PONTIFICIA UNIVERSIDAD CATOLICA DE CHILE
SCHOOL OF ENGINEERING

THERMOECONOMIC OPTIMIZATION OF SOLAR POLYGENERATION PLANTS FOR PRODUCING ELECTRICITY, DESALTED WATER, COOLING, AND PROCESS HEAT.

ROBERTO EDUARDO LEIVA ILLANES

Thesis submitted to the Office of Graduate Studies in partial fulfillment of the requirements for the Degree of Doctor in Engineering Sciences.

Advisor:
Dr. RODRIGO ESCOBAR

Santiago de Chile, September, 2018

PONTIFICIA UNIVERSIDAD CATOLICA DE CHILE

SCHOOL OF ENGINEERING

THERMOECONOMIC OPTIMIZATION OF SOLAR POLYGENERATION PLANTS FOR PRODUCING ELECTRICITY, DESALTED WATER, COOLING, AND PROCESS HEAT.

ROBERTO EDUARDO LEIVA ILLANES

Members of the Committee:

Dr. RODRIGO ESCOBAR

Dr. JOSÉ MIGUEL CARDEMIL

Dr. FRANCISCO SUAREZ

Dr. DAVID WATTS

Dr. DIEGO ALARCÓN

Dr. JORGE VÁSQUEZ

Thesis submitted to the Office of Graduate Studies in partial fulfillment of the requirements for the Degree of Doctor in Engineering Sciences.

Santiago de Chile, September, 2018

Dedicated to my father, mother, friend, and beloved God.

AKNOWLEDGEMENTS

My gratitude to:

- Dr. Rodrigo Escobar and Dr. José Miguel Cardemil, my main supervisor and co-supervisor of my dissertation, for their advices, trust, discussions and valuable feedback during these years.
- Plataforma Solar de Almeria-PSA, Spain, that is the largest and one of the most relevant solar thermal research center in Europe and worldwide, where I did an eight-month research internship, and had the privilege of working with Dr. Diego Alarcón, Director of the Solar Desalination Unit. Thanks for his valuable comments. His discussions contributed significantly to this research. Additionally, to thank all those who gave me the opportunity to discuss my research topic, I refer to other PSA researchers, such as, Dra. Patricia Palenzuela, Dr. Eduardo Zarza, Dra. Loreto Valenzuela, Dr. Bartolome Ortega, and also to Mrs. Carmen Montesinos, PSA Secretary.
- Center for Energy Resources and Consumption Research (CIRCE), and Department of Mechanical Engineering - University of Zaragoza, Spain, that is an important research center in thermoeconomic and energy. Where, I did a three-month research internship and had the privilege of working with Dr. Javier Uche and Dra. Amaya Martinez. Thanks for their suggestions, constructive dialogues, and their kindness. Their discussions contributed significantly to this research, also. Additionally, I attended the subject “Tools for Industrial Energy Analysis” of the European Master in Renewable Energy taught by professors Dr. Antonio Valero and Dr. Cesar Torres. Note that Dr. Antonio Valero and his research group developed an important thermoeconomic method that I applied in chapter 4 of this dissertation.
- The research team of Dr. Rodrigo Escobar and José Miguel Cardemil (Group of Solar Energy - DICTUC, Center for Solar Energy Technologies - Fraunhofer Chile Research, and Energy Center - PUC). Special mention to Cristian Cortés, Alan Pino, Carlos Felbol, Carlos Valenzuela, and Carlos Mata, among others.
- CONICYT, that awarded me a National Doctoral Scholarship. In particular CONICYT-PCHA/Doctorado_Nacional/año2013-folio21130634.

- Pontificia Universidad Católica de Chile (PUC), School of Engineering, that awarded me a Doctoral Scholarship, which was complemented with the CONICYT Scholarship.
- FONDECYT project Nº 1130621, which funded part of this research project as well as visits from high-level specialists such as Dr. Adrian Bejan, who along with Dr. George Tsatsaronis and Dr. Michael Moran developed one of the most widely used thermoeconomic method that was applied in chapters 2 and 3 of this dissertation.
- Universidad Técnica Federico Santa María (UTFSM), my employer, for giving me the support and ease to combine work with this research project, which made possible to complete this PhD program.
- My family, for their patience, understanding, support, and help at all times.

CONTENTS

LIST OF TABLES

LIST OF FIGURES

NOMENCLATURE

a: annum or year

A: solar field aperture area, m^2

BS: backup fossil fuel energy system

capex: capital expenditure, USD

cff: fossil fuel cost, USD/(kWh)

C: exergy cost

$\mathbf{C}_P$: exergy cost of the product

$\mathbf{C}_P^e$: exergy cost of product due to irreversibilities of the components

$\mathbf{C}_P^r$: exergy cost of product due to the residues allocation

$\mathbf{c}_e$: unit exergy cost of the external resources

$\mathbf{c}_R$: unit exergy cost of the residues

$\dot{C}$ or $\dot{C}_j$: exergy cost rate, USD/h

$\dot{C}_{D,k}$: exergy destruction cost rate, USD/h

$\dot{C}_{F,k}$: exergy fuel cost rate, USD/h

$\dot{C}_{P,k}$: exergy product cost rate, USD/h

c: unit exergy cost, USD/(kWh) or kW/kW

cfr: capital recovery factor, %

COP: Coefficient of performance, -

COCHILCO: Chilean Cooper Commission

CSP: concentrated solar power

CST: cold storage tank

DNI: direct normal irradiance, W/m^2

E: exergy flow

e: exergy specified, kJ/kg

$\dot{E}$: time rate of exergy or exergy rate, kJ/s

$\dot{E}_{sun}$: exergy rate from sun, kJ/s

$\dot{E}_D$: exergy destruction rate, kJ/s

$\dot{E}_{F,k}$: exergy fuel rate, kJ/s

$\dot{E}_{P,k}$: exergy product rate, kJ/s

$\dot{E}_{L,k}$: exergy loss rate, kJ/s

EPC: engineering, procurement, and construction

F: fuel

$\boldsymbol{F_e}$: vector of external resources

$\langle \boldsymbol{FP} \rangle$: matrix composed of distribution coefficients

FWP: feed water preheater

G: generator

HP: high pressure

HST: hot storage tank

I: irreversibility

i: discount rate, %

$\boldsymbol{K}_D$: diagonal matrix of unit exergy consumptions

k: unit exergy consumptions

f_k: exergoeconomic factor, %

LiBr/H_2O: Lithium bromide / water

LP: low pressure

LCC: levelized cooling cost, USD/(kWh)

LEC: levelized electricity cost, USD/(kWh)

LHC: levelized process heat cost, USD/(kWh)

LWC: levelized water cost, USD/m^3

MED: multi-effect distillation

n: number of time periods, years

$opex$: operational expenditure or operation and maintenance cost, USD/a

P: product

P_{elect}: electricity selling price in the grid for industrial use, USD/(kWh)

PH: process heat plant

Poly: Polygeneration

$\dot{Q}$: heat rate, kJ/s

REF: Refrigeration plant

RO: reverse osmosis

r_k: relative cost difference, %

SAM: system advisor model software

SF: solar field

T_0: reference temperature, °C

TES: thermal energy storage

$\boldsymbol{U}_D$: identity matrix

V_D: dissipative system components

y: distribution coefficients

$\dot{W}$: work rate, kJ/s

$\dot{Z}$: non-exergy-related cost rate, USD/h

$\dot{Z}_k^{CI}$: capital investment cost rates, USD/h

$\dot{Z}_k^{OM}$: operating and maintenance cost rates, USD/h

Greek symbols

β_{ir}: residue cost distribution ratio

ψ: exergy efficiency

τ: average annual time of plant operation at nominal capacity

PONTIFICIA UNIVERSIDAD CATOLICA DE CHILE

ESCUELA DE INGENIERIA

OPTIMIZACIÓN TERMOECONÓMICA DE UNA PLANTA DE POLIGENERACIÓN SOLAR PARA LA PRODUCCIÓN DE ELECTRICIDAD, AGUA DESALINIZADA, REFRIGERACIÓN, Y CALOR DE PROCESO.

Disertación enviada a la Dirección de Investigación y Postgrado en cumplimiento parcial de los requisitos para el grado de Doctor en Ciencias de la Ingeniería.

ROBERTO EDUARDO LEIVA ILLANES

RESUMEN

Esta investigación se centra en la evaluación termoeconómica para la producción conjunta de electricidad, agua, refrigeración, y calor de proceso en plantas de poligeneración solar, con el fin de crear una base de conocimiento científico para el desarrollo de tecnologías de plantas de potencia de concentración solar (CSP) en zonas con altas condiciones de irradiación solar, y el uso racional y óptimo de recursos en esquemas de poligeneración para aumentar la eficiencia global de conversión de energía del sistema, y minimizar los costos de los productos finales.

El objetivo principal de esta disertación es modelar, evaluar y optimizar plantas de poligeneración solar, configuradas con una planta CSP con un campo de colectores solares cilindro parabólico, almacenamiento térmico de energía y un sistema de respaldo, un módulo de destilación multi-efectos (MED), un módulo de refrigeración de absorción de simple efecto (REF), y un módulo de calor de proceso (PH), donde el motor impulsor es la planta CSP, considerando que las plantas de poligeneración se localiza en una zona con altas condiciones de irradiación solar y de demanda de energía y agua.

Las plantas de poligeneración solar se simulan en un régimen transitorio, en una ubicación representativa con altas condiciones de irradiación solar, como en el norte de Chile. En el desarrollo de esta disertación se utilizaron los programas IPSEpro, Microsoft Excel, MATLAB, EES, y el módulo ExIO como complemento de Microsoft Excel.

Para ampliar el análisis termoeconómico en la evaluación de esquemas de poligeneración solar, la metodología incluye el uso de dos métodos termoeconómicos; el primero, basado en el método de costo de exergía, se utilizó para evaluar el costo real de cada producto, en el análisis de sensibilidad del costo de inversión, costo de combustible y de la demanda, y para evaluar los efectos del tamaño del campo solar y el dimensionamiento del almacenamiento de energía térmica. Se investigaron tres configuraciones: dos esquemas de poligeneración y uno de sistemas independientes. Además, se comparó con el método de costo nivelado en términos de asignación de costos y del costo especifico unitario de cada producto. Mientras que el segundo método, basado en el método de exergoeconomía simbólica, se utilizó para analizar en profundidad el proceso de formación de costos de exergía, comparándolo con sistemas independientes, y para establecer la mejor configuración en cogeneración, trigeneración y poligeneración. En el cual, se investigaron veintiún configuraciones: ocho de cogeneración, ocho de trigeneración, cuatro esquemas de poligeneración, y uno de sistemas independientes.

Esta disertación fue desarrollada a través de tres artículos científicos.

Este estudio revela que una planta de poligeneración solar es más eficiente y rentable que las plantas independientes para una zona con altas condiciones de irradiación solar y proximidad a centros de consumo, como las industrias mineras, que requieren operación continua y suministro de energía y agua con una demanda fundamentalmente constante. Además, de acuerdo con el mercado del norte de Chile, las configuraciones de poligeneración solar son competitivas en cuanto a la producción de electricidad, agua dulce, refrigeración y producción de calor. A su vez, las plantas de poligeneración solar podrían aumentar el beneficio económico vendiendo créditos de carbono y créditos de cuotas de energía renovable basados en el Protocolo de Kyoto y la legislación chilena, respectivamente. También revela que el método termoeconómico es un método de asignación de costos equitativo y racional que es adecuado para ser aplicado en una planta de poligeneración solar. Otro resultado es que este método se recomienda cuando se necesita un análisis más preciso para evaluar los costos de los diferentes productos y para evaluar los beneficios de una planta de poligeneración, en comparación con las plantas independientes. Por otro lado, el método de costo nivelado es un método simple y rápido, y no se requiere un profundo conocimiento de termodinámica, siendo recomendable cuando es necesario realizar un primer acercamiento de los costos de cada producto. Otro resultado importante es que los equipos claves en los cuales el diseño debería ser mejorado en las plantas de multi-generación solar son: colectores solares, subsistemas productivos (plantas MED, REF, y PH), evaporador, y recalentador. También, las configuraciones recomendadas en las plantas de multi-generación solar (cogeneración, trigeneración, y poligeneración) son aquellas en las cuales la planta MED reemplaza al condensador, y la planta REF, así como el módulo PH, se acoplan a las extracciones de turbina.

Los resultados obtenidos brindan información útil para señalar el potencial que ofrece la poligeneración solar y podría constituir una guía para comprender estos métodos.

Miembros de la Comisión de Tesis Doctoral:

Dr. RODRIGO ESCOBAR
Dr. JOSÉ MIGUEL CARDEMIL
Dr. FRANCISCO SUÁREZ
Dr. DAVID WATTS
Dr. DIEGO ALARCÓN
Dr. JORGE VÁSQUEZ

Santiago, septiembre 2018

PONTIFICIA UNIVERSIDAD CATOLICA DE CHILE
ESCUELA DE INGENIERIA

THERMOECONOMIC OPTIMIZATION OF SOLAR POLYGENERATION PLANTS FOR PRODUCING ELECTRICITY, DESALTED WATER, COOLING, AND PROCESS HEAT.

Dissertation submitted to the Office of Research and Graduate Studies in partial fulfillment of the requirements for the Degree of Doctor in Engineering Sciences by

ROBERTO EDUARDO LEIVA ILLANES

ABSTRACT

This research is centered on thermoeconomic assessment of the joint production of electricity, fresh-water, cooling and process heat for solar polygeneration plants, to create scientific knowledge basis for the development of concentrated solar power (CSP) technologies in zones with high direct irradiation conditions, and the rational and optimal use of polygeneration schemes to increase the overall system energy conversion efficiency and minimize the costs of the final products.

The main objective of this dissertation is to model, evaluate, and optimize solar polygeneration plants in thermoeconomic terms, configured by a CSP parabolic trough collector field, thermal energy storage and backup system, a multi-effect distillation (MED) module, a single-effect absorption refrigeration (REF) module, and a process heat (PH) module, whose prime mover is the CSP plant, and considering that the polygeneration plants are located in an area with high solar irradiation conditions, and large demands of energy and water.

The solar polygeneration plants are simulated in a transient regime, in a representative location with high irradiation conditions, such as in northern Chile. In the development of this dissertation IPSEpro, Microsoft Excel, MATLAB, EES (Engineering Equation Solver), and the ExIO module as a complement of the Microsoft Excel software were used.

In order to expand thermoeconomic analysis in the assessment of solar polygeneration schemes, the methodology includes the use of two thermoeconomic methods. The first method, based on the exergy costing method, was used to assess the actual cost of each product; to conduct a sensitivity analysis of investment, fuel cost and demand, and to evaluate the effects of solar field size and the sizing of thermal energy storage. Three configurations are investigated: two polygeneration schemes and one considering stand-alone systems. Furthermore, this method was compared with the levelized cost method in terms of the costs allocation and the unit specific cost of each product. Whereas the second method, based on the symbolic exergoeconomic method, was used to analyze in depth the process of exergy cost formation, compare with stand-alone systems, and establish the best configuration in cogeneration, trigeneration and polygeneration schemes, in which twenty-one configurations are investigated: eight of cogeneration, eight of trigeneration, four polygeneration schemes, and one considering stand-alone systems.

This dissertation was developed through three journal papers.

This study reveals that a solar polygeneration plant is more efficient and cost-effective than stand-alone systems for a zone with high irradiation conditions and proximity to consumption centers, such as mining industries, which require continuous operation and energy supply with fundamentally constant demand. Furthermore, according to northern Chilean market, solar polygeneration configurations are competitive regarding electricity, fresh-water, cooling and heat productions. Additionally, solar polygeneration plants might increase the economic profit by selling carbon credits and credits of renewable-energy quotas based on the Kyoto Protocol and Chilean legislation, respectively. Also reveals that the thermoeconomic method is an equitable and rational cost allocation method which is suitable for applying in a solar polygeneration plant. Another result is that this method is recommended when a more precise analysis it is necessary to assess the proper costs of different products, and for assessing the benefits of a polygeneration plant, when compared to stand-alone systems. On the other hand, the levelized cost method is a simple and fast method, and a deep knowledge of thermodynamics is not required, being recommended when it is necessary to perform a first approached of the costs of each product. Another important result is that the key equipment, in which the design should be improved in solar multi-generation plants, are: solar collector, productive subsystems (MED, REF, and PH plants), evaporator, and reheater. Also, the recommended configurations for the integrated solar multi-generation plants (cogeneration, trigeneration, and polygeneration) are those, in which the MED plant replaces the condenser of the power cycle, and the refrigeration plant, as well as the process heat module are coupled to turbine extractions. Those plants were the most cost-effective configuration.

The results delivered provide useful information that could serve to decision-makers to point out the actual potential offered by solar polygeneration systems, and could constitute a guide to understand these methods.

Keywords: solar energy, concentrated solar power, polygeneration, thermoeconomic analysis, multi-effect distillation, absorption refrigeration.

Members of the Doctoral Thesis Committee:

Dr. RODRIGO ESCOBAR
Dr. JOSÉ MIGUEL CARDEMIL
Dr. FRANCISCO SUÁREZ
Dr. DAVID WATTS
Dr. DIEGO ALARCÓN
Dr. JORGE VÁSQUEZ

Santiago, September 2018

LIST OF PAPERS

The papers published, accepted or submitted during this PhD project are listed below. The papers are co-authored. The author of this dissertation executed the major work in writing these papers such as: creating methodology and models, simulations, interpretation of results and discussion. The contribution of the co-authors in writing these papers has been discussions, suggestions, and critical review.

This dissertation is based on the next journal papers, referred to in the text by their Roman numerals.

I. **R. Leiva-Illanes**, R. Escobar, J. M. Cardemil, and D. Alarcón-Padilla, "Thermoeconomic assessment of a solar polygeneration plant for electricity, water, cooling and heating in high direct normal irradiation conditions". *Energy Conversion and Management*, vol. 151, May, pp. 538–552, 2017.

II. **R. Leiva-Illanes**, R. Escobar, J. M. Cardemil, and D. Alarcón-Padilla, "Comparison of the levelized cost and thermoeconomic methodologies – Cost allocation in a solar polygeneration plant to produce power, desalted water, cooling, and process heat". *Energy Conversion and Management*, vol. 168, pp. 215–229, Jul. 2018.

III. **R. Leiva-Illanes**, R. Escobar, J. M. Cardemil, D. Alarcón-Padilla, J. Uche, and A. Martínez "Exergy cost assessment of CSP driven multi-generation schemes: Integrating seawater desalination, refrigeration, and process heat plants". (Submitted to Energy Conversion and Management journal)

Additionally, the author has published different conference papers, such as

International congress:

1. **R. Leiva**, T. Kaelbel, R. Escobar. “Modelamiento de una planta CSP operando en esquema de poligeneración”. XI Congreso Iberoamericano de Energía Solar (CIES) y XXXVIII - Semana Nacional de Energía Solar (SNES), Querétaro, México, octubre 2014.
2. **R. Leiva-Illanes**, R. Escobar, J. Cardemil. “Exergoeconomic assessment of a solar polygeneration plant”. Conference Proceedings, Solar World Congress 2015. Daegu, Korea, November 2015.
3. **R. Leiva**, R. Escobar, J. Cardemil. “Exergoeconomic and techno-ecnonomic analysis of a solar multi-generation plant with thermal energy storage”. Conference Proceedings, EuroSun 2016. Palma de Mallorca, Spain, October 2016.
4. **R. Leiva**, R. Escobar, J. Cardemil. “Modeling of solar polygeneration plant”. Conference Proceedings, SolarPACES Conference 2016. Abu Dhabi, UAE, October 2016.
5. **R. Leiva-Illanes**, R. Escobar, J. M. Cardemil, D. Alarcón-Padilla, J. Uche, and A. Martínez. “Exergy cost decomposition and comparison of integrating seawater desalination plant, refrigeration plant, process heat plant in a concentrated solar power plant”. Conference Proceedings, Solar World Congress 2017. Abu Dhabi, UAE, October 2017.

National congress:

1. **R. Leiva I.**, T. Kaelbel, R. Escobar. “Modelamiento de una planta de concentración solar operando en poligeneración”. XIV Jornadas de Mecánica Computacional – JMC 2014, Talca, Chile, octubre 2014.
2. **R. Leiva I.**, R. Escobar. “Modelamiento y evaluación exergoeconómica de una planta CSP+MED”. XIV Jornadas de Mecánica Computacional – JMC 2015, Concepción, Chile, octubre 2015.
3. **R. Leiva I.**, R. Escobar. “Modelamiento y evaluación exergoeconómica de una planta de cogeneración solar”. XVI Congreso Chileno de Ingeniería Mecánica - COCIM 2015, Valparaíso, Chile, noviembre 2015.

1. INTRODUCTION

1.1. Context

The mining industry in zones with high direct normal irradiation conditions, such as northern Chile presents a high demand of electricity, fresh-water, process heat, and industrial refrigeration. These products are feasible to produce in stand-alone plants that consume mainly fossil fuels. However, given the advantages offered by operating in a polygeneration scheme, it is interesting to consider the evaluation of a polygeneration plant to produce these four products or to operate in a cogeneration or trigeneration scheme. Polygeneration system is an integration process, which produces more than one product from one or more natural resources (Serra et al., 2009), whose advantages are: allowing to reduce both primary energy consumption and CO_2 emissions, avoiding the waste heat, reducing the transmission and distribution network and other energy losses, as well as decreasing energy dependency at the country level, and contributing to the diversification of energy sources (Al Moussawi et al., 2016). On the other hand, since in the north of Chile there is a high availability of solar irradiation (Escobar et al., 2014) is that a concentrated solar power (CSP) plant could be a cost-effective option to produce electricity because this type of plant allows operating directly from solar energy, storing the thermal energy captured, and operating in hybrid form using fossil fuel backup, which allows to operate in stable and constant conditions, and thus does not affect the performance of plants that are integrated into the polygeneration scheme. Therefore, CSP plants have the potential to play an important role in the production of electricity from non-conventional renewable energies, which constitute an opportunity for sustainable development. Considering that the power block, in the CSP plant, rejects heat to the environment, this heat could be recovered by technologies driven by thermal energy. Therefore also, a CSP plant is feasible to integrate it with other technologies to produce other products, such as process heat, steam, hot water, fresh-water, and cooling (Modi et al., 2017). Given the above, in this research is proposed analyzing the integration of a CSP plant that operates in polygeneration schemes where the CSP plant analyzed consists of a solar field with parabolic trough collectors, a thermal energy storage system, a power block, and a backup energy system. The CSP plant is the prime mover into the solar polygeneration plant.

Note that the prime mover, that converts thermal or chemical energy into power, is the heart of any polygeneration system (Al Moussawi et al., 2016). The technologies driven by thermal energy for producing desalted water, cooling, and process heat consist of a multi-effect distillation plant, a single-effect LiBr-H_2O absorption refrigeration plant, and a countercurrent heat exchanger module, respectively. These technologies were selected because they are commercially available and allow operating within temperature ranges of the coupling points in the CSP plant. These points were selected according to the operating temperature constraints, imposed by each technology and aiming to cause the minimum penalty in terms of power production. The process of integration of those plants is described in detail in chapters 2, 3, and 4.

Due to the complexity of dealing with many energy flows in polygeneration schemes, the integration and assessment of such technologies should be evaluated applying a rational method. A method for the allocation of resources and products allows solving this problem, considering all input and output from the system, investments, operation and maintenance costs, as well as the production units of each product. For solving this problem, several allocation cost methods have been proposed in the literature, which in general are classified in thermodynamic, economic, and thermoeconomic methods (or exergoeconomic). The thermodynamic methods are based on the First and/or Second Law of the Thermodynamics (Beretta et al., 2014; Gochenour, 2003; Tereshchenko & Nord, 2015; Ye & Li, 2013). The economic methods are similar to thermodynamic ones depending on whether lowering power or heat costs are in priority (Gochenour, 2003; Nuorkivi, 2010). Finally, the thermoeconomic methods are based on the Second Law of the Thermodynamics and economic principles (Abusoglu & Kanoglu, 2009; Bejan et al., 1996; Serra et al., 2009). However, in the evaluation of solar polygeneration plants, two methods are used: the thermoeconomic method and the levelized cost method, although, this research is based mainly on the thermoeconomic method that is described in chapters 2, 3, and 4 while the levelized cost method is described in chapter 3.

Based on a literature review, which is explained in chapters 2, 3 and 4, the following knowledge gaps have been identified:

i. Few articles reported in the literature have applied thermoeconomic assessment to solar polygeneration systems, considering a concentrated solar power plant as prime mover. In that context, some important aspects have yet to be investigated, such as the different relationships between fuels and products, the effect of investment, fuel cost, and demand in the products costs; as well as the sizing of the solar field and the TES for these solar polygeneration systems considering high irradiation conditions. This solar polygeneration plant is very attractive in zones presenting high irradiation conditions, scarcity of water, availability of flat terrain, and proximity to consumption centers, such as the mining industries in Northern Chile, Northern-Africa and Australia.

ii. Different studies have focused on assessment of CSP-polygeneration systems by the levelized cost method (Short et al., 1995) and other by the thermoeconomic method (Bejan et al., 1996); however, the results from each method are unlike and produce significant differences. Hence, it is not clear which method is more appropriate for assessing a solar polygeneration plant and which is the effect and impact of using one or other method, in terms of the complexity of calculations, rules and rationality of cost allocation, and the applicability to compare between stand-alone systems and polygeneration plants.

iii. CSP could be integrated into polygeneration schemes (Modi et al., 2017) and different studies have focused mainly on the final cost of each product. However, such those studies do not consider the evaluation of the process of exergy cost formation, the decomposition of each cost, and the configuration from stand-alone systems, following with cogeneration plants, trigeneration and finally polygeneration plants to find out new opportunities for savings, in terms of energy resources, in this complex integrated system.

This dissertation has been divided into three research papers, where each one covers one of the gaps indicated above, and it is developed in chapters 2, 3, and 4 respectively. The contribution of this dissertation seeks to fill those knowledge gaps. The objectives, hypotheses, methodology, content and contributions of the dissertation are presented below.

1.2. Objectives

The main objective of this dissertation is to model, evaluate, and optimize solar polygeneration plants in thermoeconomic terms, configured by a CSP parabolic trough collector field, thermal energy storage and backup system, a multi-effect distillation module, a single-effect absorption refrigeration module, and a process heat module to produce power, desalted water, cooling, and process heat, whose prime mover is the CSP plant, and considering that the polygeneration plants are located in an area with high solar irradiation conditions, and large demands of energy and water to create scientific knowledge basis for the development of concentrated solar power (CSP) technologies, and the rational and optimal use of polygeneration schemes to increase the overall system energy conversion efficiency and minimize the costs of the final products.

The specific objectives of this dissertation are:

i) To assess and optimize a solar polygeneration plant using a thermoeconomic method to determine the actual cost of each product; to conduct a sensitivity analysis of investment cost, fuel cost, and demand; and to evaluate the effects of solar field size and the sizing of thermal energy storage.

ii) To evaluate a solar polygeneration plant using the levelized cost and the thermoeconomic methods to analyze the costs allocation process, the unit specific costs of each product, as well as the energy and exergy efficiencies, and the main advantages of both methods evaluated.

iii) To analyze in depth the process of exergy cost formation in solar multi-generation plants, that include cogeneration, trigeneration, and polygeneration schemes, to compare with stand-alone systems, to find out new opportunities for savings, and to establish the best configuration in a cogeneration, trigeneration and polygeneration scheme, in terms of unit exergy cost of the product, total exergy cost of product, and exergy efficiency.

1.3. Hypotheses

i) Concentrated solar power plant can supply thermal energy to produce desalted water, cooling, and process heat, under different polygeneration schemes in high direct normal irradiation conditions.

ii) A solar polygeneration plant, in zones with high direct normal solar irradiation conditions and large demands of energy and water, can operate more efficiently than stand-alone systems in thermodynamic and economic terms.

iii) The thermoeconomic method is appropriate for evaluating and comparing solar polygeneration schemes and stand-alone systems.

iv) The thermoeconomic method makes a rational allocation of resources, so it is appropriate to be used in the assessment of polygeneration systems.

v) The exergy cost theory provides a general criterion that enables to assess the efficiency of polygeneration systems and rationally explains the process of cost formation of products.

1.4. Methodology

In general, the methodology considers first the modeling of stand-alone systems and their validation, following with the integration of those plants in solar multi-generation schemes, that include cogeneration, trigeneration, and polygeneration schemes, which are modeled considering solar energy and natural gas as primary resources, and the demand from the mining industry, that operates continuously and consequently presents a constant demand. The solar multi-generation schemes integrated consist of a concentrated solar power, a multi-effect distillation plant, a single-effect absorption refrigeration plant, and a process heat module. The solar polygeneration plants are simulated considering a meteorological year (Escobar et al., 2014), from the simulations, the production of the plants are determined in hourly, monthly, and annual base. The specific methodology applied in each research is explained in extenso in chapters 2, 3 and 4, respectively. Each chapter responds to a specific objective, thus, chapter 2 is associated with the first specific objective, chapter 3 with the second, and chapter 4 with the third.

Secondly, it is defined an aggregation level in each system, and it is applied the thermoeconomic and levelized cost methods. In chapter 2, it is applied the thermoeconomic method, based on the exergy costing method (Bejan et al., 1996), that was used to assess the actual cost of each product, to conduct a sensitivity analysis (investment, fuel cost and demand), and to evaluate the effects of solar field size and the sizing of thermal energy storage. Three configurations are investigated: two polygeneration schemes and one considering stand-alone systems. In chapter 3, it is compared the thermoeconomic method (Bejan et al., 1996) and the levelized cost method (Short et al., 1995) in terms of the costs allocation and the unit specific cost of each product to analyze the costs allocation process, the unit specific costs of each product, as well as the energy and exergy efficiencies, and the main advantages of both methods evaluated. Two configurations are analyzed and compared: a polygeneration scheme and stand-alone systems. Finally, in chapter 4, it is applied the thermoeconomic method, based on the symbolic exergoeconomic method

(Torres et al., 2008; Usón et al., 2012; Valero et al., 2013), that was used to analyze in depth the process of exergy cost formation to compare with stand-alone systems, and establish the best configuration in cogeneration, trigeneration, and polygeneration schemes. Twenty-one configurations are investigated: eight of cogeneration, eight of trigeneration, four polygeneration schemes, and one considering stand-alone systems. Note that chapters 2, 3, and 4 are associated with the journal papers I, II, and III respectively. Each research paper is an independent research that is concatenated with the previous research.

The present work was executed with the help of commercially available process simulation software, such as IPSEpro (modules PSE, MDK, and PSXLink) (SimTech GmbH, 2011), Microsoft Excel, MATLAB, EES (Engineering Equation Solver), and the ExIO (Torres & Valero, 2012) module as a complement of the Microsoft Excel; the post-processing was performed by MATLAB and Microsoft Excel.

1.5. Contents and research contributions

1.5.1. Contents

The present dissertation is organized in five chapters, with this introduction first. Chapter 2, 3, and 4 respond to the first, second, and third specific objective of the dissertation, respectively. These chapters constitute each one of the research paper (journal paper I, II, and III) and contain the state of the art, the literary revision, the methodology, the results, and the conclusions of this research within its scope. With the purpose of maintaining their purity and comprehension, it has avoided changing them, except if necessary. In this way, each chapter is an autonomous unity and can be read without the strict need of reading the rest of the chapters. Although this facilitates the reading of the document, it has the inevitable drawback of having to provide some redundant contents between the different chapters, especially in the introduction and the section of the different methodologies.

The content of each chapter is indicated below:

- In chapter 2, a thermoeconomic assessment of the joint production of electricity, fresh-water, cooling, and heat for a solar polygeneration plant is carried out. The aims are to assess the actual cost of each product; to conduct a sensitivity analysis of investment, fuel cost, and demand; and to evaluate the effects of solar field size and the sizing of thermal energy storage, for a polygeneration plant located in an area with high solar irradiation conditions, where there is demand for its production. The solar polygeneration plant is configured by a concentrated solar power parabolic trough collector field with thermal energy storage and backup system, multi-effect distillation module, single-effect absorption refrigeration module, and process heat module. The solar polygeneration plant is simulated in a transient regime, in a representative location with high irradiation conditions, such as in northern Chile. Three configurations are investigated: two polygeneration schemes and one considering stand-alone systems.

- In chapter 3, a comparison between the levelized cost and the thermoeconomic methods were applied to assess the performance of a solar polygeneration plant. The aim is to analyze the costs allocation process, the unit specific costs of each product, as well as the energy and exergy efficiencies. The methodology is applied in a case of study configured by a concentrated solar power with thermal energy storage and backup system, combined to a multi-effect distillation plant, an absorption refrigeration plant, and a process heat module.
- In chapter 4, a thermoeconomic analysis of solar multi-generation plants, which includes cogeneration, trigeneration, and polygeneration schemes, for the joint production of electricity, fresh-water, cooling, and process heat is carried out to analyze in depth the exergy cost formation process and compare them with stand-alone systems. That comparison allows determining the best configuration in a cogeneration, trigeneration, and polygeneration scheme, in terms of unit exergy cost of the product, total exergy cost of product, and exergy efficiency. The solar multi-generation plant considers a concentrated solar power as prime mover, which is integrated to a multi-effect distillation, an absorption refrigeration, and a process heat plants. Twenty-one configurations are investigated: eight of cogeneration, eight of trigeneration, four polygeneration schemes, and one considering stand-alone systems.
- Finally, chapter 5 presents the main conclusions of this dissertation.

1.5.2. Results

The results of this dissertation are explained in chapters 2, 3, and 4, but the main ones are explained as follows:

- In terms of total exergy cost rate of products, unit exergy cost, and exergy efficiency, the solar polygeneration schemes are more economically attractive than stand-alone systems with high irradiation conditions and proximity to consumption centers (papers I, II, and III).
- The recommended configuration for a solar polygeneration plant is the one where the MED plant has replaced the condenser of the CSP plant, the refrigeration plant is coupled in a turbine extraction, and the process heat plant is coupled between feed water preheaters. This plant was the most cost-effective configuration (paper I).
- In conformity with North Chilean market, the solar polygeneration plants are competitive. Moreover, solar polygeneration plants might increase the economic profit with the sale of carbon credits according to the Kyoto Protocol and the sale of credits, according to the renewable energy quota established by Chilean legislation (paper I).
- The sensitivity analysis of investment cost shows that the investment costs of solar field and TES are more influential on the total exergy cost rate and unit exergy cost of the plant. Therefore, the key areas where cost reductions need to be achieved are the solar field and TES (paper I).
- The thermoeconomic method is a good method for optimization a solar polygeneration plant because it uses exergy as a criterion to allocate costs and allows to perform an assessment considering the conversion efficiencies and economic benefits offered by the system (paper I).
- When more than one product is produced, there are common costs associated with the products concerned, and it is necessary to determine the share of costs attributable to one or another product. So, the cost allocation procedure needs an additional rational analysis to prevent allocation from being arbitrary (paper II).
- The levelized cost method and the thermoeconomic method are used extensively in the evaluation of this kind of plants, in which levelized cost method is a simple and fast method, and a deep knowledge of thermodynamics is not required. In the absence of a detailed knowledge of the plant, the level cost method is a good alternative and presents reasonable results. Therefore, this method is recommended when it is necessary to perform a first approximation of the costs of each product, but comparing between polygeneration plant and the stand-alone systems could lead to inaccurate conclusions.

On the other hand, the thermoeconomic method is an equitable distribution of the appropriate share of non-exergy-related cost rate ($capex$ and $opex$) and exergy cost rate in each product. It is based on the Second-Law of Thermodynamics and the Economics, in which all costs from resources consumed are charged to their useful products. This method is recommended when it is required to perform a more precise analysis of the costs of each product, and to assess the benefits of polygeneration schemes, compared to the stand-alone systems. The disadvantages of the thermoeconomic method are its complexity and additional knowledge about the internal parameters of the plant, which could not be available (paper II).

- The electricity cost calculated through the levelized cost method is higher than that estimated by the thermoeconomic method. In contrast, the water, cooling, and process heat costs are lower since in the levelized cost method, the allocation of cost does not charge all internal cost to MED, REF, and PH plants (paper II).
- The minimums unit exergy cost and levelized cost happened at the same sizing of SM and TES, however, the unit costs have different values. Hence, independently of the method employed, in an optimization process for sizing of SM and TES, the same results are delivered. Nevertheless, the thermoeconomic method allows measuring in the same unit resources and products of very different nature, such as energy and water (paper II).
- The best configurations for the integrated solar multi-generation plants (cogeneration, trigeneration, and polygeneration) are those in which the MED plant replaces the condenser of the power cycle and the REF plant, as well as the PH module are coupled to turbine extractions. Those plants deliver lower unit exergy costs of electricity, water, cooling, and heat (paper III).
- The main components that contribute to the costs formation of electricity in a solar polygeneration plant, in descending order of importance, are: solar collectors, evaporator, and reheater. In the case of the other products generated, the main components are dissipative device systems (MED and REF), solar collectors, productive subsystems (MED, REF, and PH), evaporator, and reheater. These components constitute the key equipment where the design should be improved in order to reduce the costs of products to which is necessary to first consider them in an in-depth process of analysis and optimization (paper III).

- The integrated solar multi-generation plants, that include cogeneration, trigeneration, and polygeneration schemes, are more cost-effective than stand-alone systems since these produce the lower unit exergy cost of electricity, water, cooling and heat under the conditions analyzed (paper III).

1.5.3. Contributions

The major contributions of this dissertation are the following. Note that the detailed contributions are explained in chapters 2, 3, and 4.

- It provides an exhaustive review of the literature about:
    - Solar polygeneration plants that use as prime mover a CSP plant (Paper I).
    - Levelized cost and thermoeconomic methods used in a CSP polygeneration plant (Paper II).
    - Symbolic exergoeconomic methodology that is part of the exergy cost theory (Paper III).

  The reviews are a contribution in its own right.
- It demonstrates that the five hypotheses raised are correct (Papers I, II, and III).
- It develops a thermoeconomic model for solar polygeneration plants and stand-alone systems which is flexible and could be adapted to other configurations (Papers I, II, and III).
- It develops a levelized cost model for solar polygeneration plants and stand-alone systems that could be adapted to other cases of polygeneration schemes (Paper II).
- It develops three case studies, two of them regarding solar polygeneration plants and the third one considering stand-alone systems. These case studies illustrate different potential configurations to be installed in zones with high direct normal irradiation conditions. The results delivered provide useful information that could serve to decision-makers to point out the actual potential offered by solar polygeneration systems (paper I).
- It demonstrates that the thermoeconomic method is a good method for optimization the solar polygeneration plants because it uses exergy as a criterion to allocate costs and allows to perform an assessment considering the conversion efficiencies and economic benefits offered by the system (papers I and II).

- It might constitute a guide to understand the levelized cost and the thermoeconomic methods, and to evaluate CSP-polygeneration system (paper II).
- It develops twenty different configurations of multi-generation plants: eight of cogeneration, eight of trigeneration, four polygeneration schemes, and one considering stand-alone systems (paper III).
- It determines the best configurations for the solar multi-generation plants (cogeneration, trigeneration, and polygeneration), in which the MED plant replaces the condenser of the power cycle, and both the REF plant and the PH module are coupled to turbine extractions (paper III).
- It determinates the key equipment through which the design might be improved to reduce the products costs in the solar multi-generation plants (cogeneration, trigeneration, and polygeneration). They are: solar collector, productive subsystems (MED, REF, and PH plants), evaporator, and reheater (paper III).

1.5.4. Perspectives of future work

As future studies, there are three interesting lines:

- To analyze other configurations of solar polygeneration plants using a concentrated solar power plant as prime mover, in which other alternative technologies provide desalted water and cooling, such as, multi-stage flash, reverse osmosis, and vapor compression refrigeration machine. This will allow complementing and expanding the scope of analysis regarding the equipment that can be connected to a CSP-polygeneration plant.
- To perform a thermoeconomic diagnosis of the operation of a CSP-polygeneration plant to determine the malfunction and dysfunction, in which, according to Valero and Torres (2004), the malfunction or endogenous irreversibility of a process is the variation of its irreversibilities due to a degradation of its efficiency, while the dysfunction or exogenous irreversibility of a process is the variation of its irreversibility due to the changes in its production demand.
- To analyze the effects on the products specific costs when the CSP plant is operated in a polygeneration scheme considering different modes of operation, such as generation only from solar field, generation from TES, generation from BS, generation from solar (solar field and TES), generation from TES and BS, and so on. The aim is to determine the

hourly products specific costs during a year. Additionally, it is interesting to analyze the case of operating the power block in part-load conditions and its effect over other plants.

2. THERMOECONOMIC ASSESSMENT OF A SOLAR POLYGENERATION PLANT FOR ELECTRICITY, WATER, COOLING, AND HEATING IN HIGH DIRECT NORMAL IRRADIATION CONDITIONS.

Abstract

A thermoeconomic assessment of the joint production of electricity, fresh-water, cooling and heat for a solar polygeneration plant is carried out. The aims are to assess the actual cost of each product, to conduct a sensitivity analysis of investment, fuel cost and demand, and to evaluate the effects of solar field size and the sizing of thermal energy storage, for a polygeneration plant located in an area with high solar irradiation conditions and where there is demand for its production. The solar polygeneration plant is configured by a concentrated solar power (CSP) parabolic trough collector field with thermal energy storage and backup system, multi-effect distillation (MED) module, single-effect absorption refrigeration module, and process heat module. The solar polygeneration plant is simulated in a transient regime, in a representative location with high irradiation conditions, such as in northern Chile. Three configurations are investigated: two polygeneration schemes and one considering stand-alone systems. This study reveals that a solar polygeneration plant is more efficient and cost-effective than stand-alone systems for a zone with high irradiation conditions and proximity to consumption centers, such as mining industries, which require continuous operation and energy supply with fundamentally constant demand. Furthermore, according to northern Chilean market, solar polygeneration configurations are competitive regarding electricity, fresh-water, cooling and heat productions. Additionally, solar polygeneration plants can increase the economic profit by selling carbon credits and credits of renewable-energy quotas based on the Kyoto Protocol and Chilean legislation, respectively.

2.1. Introduction

Energy and fresh water are scarce in many places, especially in locations presenting high irradiation conditions, such as desert and arid zones. Thus, the use of solar energy for producing energy and fresh water is an opportunity for economic development, energy security and climate change mitigation. Northern Chile, North-Africa and Australia are places with high irradiation conditions, availability of flat terrain, and with high consumption centers such as mining industries. Northern Chile is a good example for analysis, where its scarcity of energy and water, combined with the large mining facilities in the area, have pushed the demand for electricity, water, cooling and industrial process heat at competitive costs (COCHILCO, 2015a, 2015b). In fact, electricity, water and fuel prices have reached historical highs, negatively affecting the competitiveness of companies operating in the region. According to the Chilean Energy Ministry (2017), in 2015 the mining industry consumed 17 % and 34.4 % of the energy and electricity generated in the country, respectively, while other industries account for 23 % and 24.4 % respectively. Chile has a geography that provides an extraordinary variety of climatic conditions and availability of water resources and solar energy. Chile extends 4 270 kilometers from north to south. The north is mostly arid desert, the central zone having a more Mediterranean and the south being temperate and wet. Mining is mainly concentrated in the northern regions where minerals are more abundant. The arid Atacama Desert in northern Chile contains great mineral wealth, principally copper. So, the energy consumption in northern Chile is mostly related to mining industries, which require continuous operation and energy supply with fundamentally constant demand. The main sources of energy supply for mining are electricity and fuels. The demand for electricity in 2015 was 18.7 TWh and 12.8 TWh in northern Chile and the cooper mining industry, respectively. At regional level, the electricity demand of the cooper mining industry was 11.0 TWh in the Antofagasta region (COCHILCO, 2015b). Similarly, the demand for process heat and cooling in northern Chile is almost exclusively associated with mining. According to Chilean Cooper Commission (COCHILCO), the demand for fuels in 2015 was 21.2 TWh in the copper mining industry, of these 16.7 TWh was used in ore transportation trucks, and 4.5 TWh in mining processes that requiring process heat such as smelting, refineries, leachable mineral treatments, and services (COCHILCO, 2016). Of these processes, the leachable mineral treatments, and services require low temperatures, and its process heat demand was about 1.15 TWh. At the regional level, the fuel demand for copper mining industry was 12.1 TWh in the Antofagasta region, and the demand of the leachable mineral treatments, and services was about 0.6 TWh. On the other hand, water consumption in Chile is: 77.8 % of agriculture, 9.1 % of industry, 7.2 % of mining, and 5.9 % of drinking water. The proportions vary greatly between regions depending upon the climatic conditions. The water consumption of the copper mining industry in 2015 was of 15.8 m^3/s, which is forecast to increase to around 21.5 m^3/s by 2026 due to the development of new projects and reduced ore concentration. At the regional level, the freshwater consumption of the copper mining industry in 2015 was of 5.7 m^3/s in the Antofagasta region (COCHILCO, 2015b). In contrast, Chile presents high availability of solar energy, especially in the northern region, which stands out as one of highest solar radiation rates worldwide. In this area, the annual average of daily global horizontal irradiation reaches levels higher than 8 kWh/m^2 and the daily average of direct normal irradiation presents values higher than 10 kWh/m^2 (Escobar et al., 2015). Hence, considering the large demand for electricity, fresh water and process heat, among other utilities, in northern Chile, and the high solar energy availability, I propose to analyze the potential for implementing polygeneration schemes driven by solar energy.

A polygeneration scheme is an integrated process, which has three or more outputs that include energy flows, produced from one or more natural resources. Polygeneration systems can be classified as either topping, or bottoming cycle systems (Al Moussawi et al., 2016). In a topping cycle, the priority is power production, i.e. the supplied fuel is first used to produce power and then thermal energy. It is the most popular and widely used method of polygeneration. In contrast, in a bottoming cycle, the priority is heat production, i.e. high temperature thermal energy is the primary product produced by the process and the heat rejected from the process is recovered to generate power. A polygeneration scheme has comparative advantages over individual stand-alone systems, since it allows for reduction in both the primary energy consumption and the emissions of greenhouse gasses by displacing fossil fuels. A polygeneration scheme allows for the integration of different technologies, maximizing the rational use of resources. Due to the complexity of dealing with several energy flows, the integration of such technologies could be evaluated through a thermoeconomic approach, which combines both economic and thermodynamic relations, aiming to reduce the total exergy cost rate of the products. That approach allows performing a complete assessment, considering the conversion efficiencies and economic benefits offered by the system (Dincer & Rosen, 2012).

2.1.1. Polygeneration technologies

Concentrated solar power (CSP) systems generate solar power by using mirrors to concentrate a large area of sunlight onto a small area. Electricity is generated when the concentrated light is converted to heat, which typically drives a Rankine cycle (IRENA, 2012). CSP technologies can be classified into four categories: CSP parabolic trough collector, central receiver (solar tower), linear Fresnel and dish-Stirling. Within the CSP technologies, CSP parabolic trough collector is considered as the most mature, accounting for 85 % of the cumulative installed capacity; and presenting the lowest cost (IRENA, 2015). CSP parabolic trough collector allows for a simple integration of thermal energy storage (TES) and a backup system allowing to operate in periods of low solar radiation, increasing its capacity factor. In this context, CSP systems with TES and backup system can provide full-load, steady state electricity generation, even on cloudy days or during the night, assuring predictable dispatchability to meet peak demands. The three basic conditions for the development of concentrated solar power plants are high levels of direct solar irradiance during most of the year, availability of flat terrain, and proximity to consumption centers. Regarding water desalination, polygeneration schemes commonly consider thermal driven technologies, such as multi-effect distillation (MED) or multi-stage flash (MSF) or pressure-driven technologies, such as reverse osmosis (RO), which represent the most reliable and commercially proven technologies for desalination. Within the thermal technologies, MED is considered more attractive than MSF due to its lower energy consumption, low sensitivity to corrosion, low presence of scaling, and high development potential (Al-Karaghouli & Kazmerski, 2013). Furthermore, the possibility of operating MED plants at temperatures lower than 100 °C constitutes an interesting opportunity for coupling this technology to solar thermal systems (Al-Karaghouli & Kazmerski, 2013). Regarding the refrigeration process, absorption machines and vapor compression technologies are the most common systems employed for industrial cooling. Vapor compression systems are highly efficient refrigeration cycles that are currently dominating the market. However, it is not feasible to drive their operation using thermal energy. On the other hand, absorption refrigeration systems use thermal energy to drive a thermochemical cycle, demanding less than 1 % of the electricity consumed by a vapor compression machine. Therefore, absorption refrigeration is more attractive than vapor compression refrigeration for a solar polygeneration scheme. The commercially available solutions for absorption refrigeration are mainly single and double effect cycles, where most of the absorption systems available on the market are single-effect systems (Sarbu & Sebarchievici, 2015).

The solar polygeneration plant proposed herein consists of a CSP parabolic trough collector with TES and backup system since it is the most developed and commercially proven technology. In addition, a MED plant, a single-effect absorption refrigeration system, and a countercurrent heat exchanger as a process heat plant are considered because they are commercially available and allow for the use of thermal energy to drive the processes.

2.1.2. Integration scheme

Solar energy based heat and power systems are an attractive solution to satisfy energy demands, such as electricity, process heat, hot water, heating, space cooling, refrigeration, and water. Within solar energy alternatives, concentrated solar power technologies with parabolic trough collector, as a prime mover, allow for many integration alternatives to deliver several products. In this context, Modi et al. (2017) presented a thorough review of solar energy based heat and power plants, considering only fully renewable plants with at least the production of electricity and heat/hot water for end use. They concluded that it is economically and environmentally beneficial to invest in both small and large capacity solar-biomass hybrid plants for combined heat and power production in Nordic climatic conditions. Additionally, they also suggest that the configuration with an organic Rankine cycle with solar thermal collectors and a biomass burner is particularly attractive for large capacity plants. Recently, a new solar cogeneration plant named Aalborg CSP-Brønderslev CSP with Organic Rankine Cycle project (NREL, 2017) has been put into operation in Denmark to generate heat and power. A CSP system was integrated with a biomass-organic Rankine cycle plant. This solar cogeneration plant is the first large-scale system in the world to demonstrate how CSP with an integrated energy system design can operate efficiently. However, there are no others solar polygeneration plants or solar cogeneration plants in operation that are coupled to a CSP plant. On the other hand, due to the large potential of such schemes, the integration of CSP and desalination plants has been analyzed in several studies. Moser et al. (2013) carried out a methodology for cost comparison, where different options for producing electricity (CSP, photovoltaic system, and wind power) and desalinated water (MED and RO) were analyzed and compared in terms of levelized electricity cost (LEC) and levelized water cost (LWC). The results for the LEC and LWC were 1.6 % and 26.6 % lower, respectively, in CSP-RO compared to CSP-MED. The same authors (2014) developed a techno-economic model for the assessment of desalination plants (MED and RO), driven by conventional power plants, based on fossil fuels and renewable energies. Their results showed that despite higher investment cost, LWC of CSP-Desalination was comparable to the cost of conventional desalination, where the variability of the results depend on the different operational and financial scenarios considered. Moreover, Fylaktos et al. (2014) carried out an economic analysis of an electricity and desalinated water cogeneration plant in Cyprus. Their results revealed that the CSP-Desalination concept is financially feasible for all systems, even though the stand-alone electricity plant is economically more attractive. However, their findings also showed that LEC and LWC were 0.8 % and 11.9 % higher, respectively, for CSP-RO compared to CSP-MED. Recently, Palenzuela et al. (2015) carried out a techno-economic analysis of different MED system schemes coupled to CSP plants and compared to the CSP-RO configuration. Results showed that replacing the condenser by low-temperature MED was mostly competitive in the Arabian Gulf, but CSP-RO performs better in the Mediterranean region, where evaporative cooling is employed. As described above, the results from different authors focused on techno-economic aspects using the first law of thermodynamics and economic relations for calculating the levelized costs (LEC and LWC); but not the second law of thermodynamics, as an exergy analysis. In this context, exergy is useful in identifying the causes, locations, and magnitudes of process inefficiencies. Moreover, several studies compared MED and RO technologies where the CSP-RO is considered to be better than CSP-MED in economic terms, but CSP-MED is driven by thermal energy and has low specific electricity consumption, high reliability, simple water pretreatment and low maintenance. Thus, MED could be more attractive than RO for its integration into a polygeneration scheme.

Regarding the refrigeration process, solar absorption systems have been analyzed in several studies. In fact, Sarbu and Sebarchievici (2015) reviewed a large number of studies about solar cooling, but the integration of power plants, specifically CSP plants, and absorption plants has been reported only in some studies in the literature (Al Moussawi et al., 2016; Modi et al., 2017). Perdichizzi et al. (2015) carried out an assessment of the integration of a CSP plant coupled to a double-effect steam driven absorption chiller. The results proved that absorption chillers fed by low-grade steam save a significant amount of electricity compared to the use of compression chillers. Yet, in order to produce the same gross power in the cogeneration plant, the solar field requires a larger aperture area to deliver the heat demanded by the Rankine cycle.

Regarding the thermoeconomic analysis, the literature is extensive in polygeneration systems using fossil fuels as a main energy source. However, only a few studies have focused on thermoeconomic analyses of CSP plants. Al-Sulaiman et al. (2013a, 2013b) formulated the thermoeconomic optimization of three novel trigeneration systems based on Organic Rankine Cycle: Solid Oxide Fuel Cell -trigeneration, biomass-trigeneration, and solar-trigeneration systems. The solar-trigeneration system is made of a parabolic trough collector field including a two-tanks TES system coupled to an Organic Rankine Cycle; through a heat recovery system composed of a steam generator and a single-effect absorption chiller. The results revealed that the solar-trigeneration system offered the best thermoeconomic performance among the three configurations considered. Calise et al. (2016) presented a novel solar polygeneration system, based on a hybrid system equipped with an Organic Rankine Cycle fuelled by a parabolic trough collector solar field and by a geothermal well, a multi-effect distillation unit, and an absorption chiller. The results showed that the electricity price is quite high, thus making the production scarcely competitive in the current energy market conditions; conversely, the price of the fresh water produced is moderately competitive and it can be considered attractive in areas affected by the scarcity of water sources. Recently, Ortega et al. (2016) performed a thermoeconomic analysis of the joint production of electricity and fresh water in a CSP plant, based on parabolic trough collector, MED and RO units. Four coupling schemes were investigated: a MED plant replacing the condenser of the CSP, a MED plant fed by one extraction of the turbine, RO driven directly from the electricity generated by the CSP plant and a RO plant connected to the local grid. Results showed that the best coupling option is the RO unit connected to the local grid, which obtained the lower LWC. However, between MED configurations, the results showed that the best coupling scenario occurs when the condenser of the CSP plant is replaced with a MED system, in which case the LWC decreased by about 2.1 %.

As described above, the integration and performance between CSP, MED, cooling and process heat plants have been analyzed extensively, focusing in cogeneration schemes. Some of those studies considered the levelized cost to evaluate the benefits of the integration. Nevertheless, in polygeneration schemes it is necessary to determine the relationship between the unitary costs of the different outputs (J. Wang & Mao, 2015). Thermoeconomics allows to determine the cost of each product using cost allocation rules, allocating the resources consumed to the useful product of each component, and distributing its costs proportionally to the exergy flow. Hence, exergy is used as a basis for cost allocation of products. Few articles reported in the literature have applied thermoeconomic assessment to solar polygeneration systems, considering a CSP plant as primary driver. In that context, some important aspects have yet to be investigated, such as the different relationships between fuels and products, the effect of investment, fuel cost, and demand in the products costs; as well as the sizing of the solar field and the TES for these solar polygeneration systems considering high irradiation conditions. This solar polygeneration plant is very attractive in zones presenting high irradiation conditions, scarcity of water, availability of flat terrain, and proximity to consumption centers, such as the mining industries in the Northern Chile, Northern-Africa and Australia. Therefore, the objective of the present study is to apply a thermoeconomic assessment of CSP polygeneration plants, located in an area with high solar irradiation conditions and large demands for utilities, aiming to assess the actual cost of each product and conducting a sensitivity analysis regarding the most relevant parameters. The impact of integrating these different technologies is investigated based on the following parameters: total exergy cost rate of products and unit exergy costs. The results delivered provide useful information that could serve decision-makers to point out the actual potential offered by solar polygeneration systems.

2.2. Methodology

The methodology considers the modeling of a solar polygeneration plant and the application of thermoeconomic evaluations. In brief, it is based in the following procedure: First, each stand-alone system is modeled and, afterward, each stand-alone model is validated against data reported in the literature. Then, according to technical restrictions, each technology is integrated composing a polygeneration plant. Three configurations are investigated: two polygeneration schemes and one configuration considering only stand-alone systems. The polygeneration plant is simulated considering an hourly resolution meteorological year (Escobar et al., 2014), which represents the long-term behavior of the weather, in terms of a database of 8 760 hourly values. From the simulation, the plant's production is determined in hourly, monthly, and annual base, allowing to assess the contribution in each product from the sun, TES, and backup fossil fuel system. The solar thermal loop is composed of the solar field, the thermal energy storage, and the backup system. The modeling approach is based on a dynamic representation of the solar thermal loop and a steady state model of the power cycle, the desalination plant, the refrigeration plant, and the process heat unit. Those last operate in steady state conditions due to the energy provided by the solar thermal loop. Figure 2-1 provides a flowchart of the overall simulation.

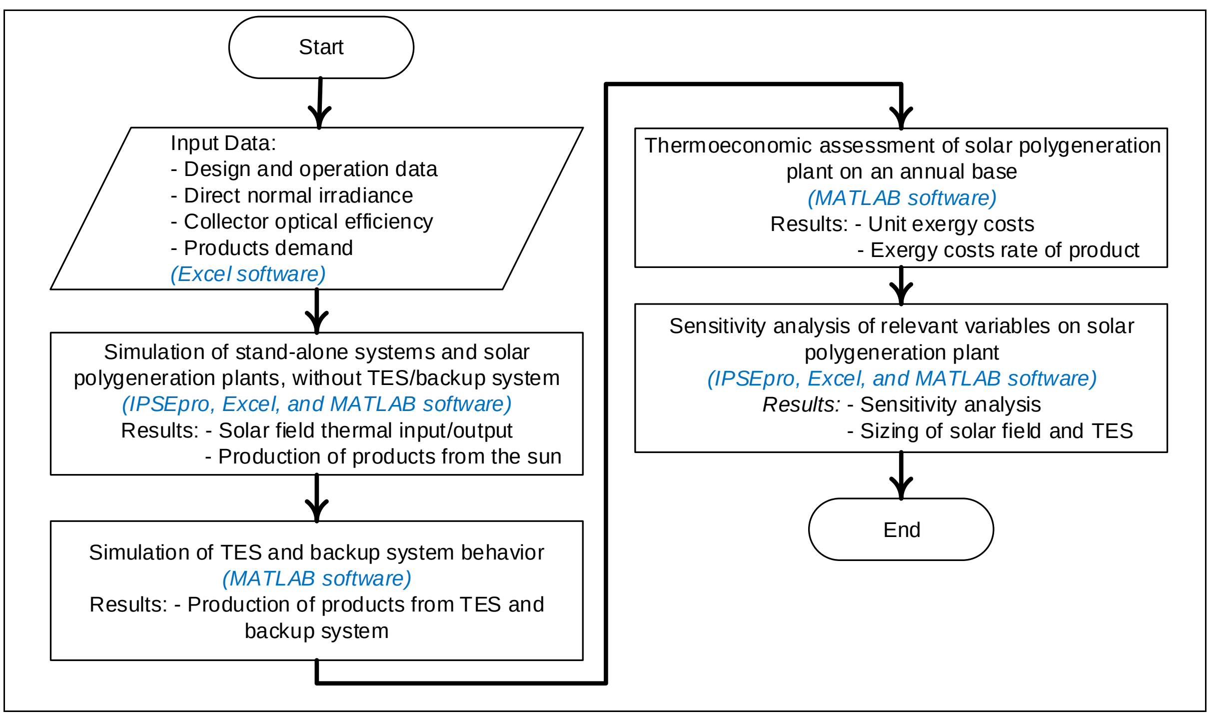

Figure 2- 1: Flowchart of the overall simulation.

The software IPSEpro (SimTech GmbH, 2011) was used for the simulations of each stand-alone plant and the solar polygeneration plants, both without TES/backup-system. IPSEpro software is composed of different modules; the main modules used in this research are IPSEpro-MDK, IPSEpro-PSE, and IPSEpro-PSXLink. IPSEpro-MDK (Model Development Kit) is a programming environment that offers all the capabilities required to define and build new component models (see Appendix A) and to translate them into a form that can be used by IPSEpro-PSE. IPSEpro-PSE (Process Simulation Environment) can establish mass and energy balances, simulating different kinds of processes, through iterative methods. These equation systems derived from the balances are solved using the Newton–Raphson method (SimTech GmbH, 2011). IPSEpro-PSXLink is an extension module that allows integrating IPSEpro-PSE projects with Microsoft Excel worksheets, which data exchange can be done in both directions: use data from Excel calculations as input for IPSEpro-PSE projects and use results of IPSEpro-PSE simulations in Excel spreadsheets for further post-processing with other software, such as in our case with MATLAB software. IPSEpro-PSE only develops steady state simulations, therefore, to analyze the dynamic behavior of the system, it is linked to a Microsoft Excel spreadsheet by IPSEpro-PSXLink where the input data, such as direct normal irradiance (Escobar et al., 2014), the collector optical efficiency of solar field (NREL, 2013; Wagner & Gilman, 2011), and the demand for products, are modified within each time-step. The results are the solar field thermal input/output, and the production of each product from the sun. After that, the simulation of the TES and backup system behavior was conducted using MATLAB software. The results are the production of each product from the TES and from the backup system; lastly, the total production of each product is the sum of production from the sun, TES, and backup system. This approach allows to simulate the polygeneration plant over a one-year period using an hourly time step.

Finally, the thermoeconomic model is solved on an annual base, for which an aggregation level is firstly selected, allowing the delimitation of boundaries (control volume) for the analysis; secondly, the physical and productive structures are determined, where fuel and product streams are established. Subsequently, different models are defined: thermodynamic, economic and thermoeconomic models (Bejan et al., 1996). The simulation of the thermoeconomic assessment was conducted using MATLAB software. The main parameters to analyze are total exergy cost rate of products and unit exergy costs. The total exergy cost rate of products is the amount of cost per unit time required to obtain the products, considering exergetic and non-exergetic parameters, by aggregating the exergy cost rate of fuel, the capital investment cost rates and the operating and maintenance cost rates. The unit exergy cost is the amount of cost per unit exergy required to generate each product.

The simulations considered the meteorological data from Crucero (Escobar et al., 2014), in Antofagasta region, northern Chile (22.14 °S, 69.3 °W). Crucero is located at 1 146 meters above sea level in extremely arid conditions. Moreover, it presents high irradiation levels: 3 389 kWh/(m^2 a) of direct normal irradiation and 2 571 kWh/(m^2 a) of global horizontal irradiation (Escobar et al., 2015). The analysis has been conducted for southern hemispherical conditions. Due to its high solar resource and its proximity to a transmission substation and different mining facilities, it is considered as one of the best sites for deploying solar energy technologies in Chile.

2.2.1. Design and modeling of a polygeneration plant

The first scheme analyzed herein is depicted in Figure 2-2 and denominated as Poly 1, considering a CSP configuration that is analogous to the features of the Andasol-1 power plant, located in Granada (Spain) (NREL, 2013; Wagner & Gilman, 2011). Based on these characteristics, the solar field is considered to be composed by parabolic trough collectors aligned on a north-south orientation, absorber tubes and organic compounds as heat transfer fluid. The collectors track the sun from east to west during the day. The design point date and time was defined as the 21st December solar noon for Crucero in Chile, where the thermal output of north-south oriented collectors is maximum at that date and time. The solar multiple is defined as a measure of the solar field aperture area as a function of the power block's nameplate capacity, the solar multiple assumed is equivalent to Andasol-1 at design point, which yields up to 510 120 m^2 of solar field aperture area as a stand-alone CSP plant. The power block consists of a regenerative Rankine cycle with reheat and six extractions, as suggested in Blanco-Marigorta et al. (2011). The condenser water of the CSP plant is cooled using a wet cooling technology. The TES is assumed as a two-tank indirect system using molten salts (60 % $NaNO_3$, 40 % KNO_3 by weight) as storage media. The full load hours of

TES are the number of hours of thermal energy delivered at the power block's design thermal input level. This value is used for sizing the TES. The backup system supplies thermal energy directly to the heat transfer fluid used in the solar field, and the heat transfer fluid supplies thermal energy to the power block. The backup system permits to maintain the plant's power generation at design conditions when there is a lack of solar radiation and/or thermal energy from TES. The capacity factor is assumed as 96 % (Palenzuela et al., 2015) considering that in Chile there is no restriction on the consumption of fossil fuel in CSP plants. The fossil fuel used was natural gas. The main modification observed in Poly-1 regarding the configuration of Andasol-1 is the replacement of the condenser by a MED plant (between states 10 and 11). In addition, a refrigeration plant (REF) is coupled to the sixth turbine extraction (between states 9 and 43), and a process heat plant (PH) is coupled between feed water preheaters FWP3 and FWP4. Considering that the power output and solar multiple are fixed, the aperture area of the polygeneration system is increased by 20.9 %, with respect to a stand-alone CSP plant.

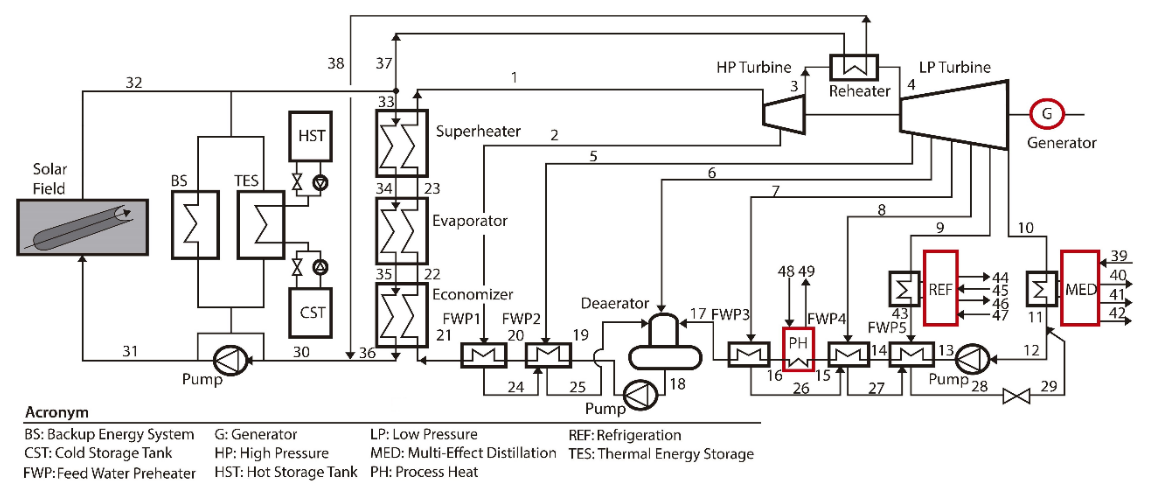

State	1	2	3	4	5	6	7	8	9	10	11	12	13	14	15	16	17	18	19	20	21	22	23	24	25
m kg/s	72.5	8.6	63.9	63.9	2.7	0.1	6.6	3.2	3.8	47.4	47.4	61.1	61.1	61.1	61.1	61.1	61.1	72.5	72.5	72.5	72.5	72.5	72.5	8.6	11.3
P bar	100.0	30.60	18.50	16.50	12.77	6.18	5.99	2.63	1.17	0.37	0.37	0.37	8.48	8.38	8.28	8.18	8.08	6.18	103.0	102.5	102.0	101.2	101.0	30.50	12.67
T °C	373.0	235.0	208.5	373.4	341.6	259.6	256.2	175.9	108.3	74.0	73.9	73.9	79.4	90.5	122.6	95.5	153.8	160.0	162.2	187.7	234.9	311.9	311.7	233.8	189.4

State	26	27	28	29	30	31	32	33	34	35	36	37	38	39	40	41	42	43	44	45	46	47	48	49
m kg/s	6.6	9.8	13.6	13.6	703.8	703.8	703.8	579.1	579.1	579.1	579.1	124.7	124.7	1588.1	430.2	555.6	602.3	3.8	281.8	297.5	297.5	281.8	61.8	61.8
P bar	5.89	2.53	0.97	0.37	8.90	12.30	11.90	11.80	11.80	11.70	11.90	11.90	8.90	1.00	1.00	1.00	1.00	1.07	1.00	1.00	1.00	1.00	1.00	1.00
T °C	157.1	126.8	97.8	73.9	292.7	293.0	393.0	379.3	379.3	313.7	292.7	393.0	292.7	25.0	52.8	35.0	39.5	101.5	35.0	10.0	6.0	25.0	63.0	90.0

Figure 2- 2: Polygeneration plant configuration. Poly 1. CSP + MED + REF + PH.

In contrast, the configuration depicted in Figure 2-3, denominated Poly 2, considers that the MED plant is coupled to the sixth turbine extraction (between states 9 and 11), the refrigeration plant is coupled to the fifth turbine extraction (between states 8 and 43) and the process heat plant is coupled between feed water preheaters FWP3 and FWP4. For this configuration, the solar field aperture area is estimated as a 17.3 % larger than a stand-alone CSP plant, which allows to ensure the power output level and to deliver the additional products.

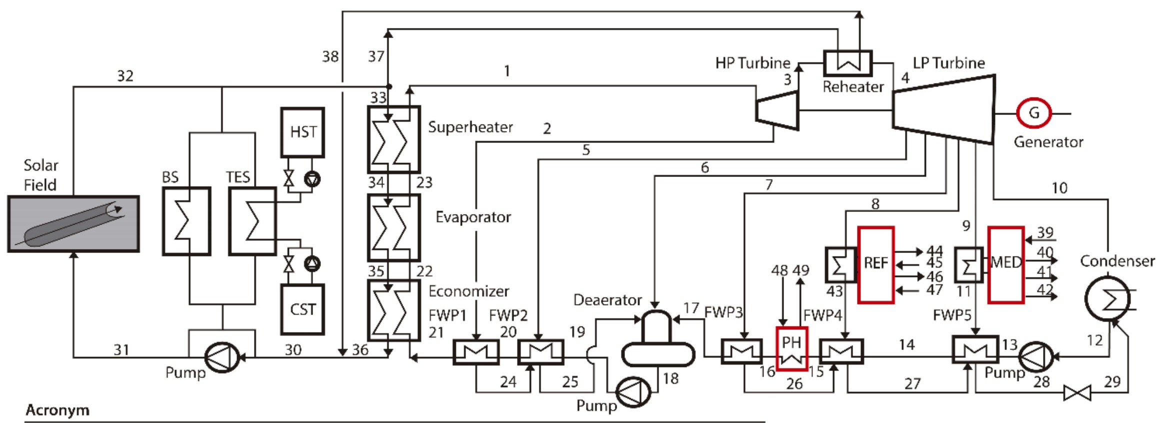

State	1	2	3	4	5	6	7	8	9	10	11	12	13	14	15	16	17	18	19	20	21	22	23	24	25
m kg/s	70.3	8.3	62.0	62.0	2.7	2.6	6.6	7.7	33.1	9.3	33.1	56.8	56.8	56.8	56.8	56.8	56.8	70.3	70.3	70.3	70.3	70.3	70.3	8.3	11.0
P bar	100.0	33.48	18.50	16.50	13.99	6.18	3.04	1.17	0.37	0.06	0.37	0.06	8.48	8.38	8.28	8.18	8.08	6.18	103.0	102.5	102.0	101.2	101.0	33.38	13.89
T °C	373.0	240.9	208.5	373.4	352.7	259.7	189.3	108.5	74.0	36.2	73.9	33.6	33.7	46.7	95.0	65.6	129.0	160.0	162.2	188.4	234.9	311.9	311.9	238.9	193.7

State	26	27	28	29	30	31	32	33	34	35	36	37	38	39	40	41	42	43	44	45	46	47	48	49
m kg/s	6.6	14.4	47.4	47.4	683.1	683.1	683.1	561.9	561.9	561.9	561.9	121.2	121.2	1107.6	300.0	387.6	420.0	7.7	281.8	297.5	297.5	281.8	61.8	61.8
P bar	2.94	0.97	0.27	0.27	8.90	12.30	11.90	11.90	11.80	11.70	11.60	11.90	8.90	1.00	1.00	1.00	1.00	1.07	1.00	1.00	1.00	1.00	1.00	1.00
T °C	131.8	97.8	65.6	65.6	292.7	293.0	393.0	393.0	397.3	313.7	292.7	393.0	292.7	25.0	52.8	35.0	39.5	101.5	35.0	10.0	6.0	25.0	63.0	90.0

Figure 2- 3: Polygeneration plant configuration. Poly 2. CSP + MED + REF + PH.

The coupling point of each technology is selected according to the operating temperature constraints, imposed by each system and aiming to cause the minimum penalty in terms of power production. For instance, the MED plant must operate within a temperature range of 64 to 74 °C (Al-Karaghouli & Kazmerski, 2013), while the desorber of the refrigeration plant should operate between 80 and 110 °C (Sarbu & Sebarchievici, 2015). Because of that, in the Poly 1 scheme the turbine back pressure is modified from 0.06 to 0.37 bar. In this configuration is not possible to regulate the amount of fresh water produced, since the MED plant is driven by the heat rejected from the power cycle and consequently any problem in the MED plant will affect the electricity production. Hence, the production of fresh water is determined by the mass flow rate of the exhaust steam from at the outlet of the low-pressure turbine. However, the production from the refrigeration plant and the process heat plant can be regulated according to demand. On the other hand, in the Poly-2 scheme the LP turbine back pressure is the same as a stand-alone CSP plant. In this scheme, the MED, refrigeration and process heat plants are considered to be coupled to turbine extractions and feed-water, respectively, therefore, their outputs can be regulated according to the demand. Furthermore, in this configuration any problem on the operation of the MED plant does not affect the CSP plant because the condensation of exhaust steam does not depend on the operation of the MED plant. However, the maximum fresh water production is limited to 385.9 kg/s, which corresponds to the case where all the turbine outlet steam is used as inlet steam in the MED plant. It should be mentioned that the output of water, cooling and process heat is dependent on the operating parameters of the rest of the plant. When it is reduced, for example, the production of process heat, the power cycle needs less input energy to generate at the nominal point (or other), and depending on the mode of operation, the control system could either reduce the energy input to power cycle by partial defocusing solar collectors, or reduce the thermal energy output from TES and/or backup system. Partial defocusing assumes that the tracking control system can adjust the collector angle in response to the capacity of the power cycle and thermal storage system.

In this study, the polygeneration plants were configured as a topping cycle, the priority is the production of electricity, and the other products are produced as a function of the thermal energy available in the power cycle. In Poly 1, the production of water is adjusted to the production of electricity. Poly 1 could run producing only electricity and water, but could not run producing the other products without producing electricity. On the other hand, Poly 2 could run producing only electricity, and in the same way, could not run producing the other products without producing electricity. Electricity and water are the priority in the mining industry.

Stand-alone configurations are also analyzed, aiming to validate the simulation models individually before integration, which also allow for comparing the performance of polygeneration plants with the same technologies, addressing the benefits of the integration.

The simulation model of the CSP plant considers that the solar field outlet temperature is constant (Montes et al., 2009), and startup and shutdown procedures are not considered. Thus, the model of the power cycle of the stand-alone CSP plant was validated at the design point against the data of Andasol-1 reported by Blanco-Marigorta et al. (2011). The results show that the differences between the IPSEpro model and the reference are about 0.03 % regarding the nominal steam mass flow rate and 0.28 % regarding the gross power. Moreover, the stand-alone CSP plant was simulated with equivalent data of Andasol-1 configuration and was validated by comparing the results between the IPSEpro/Matlab model and those obtained from SAM software (NREL, 2013). The results indicate differences of 3.6 % in terms of annual net electricity (the monthly differences are shown in Appendix B), and 1.5 % regarding the thermal efficiency.

The desalination plant is modeled considering 12 effects, parallel-cross feed MED plant and 11 feed preheaters, as suggested by Zak et al. (2012). In that context, the following assumptions are made in the thermodynamic modeling: vapors are salt free; the temperature difference between the condensation and evaporation are equal to the driving force for heat transfer in each effect; negligible heat losses to the surroundings; and the MED plant operates as a base load water station. The simulation model of the MED plant was validated considering the data reported by Zak et al. (2012) and from El-Dessouky et al. (2002). The results show no differences regarding total distillate water production, 5.46 % error in terms of specific heat transfer area, and 7.81 % regarding the Gained Output Ratio, which is defined as the mass of distillate produced for every mass unit of steam supplied to the desalination unit. Considering all the established assumptions and the large uncertainties involved in this analysis, relative errors lower than 9 % are considered as having good accuracy, as stated in Palenzuela et al. (2014).

The refrigeration plant is defined as a single-effect LiBr-H_2O absorption chiller, and modeled as suggested by Herold et al. (1996). Regarding the thermodynamic modeling, the following assumptions are considered: LiBr solutions in the generator and the absorber are in equilibrium, the refrigerant outlets at the condenser and the evaporator are in a saturated state. Moreover, to avoid crystallization of the solution, the temperature of the solution entering the throttling valve should be at least 8 ºC above crystallization temperature. The thermodynamic model of the refrigeration plant is validated against the data reported by

Herold et al. (1996). The results show differences lower than 2.6 % in terms of the cooling capacity and Coefficient of Performance (COP).

Finally, regarding the process heat plant, a countercurrent heat exchanger is configured to deliver the thermal load. Table 2-1 summarizes the main parameters of the CSP, MED, Refrigeration and Process Heat plants, according to the specifications above mentioned.

Table 2- 1: Main parameters of polygeneration plants at design point.

Property	Value in Poly 1 and Poly 2	Unit	Reference
Thermal energy storage (TES)			
Type / Storage fluid	2-tank / Molten salt	-	(NREL, 2013)
Tank temperature (cold/hot)	292 / 386	°C	(Houda et al., 2009)
Annual storage efficiency	95	%	(Houda et al., 2009)
Full load hours of TES	12	h	-
Solar field			
Parabolic trough collector model	EuroTrough collector (Skal-ET)	-	(NREL, 2013)
Absorber tube	Schott PTR-70	-	(NREL, 2013)
Heat transfer fluid	Synthetic oil (DowTherm A)	-	(NREL, 2013)
Collector optical efficiency	72.073	%	(NREL, 2013; Wagner & Gilman, 2011)
Irradiance at design day	1 010	W/m^2	(Escobar et al., 2014)
Solar Field inlet temperature (inlet/outlet)	293 / 393	°C	(NREL, 2013)
Aperture area	Poly 1: 616 650 / Poly 2: 598 510	m^2	-

Solar Multiple	2.56	-	(NREL, 2013; Wagner & Gilman, 2011)
Power block			
Gross power production	55.0	MW	(NREL, 2013)
HP turbine inlet pressure	Poly 1: 100.00 / Poly 2: 100.00	bar	(NREL, 2013)
1^{st}/ 2^{nd}/ 3^{rd}/ 4^{th}/ 5^{th}/ 6^{th} extraction pressure	Poly 1: 30.6/12.77/6.18/5.99/2.63/1.17 Poly 2: 33.48/13.99/6.18/3.04/1.17/0.37	bar	(Blanco-Marigorta et al., 2011)
LP turbine back pressure	Poly 1: 0.37 / Poly 2: 0.06	bar	(Blanco-Marigorta et al., 2011)
Isentropic efficiency (HP turbine /LP turbine)	85.2 / 85.0	%	(Blanco-Marigorta et al., 2011)
Generator and motor efficiency	98.0	%	(Blanco-Marigorta et al., 2011)
Pumps isentropic efficiency	70.0	%	(Blanco-Marigorta et al., 2011)
MED			
Feed seawater intake temperature	25	°C	(Zak et al., 2012)
Feed seawater intake salinity	0.042	kg/kg	(Zak et al., 2012)
Feed seawater after down condenser temperature	35	°C	(Zak et al., 2012)
Maximum salinity in each effect	0.072	kg/kg	(Zak et al., 2012)
Top brine temperature	65	°C	(Zak et al., 2012)

Gained Output Ratio	9.07	kg/kg	-
Fresh water production	Poly 1: 37 168 / Poly 2: 26 330	m^3/day	-
Concentration factor	1.7	-	-
Specific heat consumption	245.2	kJ/kg	-
Specific electricity consumption	1.5	kWh/m^3	(Zak et al., 2012)
Single stage absorption chiller			
Cooling capacity	5	MW_{th}	-
Chilled water temperature (inlet/outlet)	10 / 6	°C	(Herold et al., 1996)
Cooling water temperature (inlet /outlet)	25 / 35	°C	(Herold et al., 1996)
Inlet temperature desorber	108.49	°C	(Herold et al., 1996)
Coefficient of Performance (COP)	0.70	-	(Herold et al., 1996)
Process Heat			
Process heat capacity	7	MW_{th}	-
Heat exchanger temperature (inlet/outlet) (state 48/state 49)	63 / 90	°C	-

In this study, a constant demand for electricity, water, cooling and process heat was assumed, aiming to represent the large demands from the mining industry, which operates continuously and consequently presents a constant demand.

2.2.2. Thermoeconomic evaluations

The thermoeconomic evaluation was performed by selecting the proper aggregation level, allowing to delimitate the boundaries of the analysis, as depicted in Figure 2-4. Then, physical and productive structures were defined, allowing to establish the fuels and products.

After that, the thermodynamic, economic and thermoeconomic models (Bejan et al., 1996) were applied according to the aggregation level.

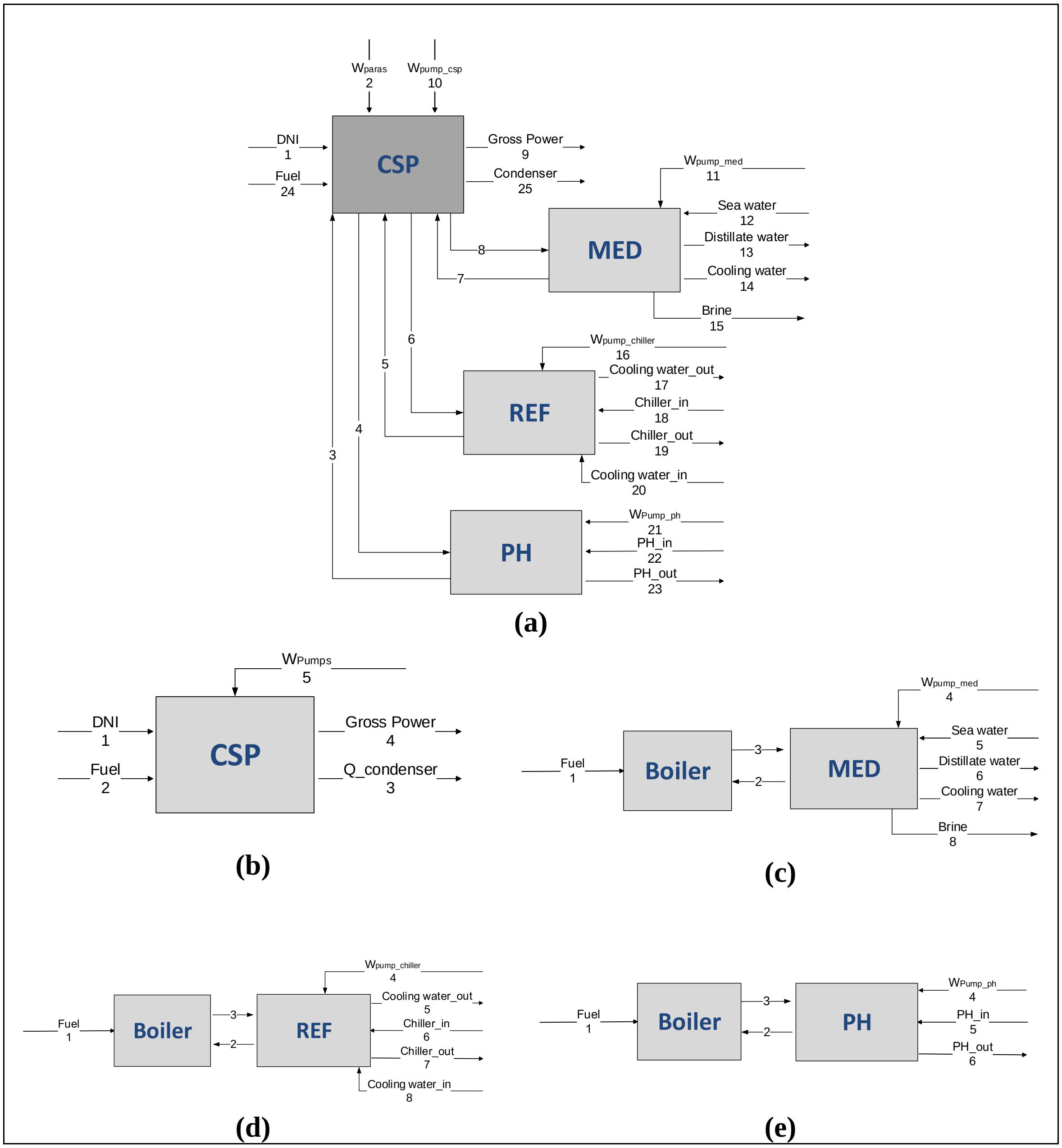

Figure 2- 4: Aggregation level for thermoeconomic assessment. (a) Polygeneration plant for Poly 1 and Poly 2 (Poly 1 does not have stream 25), (b) Stand-alone CSP, (c) Stand-alone MED, (d) Stand-alone refrigeration, e) Stand-alone process heat.

2.2.2.1. Thermodynamic model

Mass, energy and exergy balances are applied in order to perform thermodynamic modeling, aiming to determine the exergy rate in each stream. The exergy balance is expressed as:

$$\sum_{j}\left(1-\frac{T_0}{T_j}\right)\dot{Q}_j-\dot{W}+\sum_{in}(\dot{m}_{in}e_{in})-\sum_{out}(\dot{m}_{out}e_{out})-\dot{E}_D=0 \tag{2.1}$$

where $\dot{Q}$ is the heat power, T_0 is the temperature of reference, in K, $\dot{W}$ is exergy rate of work, $\dot{m}$ is the mass flow rate, e is the specific exergy, and $\dot{E}_D$ is the rate of exergy destruction. The subscripts j, in and out denote portion of boundaries, inlets, and outlets, respectively. The exergy rate from solar radiation is evaluated using the Patella's equation (Petela, 2010), defined as follows:

$$\dot{E}_{sun}=A\cdot DNI\cdot(1+\frac{1}{3}\left(\frac{T_0}{T_{sun}}\right)^4-\frac{4}{3}\left(\frac{T_0}{T_{sun}}\right)) \tag{2.2}$$

where $\boldsymbol{A}$ is the solar field aperture area, $\boldsymbol{DNI}$ is the direct normal irradiance, and $\boldsymbol{T_{sun}}$ is the apparent temperature of the sun, assumed as 6 000 K (Petela, 2010).

The exergy analysis considered an environment temperature and pressure of 25 °C and 1.013 bar (1 atm), respectively. The reference mass fraction of LiBr and water salinity were 0.5542 and 0.042 (kg/kg), respectively. Finally, all the simulations assumed that the variations of kinetic energy and potential energy are negligible.

2.2.2.2. Economic model

The economic model was developed to determine the non-exergy-related cost rate $\dot{Z}_k$ for the kth component, which is defined by aggregating the capital investment cost rate $\dot{Z}_k^{CI}$ and the operating and maintenance cost rate $\dot{Z}_k^{OM}$(not included fuel cost such as fossil fuel or biomass, fuel cost is included into exergy-related cost rate), as follows:

$$\dot{Z}_k=\dot{Z}_k^{CI}+\dot{Z}_k^{OM}=\frac{capex_k\cdot crf}{\tau}+\frac{opex_k}{\tau} \tag{2.3}$$

where τ is the annual average time of the plant's operation at nominal capacity, in hours/a; $capex$ is the capital expenditure, in USD; $opex$ is the operational expenditure, in USD/a;

and crf is the capital recovery factor, defined as:

$$crf = \frac{i(1+i)^n}{(1+i)^n - 1} \tag{2.4}$$

where i is the discount rate and n is the number periods for the analysis. Considering the particular characteristics of the Chilean conditions, a horizon of 25 years and 10 % discount rate were defined.

The economic considerations for the CSP parabolic trough collector plant are summarized in Table 2-2.

Table 2- 2: Specific cost for CSP plant.

Cost	Value	Unit	Reference
Direct Capital Cost			
Site Improvements	28	USD/m^2	(NREL, 2013)
Solar Field	200	USD/m^2	(IRENA, 2015)
Heat transfer fluid System	78	USD/m^2	(NREL, 2013)
Storage	35	USD/(kWh$_{th}$)	(Palenzuela et al., 2015)
Fossil Backup	60	USD/kW$_e$	(NREL, 2013)
Power Plant	850	USD/kW$_e$	(NREL, 2013)
Balance of plant	105	USD/kW$_e$	(NREL, 2013)
Contingency	7	%	(NREL, 2013)
EPC and Owner Cost	11	% of total direct capital cost	(NREL, 2013)
Total Land Costs	2	% of total direct capital cost	(NREL, 2013)
Sales of Tax applies of Direct Cost	4	% of total direct capital cost	(NREL, 2013)
Operational and Maintenance Costs			
Fixed Cost by Capacity	66	USD/(kW a)	(NREL, 2013)
Variable Cost by Generation	3	USD/(MWh)	(NREL, 2013)
Fossil Fuel Cost	0.0324	USD/(kWh)	(CNE, 2015)

The main economic considerations for the MED plant are listed in Table 2-3, according to the specific costs reported in the literature. This table include the costs associated with the transportation of sea water to the plant location. The distance from the coast to the plant location is about 70 km and the altitude is about 1 146 m.

Table 2- 3: Specific cost for a MED plant.

Cost	Value	Unit	Reference
Direct Capital Cost MED			
Infrastructure and construction	1 500	USD/(m^3 day)	(Mata-Torres et al., 2017)
Contingencies (%)	10	%	(Mata-Torres et al., 2017)
Total	1 650	USD/(m^3 day)	
Operational and Maintenance costs MED			
Chemical	0.025	USD/(m^3 a)	(Mata-Torres et al., 2017)
Maintenance	0.1	USD/(m^3 a)	(Mata-Torres et al., 2017)
Labor	2	% annualized total direct capital cost	(Mata-Torres et al., 2017)
Sea Water Transportation			
$capex$ of piping	736	USD/m	(COCHILCO, 2015a)
$capex$ of pumping	3.75	MUSD	(COCHILCO, 2015a)
Specific electricity consumption (pumping)	5	kWh/m^3	(COCHILCO, 2015a)

Finally, the refrigeration plant, process heat plant and boiler were modeled using unitary specific cost reported in the literature. Table 2-4 summarizes the information gathered for a refrigeration plant, and a process heat plant and the boiler.

Table 2- 4: Specific cost for a refrigeration plant, process heat plant and boiler.

Cost	Value	Unit	Reference
Refrigeration plant			
Direct and Indirect Capital Cost	548.0	USD/kW$_{th}$	(Noro & Lazzarin, 2014)
Operational and Maintenance costs	2	%	
Process heat plant			
Direct and Indirect Capital Cost	583.3	USD/kW$_{th}$	(Turton et al., 2012)
Operational and Maintenance costs	2	%	
Boiler			
Direct and Indirect Capital Cost	76.8	USD/kW$_{th}$	(Turton et al., 2012)
Operational and Maintenance costs	2	%	

2.2.2.3. Thermoeconomic model

The unit exergy cost c and exergy cost rate $\dot{C}$ for each stream are calculated by an economic balance, as follows:

$$\sum_{in}(c_{in}\dot{E}_{in})_k + \dot{Z}_k = \sum_{out}(c_{out}\dot{E}_{out})_k \tag{2.5}$$

$$\dot{C} = c(\dot{m}e) \tag{2.6}$$

where, c is the unit exergy cost, and $\dot{C}$ is the exergy cost rate. The subscript k denotes the kth component.

The exergy cost rate of product $\dot{C}_p$ is the sum of exergy cost rate of fuel $\dot{C}_f$ and non-exergy-related cost rate $\dot{Z}$. Hence, it considers exergetic and non-exergetic parameters.

For each subsystem, the fuel, product and auxiliary equations are defined to apply the economic balance for the polygeneration and stand-alone plants. In that context, the equations established for addressing that balance are summarized in Table 2-5, for the polygeneration schemes, and in Tables 2-6, 2-7, 2-8, and 2-9 for the stand-alone systems (CSP, MED, refrigeration, and process heat, respectively).

Table 2- 5: Economic balance in polygeneration plant. Poly 1 and Poly 2. Poly 1 does not have stream 25.

Subsystem	Fuel kW	Product kW	Economic balance USD/h	Auxiliary equations USD/(kWh)
CSP	$\dot{E}_1 + \dot{E}_2 + \dot{E}_{10} + \dot{E}_{24}$	$\dot{E}_9 + (\dot{E}_8 - \dot{E}_7) + (\dot{E}_6 - \dot{E}_5) + (\dot{E}_4 - \dot{E}_3)$	$\dot{C}_9 + \dot{C}_8 + \dot{C}_6 + \dot{C}_4 + \dot{C}_{25} = \dot{C}_1 + \dot{C}_2 + \dot{C}_3 + \dot{C}_5 + \dot{C}_7 + \dot{C}_{10} + \dot{C}_{24} + \dot{Z}_{csp}$	c_1=0, c_2=c_9, c_3=c_4, c_5=c_6, c_4=c_5, c_7=c_8, c_7=c_6, c_{10}=c_9, c_{24}= c_{ff}, c_{25}=0, c_3=c_9
MED	$(\dot{E}_8 - \dot{E}_7) + \dot{E}_{11} + \dot{E}_{12}$	$\dot{E}_{13}$	$\dot{C}_{13} + \dot{C}_{14} + \dot{C}_{15} + \dot{C}_7 = \dot{C}_8 + \dot{C}_{11} + \dot{C}_{12} + \dot{Z}_{med}$	c_7=c_8, c_{11}=c_9, c_{12}=0, c_{14}=0, c_{15}=0
Ref	$\dot{E}_{16} + (\dot{E}_6 - \dot{E}_5)$	$\dot{E}_{19} - \dot{E}_{18}$	$\dot{C}_{17} + \dot{C}_{19} + \dot{C}_5 = \dot{C}_6 + \dot{C}_{16} + \dot{C}_{18} + \dot{C}_{20} + \dot{Z}_{ref}$	c_5=c_6, c_{16}=c_9, c_{17}=0, c_{18}= c_{19}, c_{20}=0
PH	$\dot{E}_{21} + (\dot{E}_4 - \dot{E}_3)$	$\dot{E}_{23} - \dot{E}_{22}$	$\dot{C}_3 + \dot{C}_{23} = \dot{C}_4 + \dot{C}_{21} + \dot{C}_{22} + \dot{Z}_{ph}$	c_3=c_4, c_{21}=c_9, c_{22}= c_{23}

Table 2- 6: Economic balance cost in stand-alone CSP plant.

Subsystem	Fuel kW	Product kW	Economic balance USD/h	Aux. equat. USD/(kWh)
CSP	$\dot{E}_1 + \dot{E}_2 + \dot{E}_5$	$\dot{E}_4$	$\dot{C}_3 + \dot{C}_4 = \dot{C}_1 + \dot{C}_2 + \dot{C}_5 + \dot{Z}_{csp}$	c_1=0, c_2= c_{ff}, c_3=0, c_5=c_4

Table 2- 7: Economic balance cost in stand-alone MED plant.

Subsystem	Fuel kW	Product kW	Economic balance USD/h	Aux. equat. USD/(kWh)
Boiler	$\dot{E}_1$	$\dot{E}_3 - \dot{E}_2$	$\dot{C}_3 = \dot{C}_1 + \dot{C}_2 + \dot{Z}_{boiler}$	$c_1 = c_{ff}$, $c_2 = c_3$
MED	$(\dot{E}_3 - \dot{E}_2) + \dot{E}_4 + \dot{E}_5$	$\dot{E}_6$	$\dot{C}_2 + \dot{C}_6 + \dot{C}_7 + \dot{C}_8 = \dot{C}_3 + \dot{C}_4 + \dot{C}_5 + \dot{Z}_{med}$	$c_2 = c_3$, $c_4 = P_{elect}$, $c_5 = 0$, $c_7 = 0$, $c_8 = 0$

Table 2- 8: Economic balance cost in stand-alone refrigeration plant.

Subsystem	Fuel kW	Product kW	Economic balance USD/h	Aux. equat. USD/(kWh)
Boiler	$\dot{E}_1$	$\dot{E}_3 - \dot{E}_2$	$\dot{C}_3 = \dot{C}_1 + \dot{C}_2 + \dot{Z}_{boiler}$	$c_1 = c_{ff}$, $c_2 = c_3$
Ref	$(\dot{E}_3 - \dot{E}_2) + \dot{E}_4$	$\dot{E}_7 - \dot{E}_6$	$\dot{C}_2 + \dot{C}_5 + \dot{C}_7 = \dot{C}_3 + \dot{C}_4 + \dot{C}_6 + \dot{C}_8 + \dot{Z}_{ref}$	$c_2 = c_3$, $c_4 = P_{elect}$, $c_5 = 0$, $c_6 = c_7$, $c_8 = 0$

Table 2- 9: Economic balance cost in stand-alone process heat plant.

Subsystem	Fuel kW	Product kW	Economic balance USD/h	Aux. equat. USD/(kWh)
Boiler	$\dot{E}_1$	$\dot{E}_3 - \dot{E}_2$	$\dot{C}_3 = \dot{C}_1 + \dot{C}_2 + \dot{Z}_{boiler}$	$c_1 = c_{ff}$, $c_2 = c_3$
PH	$(\dot{E}_3 - \dot{E}_2) + \dot{E}_4$	$\dot{E}_6 - \dot{E}_5$	$\dot{C}_2 + \dot{C}_6 = \dot{C}_3 + \dot{C}_4 + \dot{C}_5 + \dot{Z}_{ph}$	$c_2 = c_3$, $c_4 = P_{elect}$, $c_5 = c_6$

The exergy efficiency is defined as the ratio between the exergy rate of product and the exergy rate of fuel. Therefore, for the polygeneration schemes the exergy efficiency is determined by

$$\psi_{polygeneration} = \frac{\dot{E}_P}{\dot{E}_F} = \frac{\dot{E}_9 + \dot{E}_{13} + \left(\dot{E}_{19} - \dot{E}_{18}\right) + (\dot{E}_{23} - \dot{E}_{22})}{\dot{E}_1 + \left(\dot{E}_2 + \dot{E}_{10} + \dot{E}_{11} + \dot{E}_{16} + \dot{E}_{21}\right) + \dot{E}_{12} + \dot{E}_{24}} \tag{2.7}$$

and for stand-alone systems, it is expressed as

$$\psi_{stand-alone} = \frac{\dot{E}_P}{\dot{E}_F} = \frac{\dot{E}_{4_{CSP}} + \dot{E}_{6_{MED}} + \left(\dot{E}_7 - \dot{E}_6\right)_{Ref} + (\dot{E}_6 - \dot{E}_5)_{PH}}{\left(\dot{E}_1 + \dot{E}_2 + \dot{E}_5\right)_{CSP} + \left(\dot{E}_1 + \dot{E}_4 + \dot{E}_5\right)_{MED} + \left(\dot{E}_1 + \dot{E}_4\right)_{Ref} + \left(\dot{E}_1 + \dot{E}_4\right)_{PH}} \tag{2.8}$$

To facilitate the thermoeconomic analysis, several assumptions were adopted along the simulation process, as listed below:

- The solar irradiance (stream 1) and the seawater intake (stream 12) have null costs.
- The unit exergy cost of fossil fuel (c_{ff}) is stated as 0.0324 USD/(kWh) (CNE, 2015).
- The unit exergy cost of electricity is equivalent for generator, pump and parasitic consumptions.
- The unit exergy costs related to the waste streams (14, 15, 17, and 20) are assumed as negligible.
- All products of the CSP plant present equivalent unit exergy cost, such as the thermal inputs for driving the MED, absorption chiller, process heat plant; and the output from the generator.
- The unit exergy cost in stand-alone plants (MED, refrigeration and process heat plants) is the electricity price from the grid for industrial use (P_{elect}), which is assumed to be 0.098 USD/(kWh) (Tariffs BT4 and AT4) (ELECDA, 2016).

The exergy destruction cost rate $\dot{C}_{D,k}$ in a component or process is a hidden cost, revealed only through a thermoeconomic analysis, as follows,

$$\dot{C}_{D,k} = c_{F,k}\dot{E}_{D,k} \tag{2.9}$$

where $\dot{C}_{D,k}$ is the exergy destruction cost rate of the kth component, $c_{F,k}$ is the unit exergy cost of fuel, and $\dot{E}_{D,k}$ is the rate of exergy destruction.

Regarding the relative cost difference $\boldsymbol{r_k}$, it expresses the relative increase in the average cost per unit exergy of the $\boldsymbol{k}$th component, between fuel $\boldsymbol{c_{F,k}}$, and product $\boldsymbol{c_{P,k}}$, as follows,

$$r_k = \frac{c_{P,k} - c_{F,k}}{c_{F,k}} \tag{2.10}$$

Finally, the exergoeconomic factor (Bejan et al., 1996) is expressed as the ratio between the contribution of the non-exergy-related costs and the exergy related costs (cost of exergy destruction and exergy losses).

$$f_k = \frac{\dot{Z}_k}{\dot{Z}_k + c_{F,k}\left(\dot{E}_{D,k} + \dot{E}_{L,k}\right)} \tag{2.11}$$

As described above, this methodology allows to assess the exergy cost rate, unit exergy cost for each product and the exergoeconomic factors to compare the performance of polygeneration schemes and stand-alone systems with the same capacity configuration. If the capacity configuration is different, as the case of Poly 1 and Poly 2 that have different capacities of MED plant, it is only possible to compare the unit exergy cost for each product, but not the exergy cost rate.

2.3. Results and discussion.

2.3.1. Production and thermoeconomic assessment in base cases.

Figure 2-5a depicts the daily average of monthly productions of electricity, desalinated water, cooling and process heat of the Poly 1 scheme from the solar (considering from the sun and TES, and without backup system). The behavior of the plant shows seasonal variation, presenting lower production during the Chilean winter (June and July) and in summer almost all the energy comes from the sun. In contrast, in February, the productions decreased because there are episodes of persistent cloud cover resulting from moisture by the Altiplanic Winter. Figure 2-5b presents the relative energy consumption from the solar and from the backup system, where the annual solar contribution is 71.6 %. The same tendency is observed in Poly 1 and Poly 2 schemes.

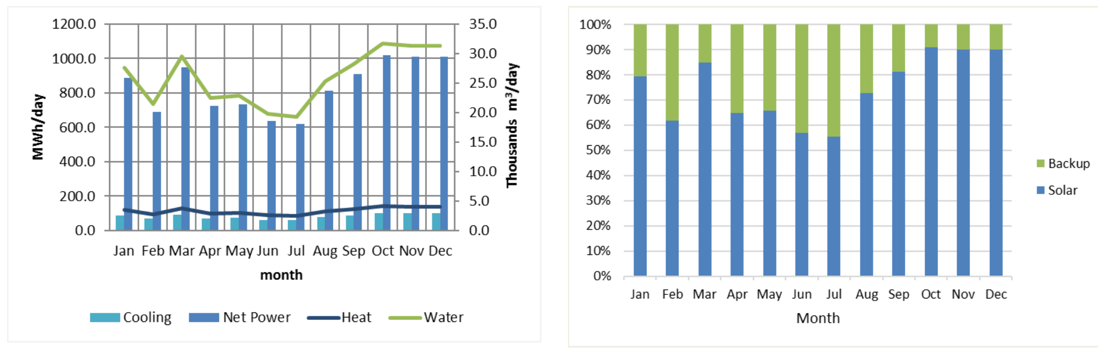

(a) (b)

Figure 2- 5: (a) Monthly productions from the solar. (b) Monthly percentage production from the solar and from the backup.

The annual production of electricity, desalinated water, cooling and process heat, and exergy efficiencies of base cases are presented in Table 2-10. The net power is the electric energy provided by the generator minus the parasitic loads of the plant. Fresh water production in Poly 1 is about 40 % higher than Poly 2, because the power block condenser was replaced by a MED plant in the Poly 1 scheme, and the MED plant was driven by all the heat rejected from the power cycle. Stand-alone MED plant produces the same amount of fresh water as Poly 1 in order to compare them. Regarding exergy efficiencies, they were calculated by equations 2-7 and 2-8 for polygeneration and stand-alone schemes respectively. Poly 2 is more efficient than Poly 1, and polygeneration is more efficient than stand-alone systems. Exergy efficiency provides a measure of how closely the operation of a system approaches the ideal, or theoretical upper limit. Exergy efficiency gives information of process performance because they weigh energy flows according to their exergy contents and they separate inefficiencies into those associated with effluent losses and those due to irreversibilities (Dincer & Rosen, 2012).

Table 2- 10: Annual productions and exergy efficiencies in base cases.

Item	Poly 1	Poly 2	Stand-alone
Gross power, GWh/a	463.1	463.1	463.1
Net power, GWh/a	408.5	415.3	449.8
Fresh water, Mm^3/a	13.2	9.2	13.2
Cooling, GWh/a	42.0	42.0	42.0
Heat, GWh/a	58.9	58.9	58.9
Exergy efficiency, %	27.1	27.6	18.7

Exergy cost rate of products and unit exergy costs of both polygeneration schemes are presented in Table 2-11. It should be mentioned that the unit exergy cost of water associated with the sea water transportation cost was included in this cost and it was calculated considering the $capex_{\text{piping}}$, the $capex_{\text{pumping}}$, the specific electric consumption, the annual water production and the electricity price from the grid for industrial use (P_{elect}). Appendix C and D present the exergy rate and unit exergy cost of each stream in the polygeneration plants and stand-alone systems, respectively.

Table 2- 11: Exergy cost rate of products and unit exergy costs.

Item	Poly 1	Poly 2	Stand-alone
$\dot{C}_{p\_total}$, USD/h	10 507.4	9 769.4	13 630.0
$c_{p\ \text{electricity}}$, USD/(kWh)	0.1058	0.1114	0.122
$c_{p\ \text{water}}$, USD/m^3	2.746	3.008	4.0355
$c_{p\ \text{cooling}}$, USD/(kWh)	0.036	0.038	0.055
$c_{p\ \text{heat}}$, USD/(kWh)	0.024	0.018	0.038

In Poly 1 and Poly 2 configurations, the unit exergy costs are lower than those of the stand-alone systems. Thus, polygeneration schemes are better than stand-alone systems. On the other hand, Poly 1 produces electricity, fresh water and cooling at a lower unit exergy cost than that of Poly 2. Therefore, Poly 1 is the best alternative, considering that the unit exergy cost is calculated from an economic balance, which the total exergy cost rate of products includes the exergy cost rate of fuel, the capital investment cost rates and the operating and maintenance cost rates.

Comparing the costs observed in the Chilean market at the proximities of Crucero, the price of electricity tender is 0.1148 USD/(kWh) (Inodú, 2014) for Cerro Dominador Solar Thermal Plant (CSP plant) in northern Chile. The unit exergy cost of electricity in Poly 1 and Poly 2 are lower than this price of electricity tender. Concerning water, the fresh water price in northern Chile is between 2.1 and 5.6 USD/m^3 (Antofagasta, 2016; COCHILCO, 2015a). The main factors in the price of water is the electricity cost and the delivery point. Moreover, the cooling price is 0.0392 USD/(kWh), considering an electricity price of 0.098 USD/(kWh) (ELECDA, 2016) (Tariffs BT4 and AT4) and a COP for a vapor compression chiller of 2.5. Finally, the process heat price is 0.036 USD/(kWh), considering a natural gas cost of 0.0324 USD/(kWh) (CNE, 2015) and a boiler efficiency of 90 % (NREL, 2013). Hence, according to the Chilean market, solar polygeneration plants are competitive in terms of electricity, fresh water, cooling and heat productions.

Additionally, solar polygeneration plants can increase the economic profit by selling carbon credits (certified emission reductions) according to the clean development mechanism of the Kyoto Protocol, and/or selling credits conforming with the renewable energy quota established by Chilean legislation (Ministerio de economía, 2008). The emission factor of Northern Chile Interconnected System grid is 0.764 tonCO_2eq/(MWh), thus, by electric production it is possible to reduce the emissions by 312 078 tonCO_2eq/a in Poly 1. Considering a carbon price of 0.39 USD/tonCO_2eq (SENDECO2, 2016), carbon credits could represent an income of 0.12 MUSD/a. With regards to the renewable energy quota, the price of renewable energy credits is assumed as 27.4 USD/(MWh), which is the fine for non-compliance of the renewables energy quota, thus, by electric production it is possible to increase the income by 11.19 MUSD/a, which would reduce the unit exergy cost of electricity by 0.2 % and 18.3 %, respectively.

In conformity with thermoeconomic indicators summarized in Table 2-12, the sum $\dot{C}_D$ plus $\dot{Z}$ shows the improvement potential to raise cost effectiveness. Components with a high cost rate ($\dot{C}_D$ plus $\dot{Z}$) and high relative cost difference, such as CSP, are significant for further comparison analysis. Moreover, the exergoeconomic factor is used to identify the major cost source, both capital investment and exergy destruction cost. CSP has a high exergoeconomic factor, the rule says that when the exergoeconomic factor is high, it is suggested to evaluate whether it is cost effective to reduce the capital investment for the component at the expense of the component efficiency (Bejan et al., 1996), in other words, the system performance may be improved by decreasing the investment cost of the CSP plant. Conversely, if the exergoeconomic factor is low, such as MED, cooling and heat plants, it is suggested to evaluate whether the component efficiency (and the investment cost) should be increased, in this case the associated cost of thermodynamic inefficiencies is more significant than the investment costs for the component under consideration. Hence, according to those criterions, the CSP plants may be improved and the other plants are not a priority for improvement. It is recommended to reduce the non-exergy-related cost rate at the expense of its efficiency at the CSP plant. It should be noted that, in general, when a plant is less efficient its investment cost is lower.

Table 2- 12: Thermoeconomic indicators in polygeneration schemes.

Plant	$\dot{C}_{D,k} + \dot{Z}_k$ USD/h		r_k %		f_k %	
	Poly 1	Poly 2	Poly 1	Poly 2	Poly 1	Poly 2
CSP	7 048.2	6 944.4	91.3	91.6	81.6	81.1
MED	4 085.9	3 127.5	94.6	94.8	61.0	62.5
Cooling	163.6	175.8	83.1	83.4	22.4	20.8
Process heat	57.3	11.0	34.5	8.8	6.6	34.2

2.3.2. Sensitivity analysis of investment cost, fuel cost and demand.

Sensitivity analyses of investment cost of TES, solar field (SF), MED plant, refrigeration plant and process heat plant were carried out. Figure 2-6 depicts the effect over total exergy cost rate of products for Poly 1 and Poly 2. The results show that the most significant changes in the total exergy cost rate of products was due to the variation of the investment costs of solar field, TES and MED. The changes are marginal in the case of refrigeration plant and process heat plant, because the investment costs of refrigeration plant and process heat plant were significantly lower with respect to the investment cost of a CSP plant.

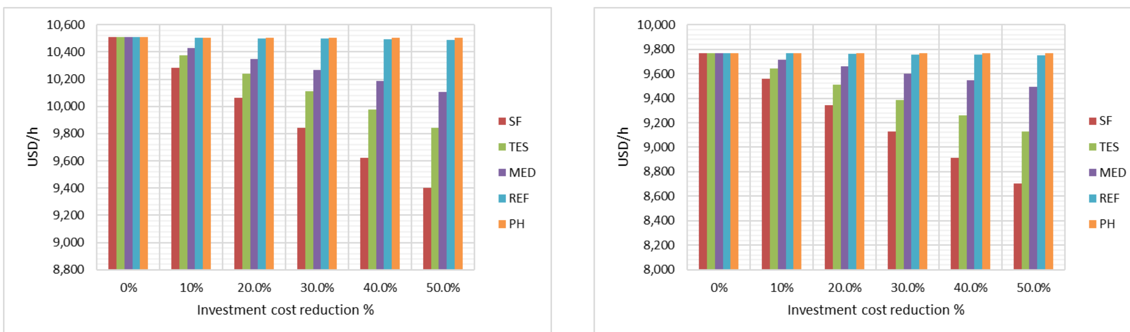

(a) **(b)**

Figure 2- 6: Sensitivity analysis of investment cost. Effect in total exergy cost rate of products. (a) Poly1. (b) Poly 2.

To illustrate the effect of investment cost over unit exergy costs, comparative graphs are presented in Figure 2-7 for Poly 1. The same tendency is observed in both configurations of polygeneration plants. According to the results, variation of investment costs of solar field and TES affects each unit exergy cost of electricity, fresh water, cooling, and heat, respectively. In contrast, variation of investment cost of MED, refrigeration plant and process heat plant affect only the unit exergy cost associated with the product that each one produces; for example, variation of investment cost of MED only influences the unit exergy cost of water, the variation of investment cost of refrigeration plant only influences the unit exergy cost of cooling, and the variation of investment cost of process heat plant only influences the unit exergy cost of heat. This behavior is due to the unit exergy costs in the streams that connect the CSP plant with MED, refrigeration plant and process heat plant have the same value, as indicated in Table 2-5. According to the thermoeconomic, if a process has more than one product, the irreversibilities of the process are distributed proportionally to the exergy of the output flows, and then the unit costs of all products are equal. On the other hand, according to the cost formation process, the unit exergy cost of water, cooling and heat are functions of the unit exergy cost of electricity, their own investment cost and exergy rates. And the unit exergy cost of electricity is function of fuel cost, exergy rates and the investment cost of CSP plant.

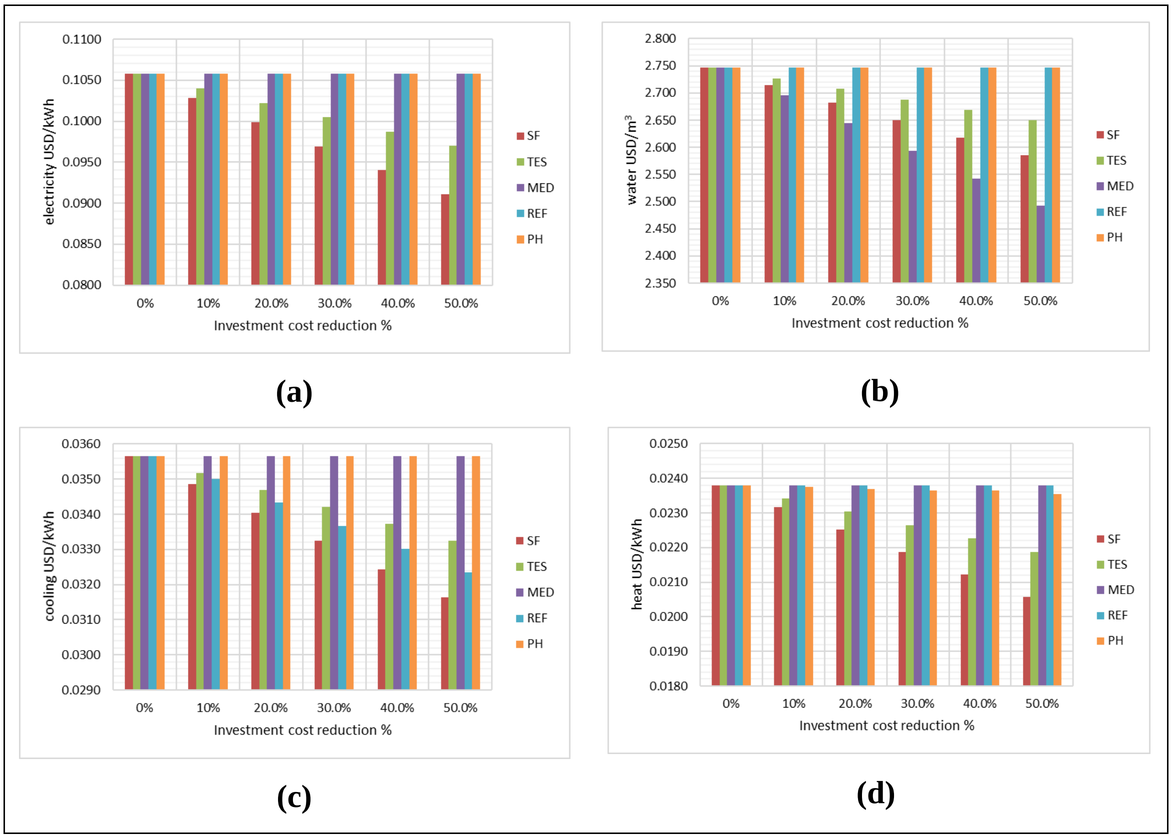

Figure 2- 7: Sensitivity analysis of investment cost in Poly 1. Effect in unit exergy cost of: (a) electricity, (b) water, (c) cooling, (d) heat.

Sensitivity analyses of fossil fuel cost, and demands of cooling, heat and fresh water were also carried out, and are depicted in Figure 2-8. Figure 2-8a shows that variation in the fuel cost impact each unit exergy cost but is more significant in the unit exergy costs of electricity, heat and water. Regarding the demand variations shown in Figures 2-8b to 2-8d, the unit exergy cost of product (cooling, heat or water) is increased as the demand of this product is reduced, because the installed capacity is underused, and the investment cost is charged to a low product production.

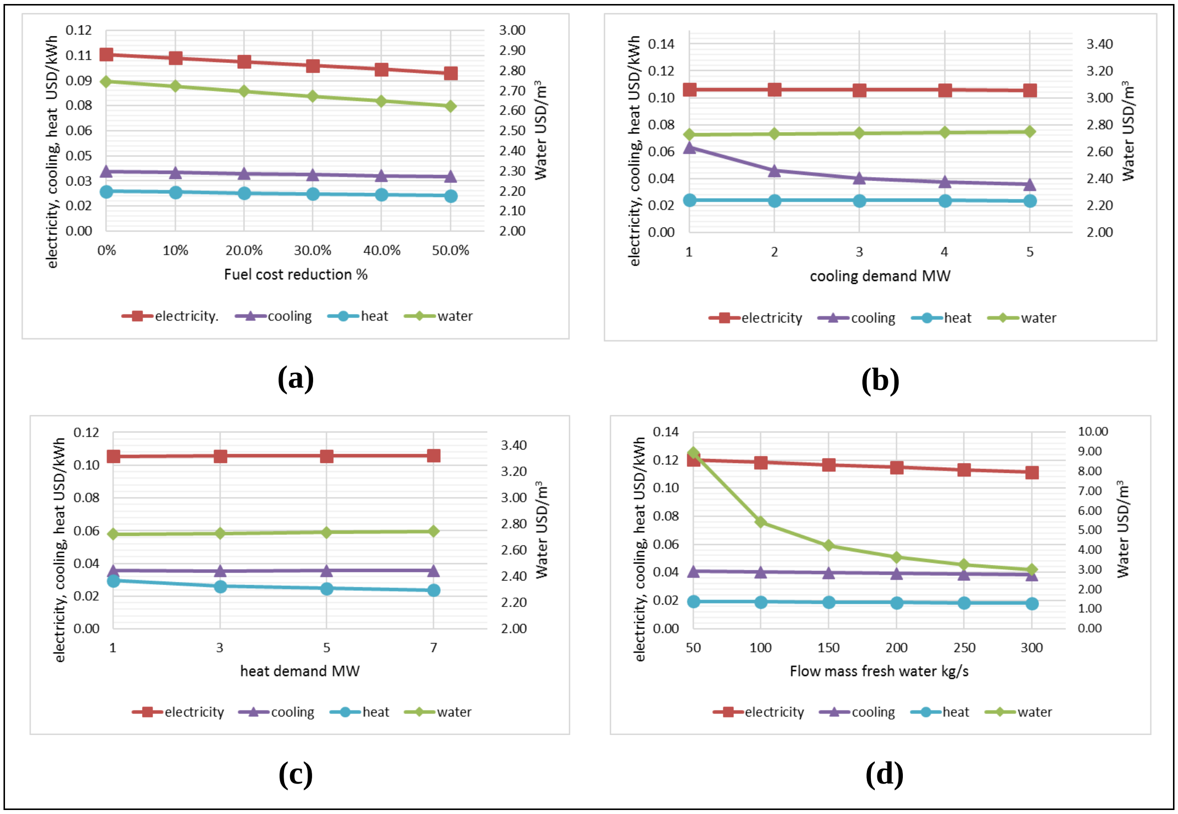

Figure 2- 8: Sensitivity analysis of: (a) fuel cost, (b) cooling demand, (c) heat demand, (d) fresh water demand.

2.3.3. Effects of sizing solar multiple and TES.

An important aspect in the CSP plant is the solar field size (solar multiple) and the amount of thermal energy storage. In this context, Figure 2-9 shows the total exergy cost rate of products as a function of the solar multiple and the storage capacities for Poly 1 and Poly 2 schemes. According to the results, the minimum total exergy cost rate of product is attained with a solar multiple of 1.4 and 1.8, and TES of 3 and 6 hours in Poly 1 and Poly 2, respectively. The values are 10 222 USD/h and 9 523 USD/h, respectively. There is a difference of 2.3 % and 2.1 % between the optimal configuration and base cases for Poly 1 and Poly 2, respectively. However, there is a relatively small difference between other configurations, such as, a plant with a solar multiple of 2.2 and 9 hours of TES, or with a solar multiple of 1.8 and 6 hours of TES. This behavior is due the total exergy cost rate is dominated by the sizing of solar field and TES, hybridization (backup system) levels, and the location of the plant (level of direct normal irradiation). The last point was not sensitized in this study. An optimal solar field area should maximize the time in a year that the field generates enough thermal energy to drive the power cycle at its rated capacity, minimize $capex$ and $opex$, and use TES and backup system efficiently and cost effectively. The problem of choosing an optimal sizing of solar field and TES involves analyzing the trade-off between a larger solar field and TES to maximize the system's output (electricity, water, cooling and process heat) and project revenue, and a smaller solar field and TES that minimizes $capex$ and $opex$.

The optimal point is very sensitive to the investment costs of solar field and TES, as well as to the fossil fuel cost. The decision about the size of solar field (solar multiple), levels of TES and backup system to develop will depend on the additional costs of their expansion, relative to the additional production to dispatch. On the other hand, without backup system, the minimum total exergy cost rate of product is attained with a solar multiple of 2.8 and TES of 15 hours in both polygeneration schemes.

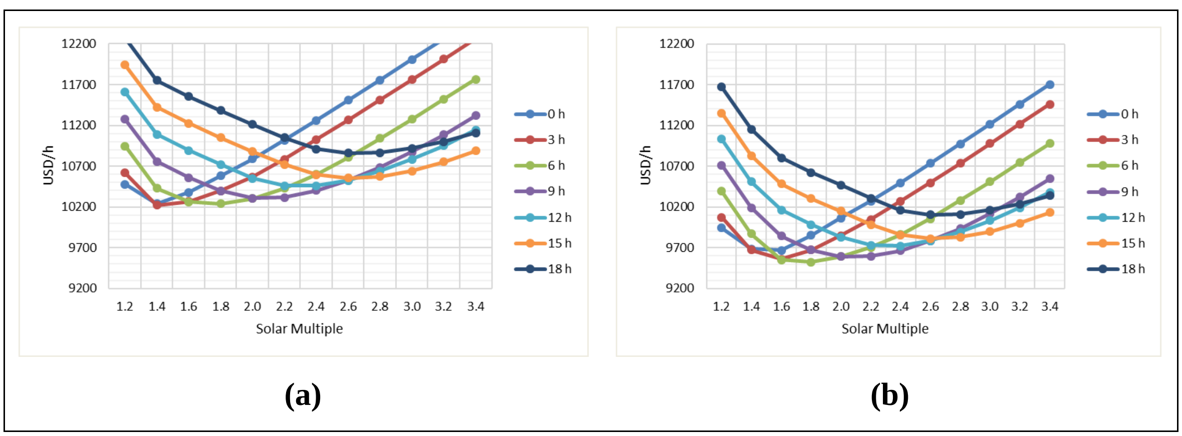

Figure 2- 9: Total exergy cost rate of products as a function of the solar multiple and the hours (h) of TES. (a) Poly 1. (b) Poly 2.

Concerning unit exergy cost, in Figure 2-10 the minimum unit exergy cost is presented for Poly 1: 0.1022 USD/(kWh), 2.705 USD/m^3, 0.035 USD/(kWh) and 0.023 USD/(kWh) for electricity, water, cooling and heat, respectively. The concept of unit exergy cost is analogous to levelized cost, where the main difference is that unit exergy cost is the amount of cost per unit exergy required to produce each product. Unit exergy cost includes exergy costs and non-exergy costs (costs of installing and operating), while the levelized cost is the amount of cost per unit energy required to produce each product. It includes only non-exergy costs (cost of installing and operating).

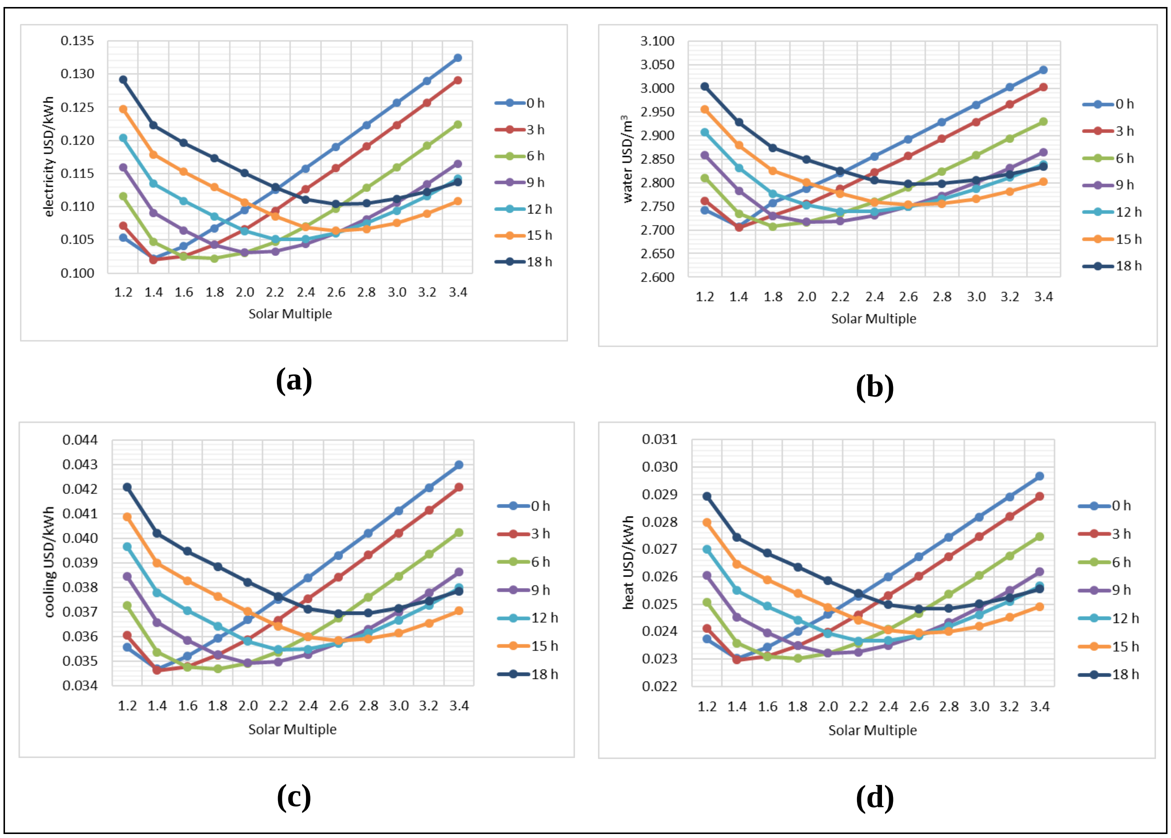

Figure 2- 10: Unit exergy cost for Poly 1 configuration (a) electricity, (b) water, (c) cooling, (d) heat.

In a CSP plant, the criterion for selecting the optimal size of the plant is the minimum LEC (Montes et al., 2009; Wagner & Gilman, 2011). However, in the case of solar polygeneration plants, the criterion should be the minimum total exergy cost rate of products $\dot{C}_p$. As the thermoeconomic method allows to charge the costs according to the type and amount of each utility employed for generating such a product, where the exergy is used for allocating the costs. Additionally, exergy cost rate of products allows to aggregate different kinds of products, such as, electricity, fresh water, cooling and process heat. On the other hand, conventional economic analysis does not provide criteria for apportioning the carrying charges, fuel costs, and *opex* to the various products generated in the same system (Bejan et al., 1996) and it is based only on the first law of thermodynamics, which states the principle of conservation of energy.

2.4. Conclusions

A solar polygeneration scheme is proposed as an alternative for the supply of electricity, fresh water, cooling and heat for a zone with high irradiation conditions, scarcity of water, availability of flat terrain, and a short distance to consumption centers, such as those in northern Chile. For that reason, a thermoeconomic assessment of a solar polygeneration plant using a CSP parabolic trough collector of 50 MW with TES and backup system, a multi-effect distillation MED plant, a single-effect absorption refrigeration plant, and a countercurrent heat exchanger for process heat was carried out. Three configurations were investigated: two polygeneration schemes and one configuration considering only stand-alone systems for comparison purposes.

The results show that, in terms of total exergy cost rate of products, unit exergy cost, and exergy efficiency, the solar polygeneration schemes are more economically attractive than stand-alone systems with high irradiation conditions and proximity to consumption centers. Therefore, a solar polygeneration plant is a cost-effective system making a more efficient use of the available resources.

According to the results, the recommended configuration for a solar polygeneration plant is the one where the MED plant replaced the condenser of the CSP plant, the refrigeration plant is coupled in the sixth turbine extraction, and the process heat plant is coupled between feed water preheaters. This plant was the most cost-effective configuration.

In conformity with North Chilean market, the solar polygeneration plants are competitive. Moreover, solar polygeneration plants can increase the economic profit with the sale of carbon credits according to the Kyoto Protocol and the sale of credits, conforming with the renewable energy quota established by Chilean legislation.

The sensitivity analysis of investment cost show that the investment costs of solar field and TES are more influential on the total exergy cost rate and unit exergy cost of the plant. Therefore, the key areas where cost reductions need to be achieved are the solar field and TES.

The traditional criterion for selecting the optimal size of a CSP plant is the minimum LEC but in the case of solar polygeneration plants, the criterion should be the minimum total exergy cost rate of products $\dot{C}_p$, as the thermoeconomic method uses exergy as a criterion to allocate costs and allows to perform an assessment considering the conversion efficiencies and economic benefits offered by the system.

In future studies, a comparison of the thermoeconomic and the levelized cost methods in a solar polygeneration plant should be conducted to determine and compare the different unit costs of each product, such as, unit exergy costs (electricity, water, cooling and heat) and levelized costs (LEC, LWC, LCC and LHC). As another prospective action, a thermoeconomic assessment with a low aggregation level in CSP plant should be done by individual components, such as turbines, preheaters, solar field, among others, to understand which specific components need improvement.

3. COMPARISON OF THE LEVELIZED COST METHOD WITH THE THERMOECONOMIC METHOD - COST ALLOCATION IN A SOLAR POLYGENERATION PLANT TO PRODUCE POWER, DESALTED WATER, COOLING, AND PROCESS HEAT.

Abstract

The present work shows a comparison between the levelized cost and the thermoeconomic methods in their application to assess the performance of a solar polygeneration plant. The aim is to analyze the costs allocation process, the unit specific costs of each product, as well as the energy and exergy efficiencies, which allows to identify the main advantages of both the evaluated methods. The methodology is applied in a case study configured by a concentrated solar power with thermal energy storage and backup system, combined to a multi-effect distillation plant, an absorption refrigeration plant, and a process heat module. The present study reveals that through the levelized cost method, the cost associated to the electricity generation is higher than it is by applying the thermoeconomic method, whereas the costs of water, cooling and process heat are significantly lower. Those differences represent an increase of about 35.1% in the case of the electricity, and a reduction in the cost associated to the water, cooling, and heat production by around 34.4 %, 78.1 %, and 97.6 %, respectively. Results show that the thermoeconomic method is an equitable and rational cost allocation method which is suitable for a solar polygeneration plant. This method is recommended when a more precise analysis is required to assess the proper costs of different products, and for assessing the benefits of a polygeneration plant, when compared to stand-alone systems. However, the levelized cost method is a simple and fast method, and a deep knowledge of thermodynamics is not required, being recommended when in need to perform a first approach of the costs of each product.

3.1. Introduction

Multi-generation or polygeneration is defined as the concurrent production of two or more energy services and/or manufactured products that, benefiting from the energy integration of the processes, seeking to extract the maximum thermodynamic potential (maximum thermodynamic efficiency) of the resources consumed (Serra et al., 2009). In general, if a multi-generation system generates two products, it is named as a cogeneration system, such as Combined Heating and Power (CHP), Combined Cooling and Power (CCP), and Combined Water and Power (CWP). Correspondingly if a multi-generation system generates three products, it is named as a trigeneration system, such as Combined Cooling, Heating and Power (CCHP). Finally, if a multi-generation system generates more than three products, it is named generically as a polygeneration system; however, to avoid any confusion, the term polygeneration is used in this paper to represent any scheme of a multi-generation system. The basic elements of a polygeneration plant is the prime mover or engine, which provides the mechanical motive power; the electrical power generator, and the heat recovery equipment including cooling, water distillation, and/or other subsystems. The typical prime mover can be a Rankine, a Brayton, a Diesel or a combined cycle.

Polygeneration systems are commonly classified as topping or bottoming cycle systems (Al Moussawi et al., 2016). In a topping cycle, the priority is power production, i.e. the supplied fuel is first used to produce power and then thermal energy. In contrast, in a bottoming cycle, the priority is for heat production, i.e. high temperature thermal energy is the primary product delivered and the heat rejected from the process is recovered to generate power. Polygeneration plants have been extensively employed within the industrial sector, where large concurrent heat and power demands are present (IEA, 2011). A polygeneration scheme has comparative advantages over stand-alone systems, since it allows reducing both primary energy consumption and emissions of greenhouse gasses displacing fossil fuels, avoiding waste heat, reducing transmission and distribution network and other energy losses, as well as decreasing energy dependency at the country level, contributing to the diversification of energy sources (Al Moussawi et al., 2016). According to the International Energy Agency (IEA, 2016) in 2014, the conversion of total primary energy supply to end use energy, in the world, was of 1.7 % and 18.1 % from CHP and electricity plants, respectively.

The average energy efficiency (First-Law of Thermodynamics) of fossil-fuelled power generation is about of 35 % to 37 %, whereas for polygeneration schemes it is around 75 % to 80 %, and up to 90 % in the most efficient plants (IEA, 2011). Thus, about two-thirds of the primary energy input, which is the overall lost in traditional power generation, could be exploited leading to a significant reduction on both energy costs and CO_2 emissions (IEA, 2011). Regarding the use of fuels in polygeneration schemes, fossil resources currently predominate. Renewable energies also have been used as primary energy sources in polygeneration schemes, allowing to generate electricity by delivering an input of thermal energy. In that context, biomass, geothermal and concentrated solar technologies have been implemented in polygeneration schemes (Modi et al., 2017).

To integrate and properly assess a polygeneration plant, in which two or more goods are produced from one or more natural resources, it is necessary to determine the production cost of each product. Due to the complexity of dealing with many energy flows in polygeneration schemes, the integration and assessment of such technologies should be evaluated applying a rational method. A method for the allocation of resources and products allows solving this problem, considering all input and output from the system, investments, operation and maintenance costs, as well as the production units of each product. To solve this problem, several cost allocation methods have been proposed in the literature, which in general are classified in thermodynamic, economic, and thermoeconomic methods (or exergoeconomic). The thermodynamic methods are based on the First-Law and/or Second-Law of Thermodynamics and include several methodologies, such as the energy balance, work flow, kW equivalence, enthalpy drop, heat discount, weighting, entropy change, and exergy methods (Beretta et al., 2014; Gochenour, 2003; Tereshchenko & Nord, 2015; Ye & Li, 2013). The economic methods are similar to thermodynamic ones depending on whether lowering power or heat costs are in priority (Gochenour, 2003; Nuorkivi, 2010). Among the available methods that exist are the proportional method, the equal distribution method, and the benefit distribution method. Finally, the thermoeconomic methods are based on the Second-Law of Thermodynamics and economic principles, which include algebraic and calculus methods (Abusoglu & Kanoglu, 2009; Bejan et al., 1996; Serra et al., 2009). The algebraic methods use algebraic balance equations and auxiliary cost equations for each component, focus mainly on the cost formation process and determine average costs. The calculus method use differential equations, such that the system cost flows are obtained in conjunction with optimization procedures based on the method of Lagrange multipliers, and it is used to determine marginal costs (Baghernejad & Yaghoubi, 2011).

3.1.1. Solar polygeneration plant

The use of the solar energy as main resource in a polygeneration system for producing energy and water is an opportunity for sustainable development. Solar energy can be captured and concentrated by Concentrated Solar Power (CSP) technologies to provide the heat required to generate electricity through a power cycle. Hence, a CSP plant could be the prime mover in a polygeneration scheme, operating as a topping cycle system. The other technologies could be integrated to generate by-products, such as desalted water, cooling and process heat. CSP is one of the promising options for electricity supply as demonstrated in some areas such as, Spain, USA, and North Africa (IRENA, 2015). To be economically attractive, CSP plants require abundant direct normal irradiation to produce electricity. This restriction limits the geographical regions in which CSP should be installed. Therefore, these areas are in general hot and dry regions. Moreover, the development of CSP plants requires availability of flat land and proximity to consumption centers. CSP can integrate thermal energy storage (TES) to increase the capacity factor and to provide dispatchable electricity to the grid and could capture peak market prices. Additionally, CSP can be hybridized with a backup energy system (BS), which supplies thermal energy to maintain the plant's power generation at design conditions when there is a lack of solar radiation and/or thermal energy from TES.

The current CSP market is dominated by parabolic trough collector technologies, comprising around 85% of the cumulative installed capacity (IRENA, 2015). CSP is considered a promising multi-purpose technology for electricity, heat and district cooling production, and water desalination (Modi et al., 2017), as it is easily integrated to thermal driven cycles that can produce fresh water, refrigeration and process heat. Within the industrial thermal desalination technologies, multi-effect distillation (MED) is considered the most attractive option due to its lower energy consumption (compared to the rest of the thermal technologies as multi-stage flash and solar stills), low sensitivity to corrosion, low presence of scaling, high development potential, and the possibility of operating at temperatures lower than 100 ºC (Al-Karaghouli & Kazmerski, 2013). In the line of refrigeration systems driven by thermal energy, the single-effect absorption cycle is driven at low temperatures, between 80 and 110 ºC (Sarbu & Sebarchievici, 2015), and is available in the market, making it a good alternative to be considered in a polygeneration scheme. Each technology can be integrated into the CSP plant taking into account its technical restrictions and the demand of each product. The size of the plants has been established to satisfy a large-scale supply from the mining industry (northern Chile, Australia, and North Africa), which operates continuously and presents a constant demand. The CSP plant has been chosen considering the already existing commercial plant, called Andasol 1, due to the technical data of this plant is available in different technical reports. The electric power is produced in the CSP plant and the heat rejected from the power production is then used to produce the other products (desalted water, cooling and process heat), whose production is limited by the availability of the heat rejected from the CSP plant. This also limits the size of the desalination, cooling, and process heat plants.

For the aforementioned, a solar polygeneration system is configured and simulated to produce electricity, desalted water, industrial cooling and process heat. The solar polygeneration plant proposed herein consists of a concentrated solar power parabolic trough collector field with TES and BS as prime mover, integrated to a MED plant, a single-effect absorption refrigeration system, and a counter-current heat exchanger as process heat plant. This solar polygeneration scheme was previously analyzed by Leiva-Illanes et al. (2017), in which a thermoeconomic assessment was performed considering that the plant operates in high direct normal irradiation conditions. The present work constitutes the continuation of that research, where its main contribution is a comparison between the levelized cost and the thermoeconomic methods applied to a solar polygeneration plant. The aim of that evaluation is to determine and compare the different unit costs of each product obtained by each method, such as levelized costs and unit exergy costs (electricity, water, cooling and heat); the cost allocation process; and the energy and exergy efficiencies.

3.1.2. Assessment of a solar polygeneration plant

Concentrated Solar Power plants as the prime mover could be easily integrated into polygeneration systems, as demonstrated elsewhere (Fernández-García et al., 2010; Modi et al., 2017). Due to the potential of such systems, the integration of a CSP plant and desalination, refrigeration and process heat technologies has been analysed in several studies as described below, focusing mainly in cogeneration and trigeneration schemes.

Nonetheless, currently there is only one CSP plant configured in a polygeneration system, the "Aalborg CSP-Brønderslev CSP with organic Rankine cycle project" (NREL, 2017) located in Denmark, a solar cogeneration plant for generating heat and power of 16.6 MW.

Two assessment methodologies have been intensively employed for analyzing solar polygeneration plants: the levelized cost method (Short et al., 1995) and the thermoeconomic method (Bejan et al., 1996). Both methodologies allow estimating separately the costs of each product generated by the system. The first method determines the present value of the total cost of investment, maintenance and operation, fuels, and revenues from the sales of by-products (such as carbon credits) of a productive plant over its economic life, considering equivalent annualized payments (IEA-NEA, 2015), levelized in monetary units per unit of annual production. The levelized cost (LC) allows alternative technologies to be compared considering different scales of operation or different investment and operating periods. In this context, several studies have focused on assessment of CSP-polygeneration systems using the levelized cost method. Olwig et al. (2012) carried out a techno-economic analysis of integrated CSP and desalination plants, including MED and reverse osmosis (RO) systems. The authors determined the levelized water cost (LWC), considering a cash flow that includes the total investment costs (CSP and desalination plants), the fuel for backup, the maintenance and operation cost associated to desalination, while the annual revenues due to electricity sales were subtracted from the costs. Later, Moser et al. (2014) developed a techno-economic model for the assessment of desalination plants, driven by renewable energies, based on CSP plant, MED and RO technologies. The model considers a detailed method for cost allocation to determine the LWC and levelized electricity cost (LEC), considering capital and operational costs. The operational cost includes fixed and variable operating costs, where the last one was determined using the reference-cycle method, in which the evaluation of heat cost is approached based on the comparison of steam turbine performances in two cases (MED case and reference case). The reference cycle is defined as a power block with standard cooling such as once-through or evaporative tower. Heat cost is defined as the cost needed to compensate the missing income that would be generated in the reference case, that constitutes the consistency in the allocation method employed.

Fylaktos et al. (2014) carried out an economic analysis of an electricity and desalinated water cogeneration plant in Cyprus. Three different CSP schemes were examined: a stand-alone

CSP plant, CSP-RO, and CSP-MED. They calculated the LEC for the whole plant using the kWh-equivalent method that consist in converting the revenues from water and from selling CO_2 allowances into equivalent electricity production units (kWh). Through this approach the plant is considered as an electricity-only system, and all the production is added and expressed in terms of the LEC. The estimation of the levelized cost was based on the substitution method, consisting in separate the LEC and LWC. In this context, for determining separately the LWC, it assumed that the difference of possible revenue streams between a stand-alone CSP plant and the cogeneration plant has occurred because of the integration of the desalination subsystem. Recently, Palenzuela et al (2015) carried out a techno-economic analysis of different CSP-MED systems and compared them with a CSP-RO configuration, based on the assessment of the LEC and LWC. LEC contemplates the total investment cost of the CSP plant, the annual operation and maintenance costs, the annual fuel cost due the backup system, and the annual net electricity delivered to the grid. While LWC considers the investment, operation and maintenance cost, and the fresh water production. The steam energy cost and the electricity consumption by the MED were considered as internal costs, therefore neglected. In other recently study, Mata-Torres et al. (2017) carried out an investigation on solar polygeneration for electricity production and desalination, considering two configurations of CSP-MED plants in two potential locations. Their economic analysis was based on LEC and LWC, where the annual fuel cost was only assigned to the LEC, since water is extracted as an additional product from the CSP plant and does not represent an additional fuel cost. At the same time, the electric and steam costs of the MED plant were considered as internal costs of the plant.

The main feature of the thermoeconomic method is that it proposes a cost balance equation applying the unit exergy cost to the exergy balance equation according to specific principles and rules (Abusoglu & Kanoglu, 2009) and, at the same time, it allows to understand the cost formation process and the flow of costs in the system. Only a few studies have focused on thermoeconomic evaluation of CSP-polygeneration plants. In this context, Al-Sulaiman et al. (2013a, 2013b) carried out an thermoeconomic optimization of three trigeneration systems using organic Rankine cycle for power, cooling and heating production. One of those trigeneration systems is a solar-trigeneration system, which consist of a CSP plant (including a parabolic trough collector field, TES, and an Organic Rankine Cycle as power block), and the heat recovery system composed of a steam generator and a single-effect absorption chiller. They used the specific exergy costing (SPECO) method as the thermoeconomic approach. This method is based on the notion that exergy is the only rational basis for assigning costs to the interactions that a thermal system experiences with its surroundings and to the sources of inefficiencies (Bejan et al., 1996). Along the same lines, Calise et al. (2016) carried out an exergy and exergoeconomic analysis of a novel hybrid solar geothermal polygeneration system that produces energy and water, based on a hybrid system equipped with an organic Rankine cycle driven by a parabolic trough collector solar field and a geothermal well, a multi-effect distillation unit, and an absorption chiller. They applied an accounting of exergoeconomic costs to establish a monetary value to all material and energy flows, providing a reasonable basis for cost allocation. Recently, Ortega et al. (2016) carried out a thermoeconomic comparison of the joint production of electricity and fresh water in a parabolic trough CSP plant, MED and RO units. The authors applied the largely used thermoeconomic method developed by Bejan et al. (1996). The thermoeconomic methodology was selected to assess the actual cost of the steam consumption of the distillation process, which allows assessing the cost of production for each asset and the services used to generate them so that these costs can be properly charged. Finally, in a recent publication by Leiva-Illanes et al. (2017) carried out a thermoeconomic assessment of the joint production of electricity, fresh-water, cooling and heat from a solar polygeneration plants. Three configurations were investigated, two CSP-polygeneration schemes and one considering stand-alone systems. The authors applied the same thermoeconomic method developed by Bejan et al. (1996) and evaluated the plants in terms of the total exergy cost rate of products and unit exergy costs. This method allowed to determine the cost of each product using cost allocation rules, allocating the resources consumed to the useful product of each component, and distributing its costs proportionally to the exergy flow. The present work constitutes the continuation of this research were a comparison between the unit exergy cost and the levelized cost is deeply analyzed.

As described above, different studies have been focused on assessment of CSP-polygeneration systems by the levelized cost method (Short et al., 1995) and other by the thermoeconomic method (Bejan et al., 1996); however, the results from each method are unlike and produce significant differences. Hence, the present work aims to deliver insights about which method is more appropriate for assessing a solar polygeneration plant. For that reason, it is proposed an analysis in a CSP-polygeneration plant, in which the levelized cost and the thermoeconomic methods are applied, allowing to compare the costs allocation method used, the unit specific costs of each product, and the efficiencies according to the First-Law and Second-Law of Thermodynamics. Therefore, the main advantages of each method are determined in terms of the complexity of calculations, rules and rationality of cost allocation, and the applicability to compare between stand-alone systems and polygeneration plants. The results give relevant information for decision-makers to evaluate CSP-polygeneration systems and could constitute a guide to understand these methods.

3.2. Methodology

The methodology considers modelling stand-alone plants, and the integration of those plants in a solar polygeneration scheme. The solar polygeneration plant is modelled using a computational simulation platform, allowing the application of both evaluation methods: the levelized cost (Short et al., 1995) and the thermoeconomic method (Bejan et al., 1996). The solar polygeneration plant is configured as a topping cycle, in which the priority is the production of electricity, and the by-products are generated according to the availability of thermal energy in the power cycle.

The software IPSEpro (SimTech GmbH, 2011) was employed for modelling and simulating the solar polygeneration and stand-alone plants, without TES/backup-system. Three modules of IPSEpro were employed: IPSEpro-MDK, IPSEpro-PSE, and IPSEpro-PSXLink. IPSEpro-MDK is a model development kit that offers all the capabilities required to define and build new component models and to translate them into a form that can be used by IPSEpro-PSE. IPSEpro-PSE is a process simulation environment that allows establishing mass and energy balances, simulating different kinds of processes, through iterative Newton-Raphson method. IPSEpro-PSE provides only steady state solutions, so in order to assess the transient behavior of the system, IPSEpro-PSE is linked to Microsoft Excel through the IPSEpro-PSXLink tool. Using this module the input data, such as direct normal irradiance (Escobar et al., 2014), the collector optical efficiency of solar field (NREL, 2013; Wagner & Gilman, 2011), and the demand for products, are modified for each time-step. The polygeneration plant is simulated considering an hourly resolution meteorological database

(Escobar et al., 2014). The partial results are the solar field thermal input/output, and the production level of the solar field. Afterward, the simulation of the TES and backup system behavior was implemented using the MATLAB software. Hence, the total production of each product is the sum of the production from the solar field, the TES, and the backup system. This approach allows to simulate the polygeneration plant over a one-year period using an hourly time step, and to apply the levelized cost and the thermoeconomic method on an annual basis. Appendix E provides a flowchart of the overall simulation.

The polygeneration plant is evaluated disregarding the variations of kinetic energy, potential energy, and pressure drops in the lines, and considering the environmental conditions of the Atacama Desert in northern Chile. The Atacama Desert has one of the highest solar resources in the world; this region has flat and unused terrains, and it is close to consumption centres, such as mining facilities, which have large energy and water demands. In particular, the simulation considered the meteorological conditions of the vicinity of the Crucero substation (22.14 °S, 69.3 °W, 1 146 meters above sea level), considered as one of the most relevant places for CSP development in Chile, due to the 3 389 kWh/(m^2 a) of annual direct normal solar irradiation (Escobar et al., 2014).

3.2.1. Design parameters

A CSP plant is based on a number of sub-systems, such as solar thermal loop (composed of the solar field, thermal energy storage, and backup system), and a power block. Figure 3-1 shows the CSP plant, which is configured considering the configuration of Andasol-1 power plant (NREL, 2013; Wagner & Gilman, 2011), located in southern Spain. The solar field (SF) consists of EuroTrough collectors aligned in a north-south orientation, Schott PTR-70 absorber tubes, and synthetic oil type Dowtherm A as heat transfer fluid. The design temperature of the SF considers 393 ºC and 293 ºC as the outlet and inlet values, correspondingly. The collectors track the sun from east to west during the day. The design point was considered as the 21st December at solar noon for Crucero (in the southern hemisphere), where the direct normal irradiance is 1 010 W/m^2 and the collector optical efficiency is 72 % (NREL, 2013). The solar multiple (SM) is a measure of the solar field aperture area as a function of the power block's nameplate capacity. This parameter is very important because allows sizing the SF and it is expressed as:

$$\mathrm{SM} = \frac{\dot{\mathrm{Q}}_{\mathrm{th,solar\ field}}}{\dot{\mathrm{Q}}_{\mathrm{th,power\ block}}} \tag{3.1}$$

where $\dot{\mathrm{Q}}_{\mathrm{th,solar\ field}}$ is the thermal energy delivered by the solar field at the design point and $\dot{\mathrm{Q}}_{\mathrm{th,power\ block}}$ is the thermal energy required by the power block at nominal conditions. The solar multiple (SM) is assumed as 2.56, according to the design point of Andasol-1. That SF represents an area of 510 120 m^2 (NREL, 2013). This is the aperture area that collects solar insolation, and it does not include any reduction due to angle of incidence effects, shadowing or end losses.

The TES is assumed as a two-tank indirect system using molten salts as storage media. It presents 95 % of annual storage efficiency (Houda et al., 2009), and the design temperature is 386 ºC and 292 ºC for the hot and cold tanks, respectively. TES_{th} is the equivalent thermal capacity of the storage tanks and is defined as:

$$\mathrm{TES_{th}} = \frac{\dot{\mathrm{W}}_{\mathrm{des.gross}}}{\eta_{\mathrm{des}}} \cdot \mathrm{t}_{\mathrm{full\ load}} \tag{3.2}$$

where, $\dot{W}_{des.gross}$ is the gross power, η_{des} is the efficiency of Rankine cycle at design point, and $t_{full\ load}$ is the number of hours of thermal energy delivered at the power block's design thermal input level, being assumed as 12 h. $t_{full\ load}$ is a key parameter since it allows sizing the TES, i.e. determines the system's maximum storage capacity.

A natural gas heater is considered as a backup system, supplying thermal energy directly to the heat transfer fluid used in the SF. The capacity factor is assumed as 96 %, as suggested by Palenzuela et al. (2015), considering that the solar polygeneration plant does not have restriction on the consumption of fossil fuel.

The power block consists of a regenerative Rankine cycle with reheat and six extractions, as described in Blanco-Marigorta et al. (2011). The gross power production is 55.0 MW_e, the high-pressure turbine inlet pressure is 100.0 bar and the low-pressure turbine backpressure is 0.06 bar. The high and low-pressure turbines present isentropic efficiencies of 85.2 % and 85.0 %, respectively. The generator efficiency is 98.0 %, and the pumps isentropic efficiency is 70.0 %.

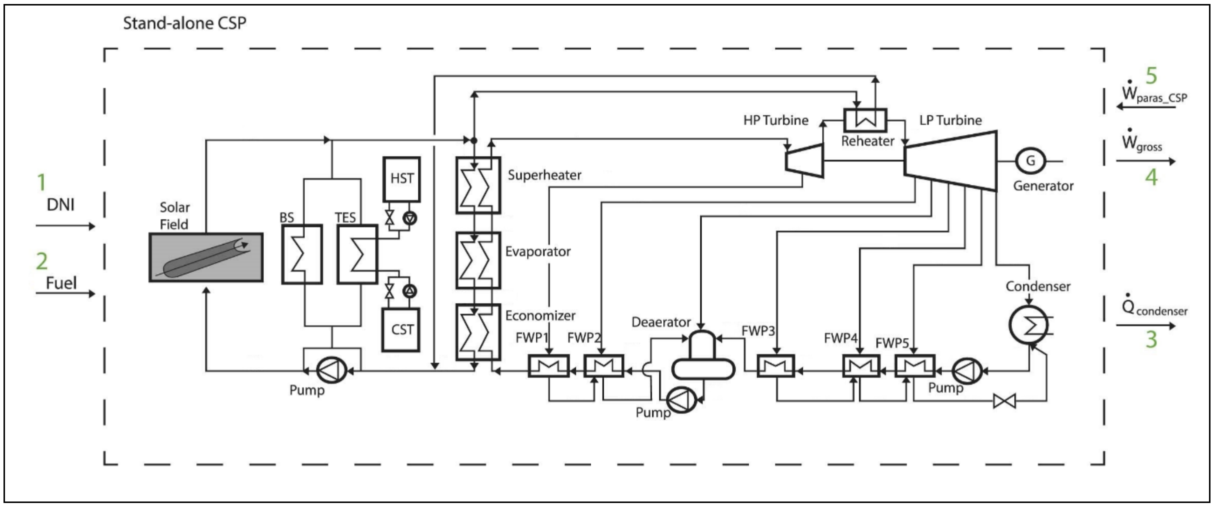

Figure 3- 1: Stand-alone CSP plant. DNI: direct normal irradiance, CST: cold storage tank, FWP: feed water preheater, G: generator, HP: high pressure, HST: hot storage tank, LP: low pressure.

Figure 3-2 shows the MED desalination plant, which considers 12 parallel-cross feed effects and 11 feed preheaters, as described by Zak et al. (2012). The feed seawater intake temperature is 25 °C and its salinity is 0.042 kg/kg, the feed seawater temperature after down condenser is 35 °C whereas the maximum salinity in each effect is 0.072 kg/kg. The top brine temperature is 65 °C, the fresh water production is 37 168 m^3/day, and the Gained Output Ratio (GOR) is 9.1, which is defined as the amount of distillate produced per unit mass of the input thermal energy (steam from CSP plant). The concentration factor is 1.7, while the specific heat consumption is 245.2 kJ/kg, and the specific electricity consumption is 1.5 and 5 kWh/m^3 at the MED and the seawater pumping system (COCHILCO, 2015a), respectively.

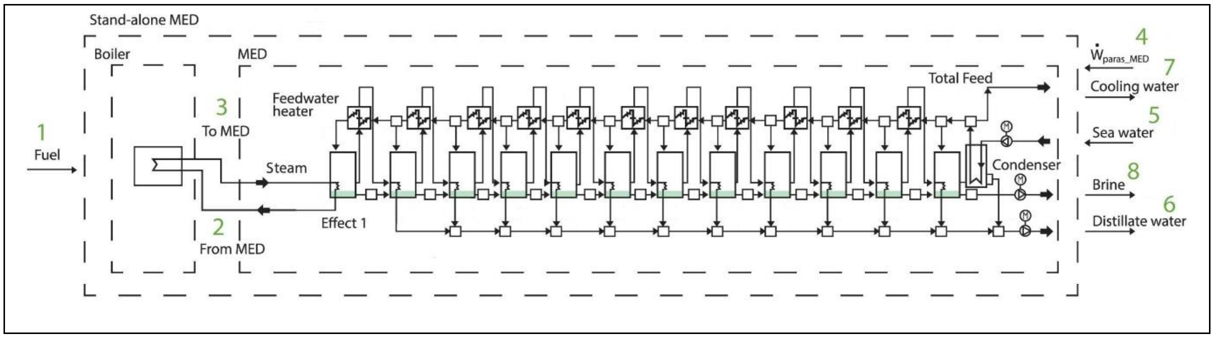

Figure 3- 2: MED plant.

Figure 3-3 shows the refrigeration plant (REF), that is configured with a single-effect LiBr-H_2O absorption chiller, as described in Herold et al. (1996). It has a cooling capacity of 5 MW_{th} (1 421.73 tons) and a nominal coefficient of performance of 0.7. The chilled water inlet temperature is 10 °C and is discharged at 6 °C. The nominal cooling water temperature inlet and outlet are 25 °C and 35 °C, respectively. Moreover, the desorber inlet temperature is 108.49 °C.

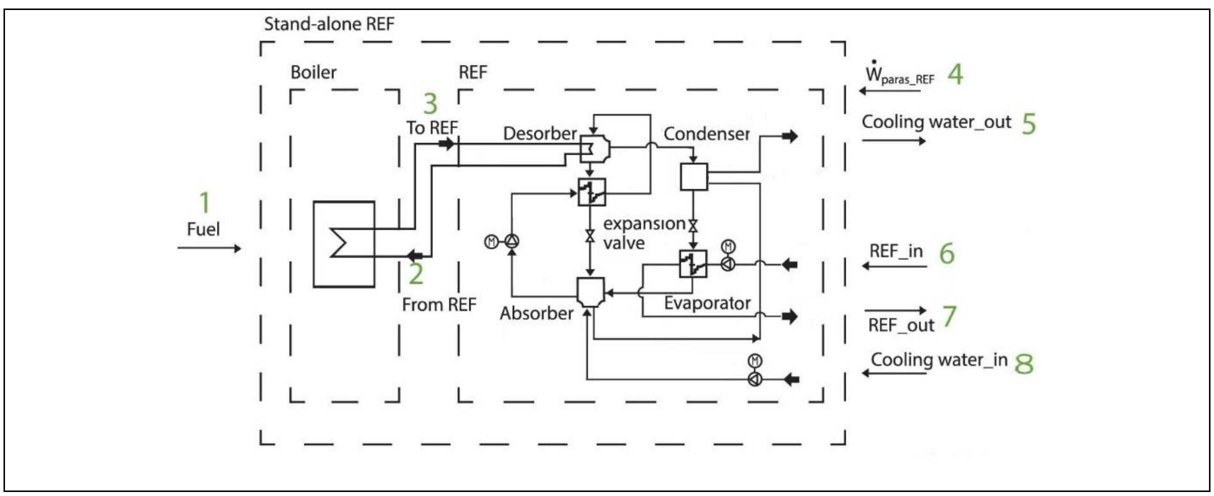

Figure 3- 3: Refrigeration plant.

Figure 3-4 shows the process heat (PH) plant, configured by a counter-current heat exchanger, which delivers process heat at nominal thermal load of 7 MW_{th}. The heat exchanger inlet and outlet temperatures are 63 °C and 90 °C, respectively.

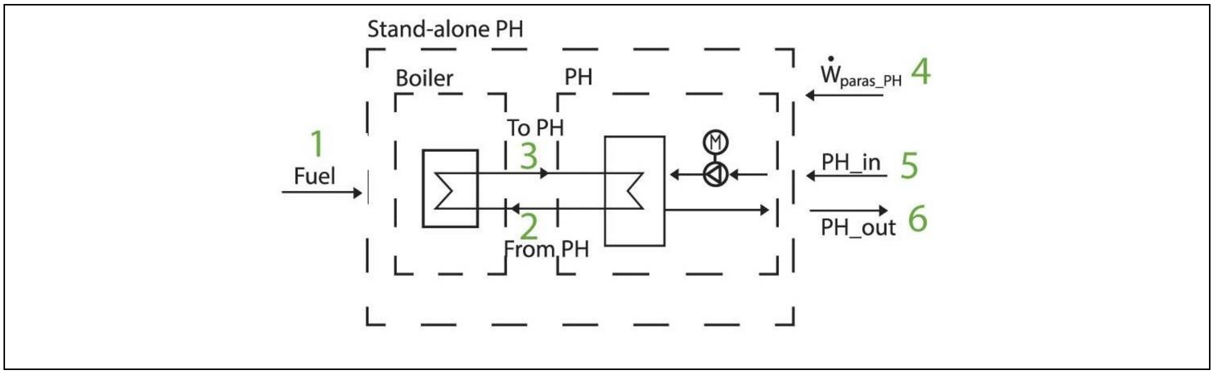

Figure 3- 4: Process heat plant.

The solar polygeneration scheme considers the integration of the desalination, refrigeration, and process heat plants, into the CSP plant, where this last one is the prime mover. Figure 3-5 shows the configuration of the CSP polygeneration plant, in which the MED plant replaces the condenser of the power cycle, the REF plant is coupled to the sixth turbine extraction, and the PH plant is coupled between feed water preheaters (FWP3 and FWP4). The coupling point of each plant was selected considering the operating temperatures constraints of each technology, aiming to cause the minimum performance penalty on the SF aperture area for the same power production. Those constraints produce changes at the design point parameters of the CSP plant. For this reason, the low-pressure turbine back-pressure is modified to 0.37 bar, since the MED plant must operate within a temperature range of 64 to 74 °C (Al-Karaghouli & Kazmerski, 2013), and the sixth extraction pressure is modified to 1.17 bar, considering the operating constraints of the refrigeration plant, which must operate within a temperature range of 80 to 110 °C (Sarbu & Sebarchievici, 2015). Additionally, to develop the same gross power of the stand-alone CSP plant, the aperture area of the SF was modified to 616 650 m^2, i.e. a 20.9 % larger than a stand-alone CSP plant.

In this CSP-polygeneration configuration is not possible to regulate the production of desalted water because the MED plant is driven by the heat rejected from the power cycle. Hence, the production of desalted water is linked to the production of electricity; if the electricity production decreases then the production of desalted water decreases too and vice-versa. The desalted water production depends on the mass flow rate of the exhaust steam from the outlet of the low-pressure turbine. Unfortunately, any problem, as a failure event or maintenance stop in the MED plant or in the CSP plant, will affect both productions, since the MED plant replaces the condenser of the power cycle. The presence of the MED plant allows closing the thermodynamic cycle through the condensation of the exhaust steam from the turbine for reuse in the cycle, then any problem in the MED plant consequently represents a problem in the condenser of the power cycle. On the other hand, the production from REF plant and PH plant can be regulated according to the demand. The output of cooling and process heat depends on the operating parameters of the rest of the plant. When process heat and cooling production are jointly or individually reduced, the power cycle needs less input thermal energy to generate electricity at the nominal rate. Thus, the control system could either reduce the energy input to the power cycle by partial defocusing solar collectors or reduce the thermal energy output from TES and/or backup system.

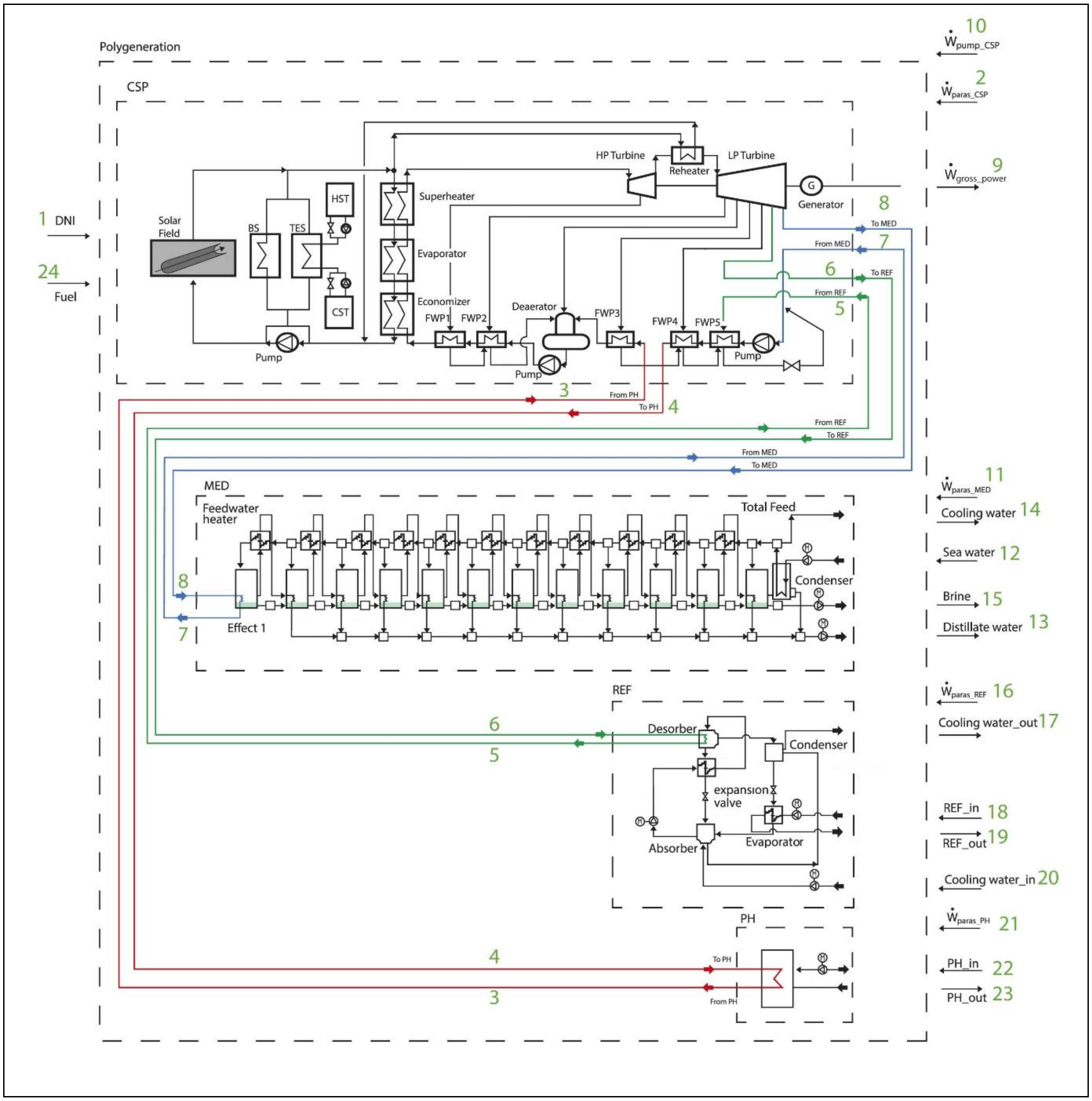

Figure 3- 5: CSP polygeneration plant.

For validating the polygeneration plant it was necessary to validate each stand-alone system, because currently there is no solar polygeneration plant of these characteristics. Therefore, the polygeneration plant model is the combination of the validated model for each stand-alone system. The power cycle was validated at the design point using the nominal data of Andasol-1 reported by Blanco-Marigorta et al. (2011). Furthermore, the CSP plant was validated by comparing the results between the IPSEpro/Matlab model and the case study

(Andasol-1) of SAM software (NREL, 2013). The results indicate differences of 3.6 % in terms of annual net electricity, and 1.5 % regarding the thermal efficiency. Regarding the MED plant, it was validated considering the data reported by Zak et al. (2012) and from El-Dessouky et al. (2002). The results show no differences in the total distillate water production, 5.46 % error in terms of specific heat transfer area, and 7.81 % regarding the GOR, that are considered as having good accuracy, as stated in Palenzuela et al. (2014). Finally, the thermodynamic model of the REF plant was validated using the data reported by Herold et al. (1996). The results show differences lower than 2.6 % in terms of the cooling capacity and COP.

A constant demand for electricity, water, cooling and process heat was assumed to meet the demand profile in the mining industry, which requires continuous operation and energy supply. Therefore, the power cycle, the desalination, the refrigeration, and the process heat units operate at full-load condition. The thermal energy storage and backup system allow to operate in periods of low solar radiation, delivering full-load steady state generation, even on cloudy days or during the night, assuring predictable dispatchability. The transient state conditions affect the solar field, the thermal energy storage, and the backup system. Those subsystems can operate at part-load conditions although the solar thermal loop provides thermal power at rated condition. In this study, the part-load condition of the solar thermal loop was simulated considering a variable efficiency of solar field, in terms of the direct normal irradiance, aperture area, optical efficiency, and the incidence angle (Leiva-Illanes et al., 2017). Finally, start-up and shut-down procedures were not evaluated.

3.2.2. Economics considerations

The main economic considerations for the CSP plant are summarized in Table 3-1.

Table 3- 1: Specific cost for the CSP plant.

Cost	Value	Unit	Reference
Direct Capital Cost			
Site Improvements	28	USD/m^2	(NREL, 2013)
Solar Field	200	USD/m^2	(IRENA, 2015)
Heat transfer fluid system	78	USD/m^2	(NREL, 2013)
Storage	35	USD/kWh_{th}	(Palenzuela et al., 2015)
Fossil Backup	60	USD/kW_e	(NREL, 2013)
Power Plant	850	USD/kW_e	(NREL, 2013)
Balance of plant	105	USD/kW_e	(NREL, 2013)
Contingency	7	%	(NREL, 2013)
EPC and Owner Cost	11	% of total direct capital cost	(NREL, 2013)
Total Land Costs	2	% of total direct capital cost	(NREL, 2013)
Sales of Tax applies of Direct Cost	4	% of total direct capital cost	(NREL, 2013)
Operational and Maintenance Costs			
Fixed Cost by Capacity	66	USD/(kW a)	(NREL, 2013)
Variable Cost by Generation	3	USD/MWh	(NREL, 2013)
Fossil Fuel Cost	0.0324	USD/kWh	(CNE, 2015)

The main economic considerations for the other plants are listed in Table 3-2. In the case of MED plant, it includes the costs associated to the transportation of sea water to the plant location.

Table 3- 2: Specific cost for a MED plant, refrigeration plant, process heat plant and boiler.

Cost	Value	Unit	Reference
MED plant			
Direct Capital Cost MED			
Infrastructure and construction	1 500	USD/(m^3 day)	(Mata-Torres et al., 2017)
Contingencies (%)	10	%	(Mata-Torres et al., 2017)
Total	1 650	USD/(m^3 day)	
Operational and Maintenance costs MED			
Chemical	0.025	USD/(m^3 a)	(Mata-Torres et al., 2017)
Maintenance	0.1	USD/(m^3 a)	(Mata-Torres et al., 2017)
Labor	2	% annualized total direct capital cost	(Mata-Torres et al., 2017)
Sea Water Transportation			
$capex$ of piping	736	USD/m	(COCHILCO, 2015a)
$capex$ of pumping	3.75	MUSD	(COCHILCO, 2015a)
Specific electricity consumption (pumping)	5	kWh/m^3	(COCHILCO, 2015a)
Distance from the coast to the plant location	70	km	
Location altitude	1 146	meters above sea level	
Refrigeration plant			
Direct and Indirect Capital Cost	548.0	USD/kW_{th}	(Noro & Lazzarin, 2014)
Operational and Maintenance Cost	2	%	
Process heat plant			
Direct and Indirect Capital Cost	583.3	USD/kW_{th}	(Turton et al., 2012)
Operational and Maintenance Cost	2	%	
Boiler			
Direct and Indirect Capital Cost	76.8	USD/kW_{th}	(Turton et al., 2012)
Operational and Maintenance costs	2	%	

In the economic evaluation a horizon of 25 years and a discount rate of 10%. have been considered.

3.2.3. Energy and exergy evaluation

To evaluate the cost allocation in the stand-alone and polygeneration plants, it was defined an adequate aggregation level, which allows delimiting the boundaries of the system. Figures 3-1 to 3-5 show the boundaries of each system, with dashed lines, in which the fuels and products of each subsystem are established. The fuels are defined as the resources expended to generate the product; it could be any input that constitutes a resource. For example, seawater, steam, and electricity in a MED plant. Conversely, the products represent the desired result produced by the system or the purpose of the system. The relations between resources and products for each subsystem are detailed in Leiva-Illanes et al. (2017). Subsequently, First-Law and Second-Law of Thermodynamics are applied, as follows:

$$\sum_{in}(\dot{m}_{in} \cdot h_{in}) - \sum_{out}(\dot{m}_{out} \cdot h_{out}) - \dot{W} + \dot{Q} = \frac{dEn_{cv}}{dt} \tag{3.3}$$

$$\dot{E}_Q - \dot{E}_W - \dot{E}_D + \sum_{in}(\dot{m}_{in} \cdot e_{in}) - \sum_{out}(\dot{m}_{out} \cdot e_{out}) = \frac{dE_{cv}}{dt} \tag{3.4}$$

where $\dot{m}$ is the mass rate, h is the specific enthalpy, $\dot{W}$ is the rate of work, $\dot{Q}$ is the heat power, dEn_{cv}/dt is the energy change rate in the control volume, $\dot{E}$ is the rate of exergy, e is the specific exergy, and dE_{cv}/dt represent the exergy change rate in the control volume. Both dEn_{cv}/dt and dE_{cv}/dt are null in steady-state conditions. The subscripts in, out, cv, Q, W, and D are inlets, outlets, control volume, heat transfer, work, and destruction, respectively.

The exergy rate of heat ($\dot{E}_Q$) and work ($\dot{E}_W$) that cross the boundaries of a control volume (j) are defined as follows

$$\dot{E}_Q = \left(1 - \frac{T_0}{T_j}\right) \cdot \dot{Q}_j \tag{3.5}$$

$$\dot{E}_W = \dot{W}_j \tag{3.6}$$

where T_0 is the temperature of reference, in K. The reference environment assumed in this study is T_0=25 °C and P_0=1.013 bar, respectively. Additionally, the reference mass fraction of LiBr and water salinity is considered of 0.5542 kg/kg and 0.042 kg/kg, respectively.
The specific exergy is defined as follows

$$e = e_{phy} + e_{che} + e_{Pot} + e_{kin} \tag{3.7}$$

where the subscripts phy, che, pot, and kin are related to physical, chemical, potential, and kinetic portion of exergy, respectively. In this study, the potential and kinetic exergy rates are neglected. The physical and chemical exergy are defined by

$$e_{phy} = (h - h_0) - T_0 \cdot (s - s_0) \tag{3.8}$$

$$e_{che} = -\Delta G + \left(\sum_{Pr} n \cdot e_{che} - \sum_{Re} n \cdot e_{che} \right) \tag{3.9}$$

where s is the specific entropy, G is Gibbs function for the reaction, n is the number of moles, the subscripts Pr and Re denote the products, and the reactants of the reaction, respectively. However, the exergy rates from the fossil-fuel is calculated with the following simplification (Ahmadi et al., 2011):

$$\dot{E}_{ff} = \dot{m}_{ff} \cdot \xi \cdot LHV \tag{3.10}$$

where ξ is an experimental correlation (Ahmadi et al., 2011), LHV is the lower heating value of the fossil-fuel. The subscript ff denotes fossil-fuel.

$$\xi = 1.033 + 0.0169 \cdot \frac{y}{x} - \frac{0.0698}{x} \tag{3.11}$$

where x and y are the composition $C_xH_y$in a general gaseous fuel, which in the case of natural gas is considered as CH_4, this value is close to unity.
Regarding to the exergy rates of solar radiation, the Patela's equation (2010) is considered, which is one of the most cited models in the literature and few differences are observed against other models. For example, between Petela's and Spanner's models (Petela, 2010) the difference is about 0.0002 %, and between Petela's and Jeter's (Petela, 2010) is about 1.8 %, for temperatures of 298 K and 6 000 K.

The First-Law or energy efficiency (η) defined as the ratio between energy output and energy input, and the Second-Law or exergy efficiency (ψ) defined as the ratio between the exergy rate of product and the exergy rate of fuel, are determined through the following equations:

$$\eta = \frac{\dot{E}n_{net}}{\dot{E}n_{in}} \tag{3.12}$$

$$\psi = \frac{\dot{E}_P}{\dot{E}_F} = \frac{\sum \Delta\dot{E}_{out}}{\sum \Delta\dot{E}_{in}} \tag{3.13}$$

where $\dot{E}n$ is the energy rate, $\dot{E}$ is the exergy rate, the subscript P, and F mean products and Fuel, respectively. Note that the energy efficiency applied to a polygeneration plant is known as utilization factor, also. In the case of the stand-alone MED, it is used the GOR as the indicator of energy efficiency considering that its product is a mass (fresh-water). Table 3-3 summarizes the expressions for these performance parameters applied to the boundaries considered in each subsystem.

Table 3- 3: Energy and exergy efficiencies.

	Polygeneration
η	$\frac{\dot{W}_{net\_polygen} + \dot{m}_{distillate} \cdot h_{distillate} + \dot{Q}_{REF} + \dot{Q}_{PH}}{\dot{Q}_{in\_polygeneration}} = \frac{(\dot{E}n_9 - \dot{E}n_2 - \dot{E}n_{10} - \dot{E}n_{11} - \dot{E}n_{16} - \dot{E}n_{21}) + \dot{E}n_{13} + (\dot{E}n_{18} - \dot{E}n_{19}) + (\dot{E}n_{23} - \dot{E}n_{22})}{\dot{E}n_1 + \dot{E}n_{24}}$
ψ	$\frac{\dot{E}_9 + \dot{E}_{13} + (\dot{E}_{19} - \dot{E}_{18}) + (\dot{E}_{23} - \dot{E}_{22})}{\dot{E}_1 + (\dot{E}_2 + \dot{E}_{10} + \dot{E}_{11} + \dot{E}_{16} + \dot{E}_{21}) + \dot{E}_{12} + \dot{E}_{24}}$
	Stand-alone CSP
η	$\frac{\dot{W}_{net}}{\dot{Q}_{in}} = \frac{\dot{E}n_4 - \dot{E}n_5}{\dot{E}n_1 + \dot{E}n_2}$
ψ	$\frac{\dot{E}_4}{\dot{E}_1 + \dot{E}_2 + \dot{E}_5}$
	Stand-alone MED
η	$\frac{\dot{m}_{distillate} \cdot h_{distillate}}{\dot{Q}_{in\_boiler} + \dot{W}_{pumps}} = \frac{\dot{E}_6}{\dot{E}_1 + \dot{E}_4}$
ψ	$\frac{\dot{E}_6}{\dot{E}_1 + \dot{E}_4 + \dot{E}_5}$

	Stand-alone REF
η	$\frac{\dot{Q}_{REF}}{\dot{Q}_{in\_boiler}+\dot{W}_{pumps}}=\frac{\dot{E}n_6-\dot{E}n_7}{\dot{E}n_1+\dot{E}n_4}$
ψ	$\frac{\dot{E}_7-\dot{E}_6}{\dot{E}_1+\dot{E}_4}$
	Stand-alone PH
η	$\frac{\dot{Q}_{PH}}{\dot{Q}_{in\_boiler}+\dot{W}_{pump}}=\frac{\dot{E}n_6-\dot{E}n_5}{\dot{E}n_1+\dot{E}n_4}$
ψ	$\frac{\dot{E}_6-\dot{E}_5}{\dot{E}_1+\dot{E}_4}$
	Stand-alone systems
η	$\frac{\dot{W}_{net\_CSP}+\dot{m}_{distillate}\cdot h_{distillate}+\dot{Q}_{REF}+\dot{Q}_{PH}}{\dot{Q}_{in\_CSP}+\dot{Q}_{in\_MED}+\dot{Q}_{in\_REF}+\dot{Q}_{in\_PH}}=\frac{(\dot{E}n_4-\dot{E}n_5)_{CSP}+\dot{E}n_{6_{MED}}+(\dot{E}n_6-\dot{E}n_7)_{REF}+(\dot{E}n_6-\dot{E}n_5)_{PH}}{(\dot{E}n_1+\dot{E}n_2)_{CSP}+(\dot{E}n_1+\dot{E}n_4)_{MED}+(\dot{E}n_1+\dot{E}n_4)_{REF}+(\dot{E}n_1+\dot{E}n_4)_{PH}}$
ψ	$\frac{\dot{E}_{4_{CSP}}+\dot{E}_{6_{MED}}+(\dot{E}_7-\dot{E}_6)_{REF}+(\dot{E}_6-\dot{E}_5)_{PH}}{(\dot{E}_1+\dot{E}_2+\dot{E}_5)_{CSP}+(\dot{E}_1+\dot{E}_4+\dot{E}_5)_{MED}+(\dot{E}_1+\dot{E}_4)_{REF}+(\dot{E}_1+\dot{E}_4)_{PH}}$

3.2.4. Levelized cost method

The levelized cost is the total cost of installing and operating the plant, expressed in monetary unit per unit of product generated by the system over its life (Palenzuela et al., 2015; Short et al., 1995). Therefore, the levelized electricity cost, in USD/kWh, is defined by:

$$LEC=\frac{capex\cdot crf+opex+C_{fuel}}{En_{el}}=\frac{\dot{Z}\cdot\tau+C_{fuel}}{En_{el}} \tag{3.14}$$

where $capex$ is the capital expenditure, $opex$ is the operational expenditure, crf is the capital recovery factor, C_{fuel} is the annual fuel cost, En_{el} is the annual production of net electricity delivered by the CSP plant, considering the parasitic loads (Note that the polygeneration plant does not include electric consumption of MED, REF, and PH), $\dot{Z}$ is the non-exergy-related cost rate, τ is the annual average time of the plant's operation at nominal capacity, in h/a. Fuel cost is calculated by:

$$C_{fuel} = c_{ff} \cdot \frac{Q_{\text{th,power block}_{\text{BS}}}}{\eta_{\text{boiler}}} + c_{sun} \cdot \frac{Q_{\text{th,power block}_{\text{solar}}}}{\eta_{\text{collector}}} \quad (3.15)$$

where c_{ff} is the fossil fuel cost, in USD/kWh, $Q_{\text{th,power block\_BS}}$ is the thermal energy required by the power block from BS, in kWh/a, and η_{boiler} is the boiler efficiency, assumed as 0.9, c_{sun} is the sun fuel cost, in USD/kWh, $Q_{\text{th,power block\_solar}}$ is the thermal energy required by the power block from Solar (SF and TES), in kWh/a, and $\eta_{\text{collector}}$ is the collector optical efficiency. The cost of solar energy is neglected.

The total investment, and operating and maintenance cost rate is defined by

$$\dot{Z} = \dot{Z}^{CI} + \dot{Z}^{OM} = \frac{capex \cdot crf + opex}{\tau} \quad (3.16)$$

where $\dot{Z}^{CI}$ is the investment cost rate, $\dot{Z}^{OM}$ is the operation and maintenance cost rate (not include fossil-fuel cost).

A similar procedure was used for the others levelized costs estimation. The levelized water cost (LWC), in USD/m^3, is defined by:

$$LWC = \frac{capex \cdot crf + opex + C_{fuel}}{V_w} = \frac{\dot{Z} \cdot \tau + C_{fuel}}{V_w} \quad (3.17)$$

where V_w is the annual production of water, in m^3/a, and C_{fuel} is the fuel cost, in USD/a. Fuel cost in the case of MED, refrigeration and process heat plants is the cost associated with electric and thermal consumptions supplied from the CSP plant (in the case of stand-alone plant is from the grid and boiler, respectively), and the sea-water cost. The latter cost applies only to the MED plant. In a polygeneration scheme, the thermal energy cost is considered as an internal cost (it is assumed by the power cycle because is a waste heat), and the sea-water cost is assumed null too. Additional discussion about cost allocation can be found in the literature (Piacentino, 2015; Wang & Mao, 2015; Wang & Lior, 2007). Fuel cost is calculated by:

$$C_{fuel} = LEC \cdot \text{En}_{\text{pumps}} + C_{thermal} \cdot En_{thermal} + C_{sw} \cdot V_w \quad (3.18)$$

where $\mathrm{En_{pumps}}$ is the annual energy consumption from pumps, in kWh/a, $C_{thermal}$ is the thermal energy cost, in USD/kWh, $En_{thermal}$ is the annual thermal energy consumption, in kWh/a, and C_{sw} is the sea-water cost.

Similarly, the levelized cooling cost (LCC), in USD/kWh, is defined by:

$$LCC = \frac{capex \cdot crf + opex + C_{fuel}}{En_c} = \frac{\dot{Z} \cdot \tau + C_{fuel}}{En_c} \tag{3.19}$$

where En_c is the annual production of cooling, in kWh/a. Finally, the levelized process heat cost (LHC), in USD/kWh, is defined by:

$$LHC = \frac{capex \cdot crf + opex + C_{fuel}}{En_h} = \frac{\dot{Z} \cdot \tau + C_{fuel}}{En_h} \tag{3.20}$$

where En_h is the annual production of process heat, in kWh/a.

It should be noted that the fuel costs are part of the operating and maintenance costs. However, because of the importance of fuel costs in thermal systems, fuel costs are considered separately from the $opex$. Other revenues, such as selling carbon credits and selling renewable credits conforming with the renewable energy quota established by Chilean legislation, are not considered in this study.

3.2.5. Thermoeconomic method

A thermoeconomic evaluation was also applied, considering the method proposed by Bejan et al. (1996). The economic balance is applied to determine the unit exergy cost c_j and the exergy cost rate $\dot{C}_j$ of each stream. That economic balance is expressed by:

$$\sum_{\mathrm{in}} (\mathrm{c_{in}} \cdot \mathrm{\dot{E}_{in}})_\mathrm{k} + \mathrm{\dot{Z}_k^{CI}} + \mathrm{\dot{Z}_k^{OM}} = \sum_{\mathrm{out}} (\mathrm{c_{out}} \cdot \mathrm{\dot{E}_{out}})_\mathrm{k} \tag{3.21}$$

where, c is the unit exergy cost. The subscript k, in, and out denote the kth component, inlets, and outlets, respectively. This equation can be expressed as the sum of total cost rate of fuel $\dot{C}_f$ and non-exergy-related cost rate $\dot{Z}$, equivalent to the total cost rate of product $\dot{C}_p$. The exergy cost rate is expressed as function of the unit exergy cost by:

$$\mathrm{\dot{C}} = \mathrm{c} \cdot \mathrm{\dot{E}} = \mathrm{c} \cdot \mathrm{\dot{m}} \cdot \mathrm{e} \tag{3.22}$$

For each subsystem, the fuel, product, and auxiliary equations are defined to apply the economic balance for the polygeneration and stand-alone plants. More details are stated elsewhere Leiva-Illanes et al. (2017). Table 3-4 summarizes the equations of those balances and report the auxiliary equations.

Table 3- 4: Unit exergy cost of electricity, water, cooling and heat.

c	Polygeneration plant	Stand-alone plant
Electricity	$c_9 = \frac{\dot{C}_1+\dot{C}_{24}-(\dot{C}_4-\dot{C}_3)-(\dot{C}_6-\dot{C}_5)-(\dot{C}_8-\dot{C}_7)+\dot{Z}_{csp}}{\dot{E}_9-\dot{E}_2-\dot{E}_{10}}$ $c_1=0$, $c_2=c_9$, $c_3=c_4$, $c_5=c_6$, $c_4=c_5$, $c_7=c_8$, $c_7=c_6$, $c_{10}=c_9$, $c_{24}= c_{ff}$, $c_3=c_9$	$c_4 = \frac{\dot{C}_1+\dot{C}_2-\dot{C}_3+\dot{Z}_{csp}}{E_4-E_5}$ $c_1=0$, $c_2= c_{ff}$, $c_3=0$, $c_5=c_4$
Water	$c_{13} = \frac{(\dot{C}_8-\dot{C}_7)+\dot{C}_{11}+\dot{C}_{12}-\dot{C}_{14}-\dot{C}_{15}+\dot{Z}_{med}}{E_{13}}$ $c_7=c_8$, $c_{11}=c_9$, $c_{12}=0$, $c_{14}=0$, $c_{15}=0$	$c_6 = \frac{\dot{C}_1+\dot{C}_4+\dot{C}_5-\dot{C}_7-\dot{C}_8+\dot{Z}_{med}+\dot{Z}_{boiler}}{E_6}$ $c_1= c_{ff}$, $c_2=c_3$, $c_2=c_3$, $c_4= P_{elect}$, $c_5=0$, $c_7=0$, $c_8=0$
Cooling	$c_{19} = \frac{(\dot{C}_6-\dot{C}_5)+\dot{C}_{16}+(\dot{C}_{20}-\dot{C}_{17})+\dot{Z}_{ref}}{E_{19}-E_{18}}$ $c_5=c_6$, $c_{16}=c_9$, $c_{17}=0$, $c_{18}= c_{19}$, $c_{20}=0$	$c_7 = \frac{\dot{C}_1+\dot{C}_4+(\dot{C}_8-\dot{C}_5)+\dot{Z}_{ref}+\dot{Z}_{boiler}}{E_7-E_6}$ $c_1= c_{ff}$, $c_2=c_3$, $c_2=c_3$, $c_4=P_{elect}$, $c_5=0$, $c_6= c_7$, $c_8=0$
Process Heat	$c_{23} = \frac{(\dot{C}_4-\dot{C}_3)+\dot{C}_{21}+\dot{Z}_{ph}}{E_{23}-E_{22}}$ $c_3=c_4$, $c_{21}=c_9$, $c_{22}= c_{23}$	$c_6 = \frac{\dot{C}_1+\dot{C}_4+\dot{Z}_{ph}+\dot{Z}_{boiler}}{E_6-E_5}$ $c_1= c_{ff}$, $c_2=c_3$, $c_2=c_3$, $c_4=P_{elect}$, $c_5= c_6$

where P_{elect} is the electricity price from the grid for industrial use, which is assumed to be 0.098 USD/(kWh) (Tariffs BT4 and AT4) (ELECDA, 2016).

3.3. Results and discussion.

3.3.1. Production and cost in the base case.

The CSP-polygeneration plant receives 2 039.3 and 399.6 GWh/a from the solar field and the backup system, respectively. Consequently, the annual productions are 463.1 GWh/a of gross power, 408.5 GWh/a of net power, 13.2 Mm^3/a of fresh water, 42.0 GWh/a of cooling, and 58.9 GWh/a of process heat. The plant is hybridized with natural gas. In Figure 6 the

Sankey and the Grassmann diagrams of the polygeneration plant are presented, in which the width of the arrows is shown proportionally to the flow of energy and exergy rates. The Sankey diagram shows energy inputs and outputs, as well as energy efficiency. However, when resources and products of different energy nature (such as water) are present the Sankey diagram is limited. A partial solution is using an appropriate definition, in terms of energy, of those resources and/or products. Therefore, it is not appropriate to express the energy efficiency for the overall system in a polygeneration plant that generates non-energy products. This problem does not occur when using the Grassmann diagram (and the Second-Law or exergy efficiency), because it is based on the exergy rate. The exergy flows and irreversibilities are represented in the Grassmann diagram, in which each component represents an exergy balance and shows how part of the exergy input is lost in the successive transformation processes. As observed in the Sankey diagram, the energy input is transformed into useful energy in a ratio of 53.7 % that is distributed with respect to the energy input as 16.7 %, 32.8%, 1.7 %, and 2.4 % in electricity, water, cooling, and process heat, respectively. On the other hand, the Grassmann diagram shows that the exergy input is transformed into useful exergy flows in about 27.1 %, distributed as 25.4 %, 1.0 %, 0.1 %, and 0.5% in electricity, water, cooling, and process heat, respectively, while the main irreversibilities or exergy destruction are in the solar thermal loop. The high exergy destruction is explained due the large temperature difference between the source temperature (sun) and the heat transfer fluid, while exergy destruction in the power block is mainly due to the large temperature differences between the hot and cold fluids. The main reasons for the high exergy destruction in the BS (combustion chamber) are the chemical reactions and heat exchange between streams with large temperature differences. Note that in a conventional steam power plant, the boiler is the main source of irreversibility.

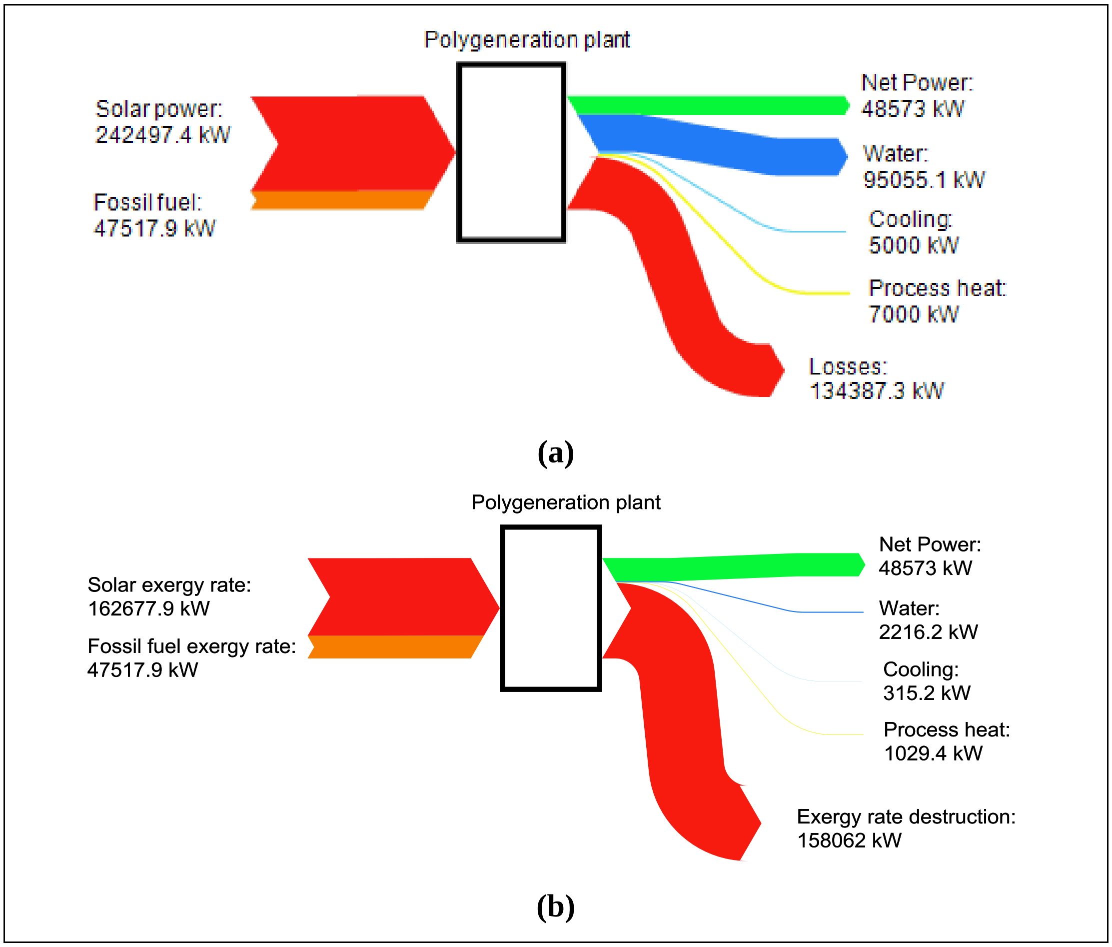

Figure 3- 6: Polygeneration plant. (a) Sankey diagram. (b) Grassmann diagram.

Table 3-5 shows the energy and exergy efficiencies of each subsystem. The polygeneration plant is more efficient than the overall stand-alone systems in terms of both energy and exergy efficiencies, due to the fact that there is a better utilization of the resources. Exergy analysis provides more information for a better understanding of the process, to quantify sources of inefficiency, and to distinguish quality of energy used. Energy analysis provides only partial information, because it does not provide a measure of how close is to ideal processes, and losses of energy could be large but with low quality (thermodynamically insignificant). On the other hand, the product of the MED plant is a mass and the efficiency of a stand-alone MED plant, in terms of consumed energy, is usually measured for any of the following indicators: GOR ($kg_{distillate}/kg_{steam}$), the Performance Ratio ($kg_{distillate}/kJ_{steam}$), the Specific Heat Consumption ($kWh_{steam}/m^3_{distillate}$), or the Unit Operating Cost

(USD/$m^3_{distillate}$). In this study the GOR is used as indicator. Note that the energy efficiency, defined as the ratio between energy output and energy input, is not an appropriate indicator since the product is not an energy but a mass (fresh-water).

Table 3- 5: Energy and exergy efficiencies.

	Energy efficiency %	Exergy efficiency %
Polygeneration	53.7	27.1
Overall stand-alone systems	41.6	18.7
Stand-alone CSP	21.5	30.9
Stand-alone MED	79.5	1.9
Stand-alone REF	63.0	4.0
Stand-alone PH	90.0	13.2

If a system produces more than one product, as in a polygeneration system, an allocation criterion of costs is needed to determine each product cost. The unit exergy costs (UEC) and levelized costs (LC) is presented in Table 3-6. For the polygeneration plant, the UEC of electricity is lower than the LEC, conversely, the UEC of water, cooling and heat are higher than LWC, LCC, and LHC, respectively. The numeric difference between unit exergy cost and levelized cost is due to the form of cost allocation. Through the levelized cost method, the thermal energy cost is considered as an internal cost, so the thermal energy cost is assumed completely by the electricity production. Hence, the $\dot{Z}_{csp}$ is completely allocated to the electricity cost, since the LEC equation (see Equations 3-14) does not consider the cost of the other product generated by the CSP plant in this scheme, i.e. thermal energy. In contrast, by applying the thermoeconomic method, the thermal energy cost is shared with MED, REF and PH plants and is distributed according to its exergy rate. Consequently, the $\dot{Z}_{csp}$ is allocated to the electricity cost and the thermal energy cost, in such a way that the $\dot{Z}_{csp}$ is allocated to the electricity, water, cooling and process heat costs (see Equations on Table 3-4). For that reason, the thermoeconomic method is considered as a rational cost allocation method. The levelized cost method overestimates the cost of electricity and underestimates the costs of the by-products and induce a bias that could lead to a misevaluation of the project; for instance, if the LEC calculated is higher than the selling price of the grid. Conventional economic analysis, as the levelized cost method, does not provide a rational criteria for apportioning the carrying charges, fuel costs, and $opex$ to the several products generated in the same system (Bejan et al., 1996).

Regarding stand-alone systems, both methods give the same results because each plant produces only one product, and it is not necessary to allocate any cost between products.

By comparing the result between polygeneration and stand-alone plants, the unit exergy cost of each product is lower in polygeneration schemes, therefore, when the thermoeconomic method is used, the results show that the polygeneration plant is more cost-effective than stand-alone systems. However, comparing by levelized cost, the LEC in the polygeneration plant is higher than in the stand-alone plant, and the other costs (LWC, LCC, and LHC) are lower. These results are explained by the increase in the solar field aperture area, which increases the $capex$ and $opex$, that is allocated to the LEC and also the fact that the cost of the steam (consumed by the MED, REF, and PH plants) is considered as an internal cost. In this case, it is not possible to establish which scheme is better, whether the polygeneration plant or the stand-alone systems, considering that electricity and water are the priority in the mining industry. Thus, additional metrics are needed to discriminate which scheme is more attractive. For example, the overall cost of products or the total exergy cost rate could be used, whose values in the polygeneration plant are lower than in the case of stand-alone systems. The total exergy cost rate of products, calculated using the thermoeconomic method (Bejan et al., 1996), is 10 504.4 USD/h for polygeneration plant, which is distributed in 55.4 % in electricity, 41.1 % in fresh water, 1.9 % in cooling, and 1.6 % in process heat, while in the stand-alone systems is 13 630.0 USD/h, which is distributed in 49.3 % in electricity, 46.6 % in fresh water, 2.2 % in cooling, and 1.9 % in process heat. Thus, the polygeneration scheme offers a more attractive solution than the stand-alone systems.

Table 3- 6: Unit exergy costs and levelized costs.

Item	Polygeneration plant		Stand-alone plants
	UEC	LC	UEC and LC
Electricity, USD/kWh	0.1058	0.1429	0.122
Water, USD/m^3	2.746	1.804	4.036
Cooling, USD/kWh	0.036	0.008	0.060
Heat, USD/kWh	0.0238	0.0006	0.038

The monthly production of electricity, fresh water, cooling and process heat, in the solar polygeneration plant, follows the same trend of capacity factor as shown in Figure 3-7, which unfolds the contribution from the solar (SF and TES) and from the backup system. The contribution from the solar is largest in the summer due to the seasonal variation in direct normal irradiation available for collection, although in summer there is a significant decrease in February, due to a local meteorological phenomenon called "Altiplanic Winter", which is characterized by an increase on the air humidity coming from the east, bringing unsettled weather and clouds. Thus, the consumption of fossil fuel is higher in February, June, and July, reaching 38.3 %, 43.0 %, and 44.6 %, respectively.

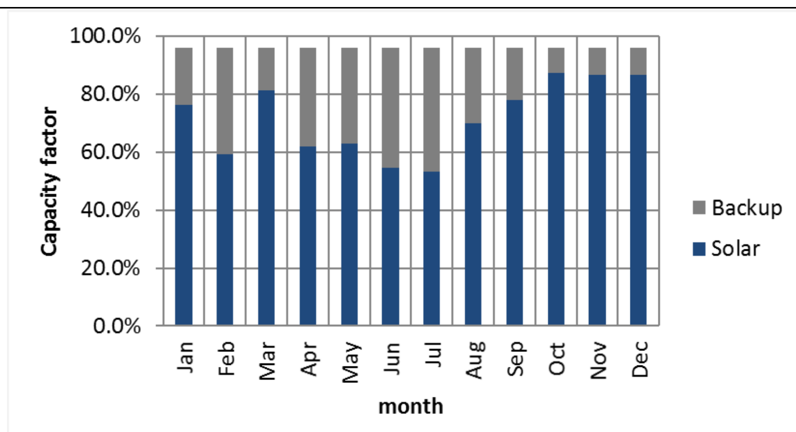

Figure 3- 7: Monthly capacity factor in polygeneration plant.

The monthly specific cost of products, such as unit exergy cost and levelized cost of electricity, fresh water, cooling, and process heat, in the polygeneration plant, are shown in Figure 3-8. The specific cost of the products, calculated through both methods follows the same trend, reaching high values in winter and decreases during summer (except in February). Considering that the capacity factor is fixed, then when the fossil fuel consumption increases, the costs of products increase too. Consequently, the costs of products are higher in February, June, and July. Note that, in stand-alone systems, the specific costs of the product vary only in the CSP plant as this is driven by solar radiation and fossil-fuel, while for the other plants the specific cost remains constant, since they are driven only by fossil fuel. Regarding the comparison of both methods, the levelized cost method gives a higher cost of electricity, lower cost of fresh water, cooling, and process heat compared to the thermoeconomic method, as observed before.

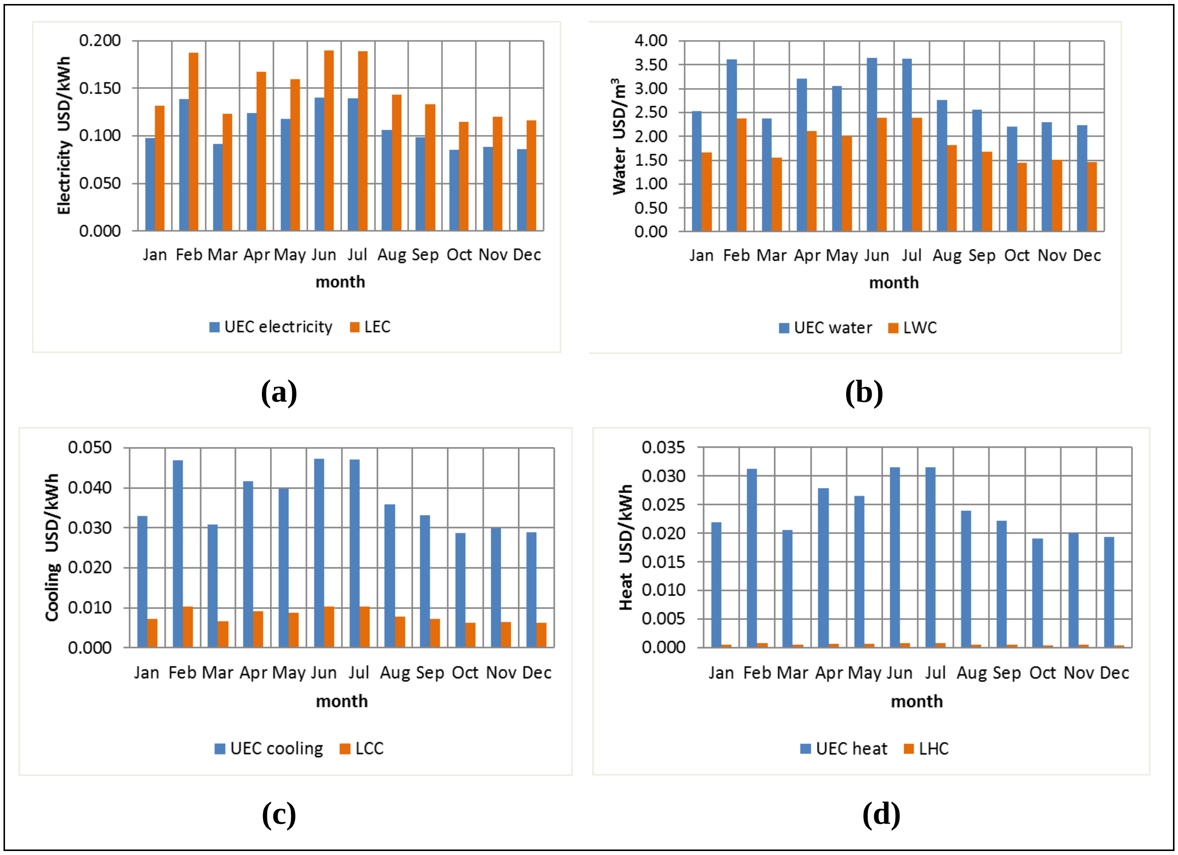

Figure 3- 8: Comparison between the levelized cost method and thermoeconomic method in polygeneration plant. Monthly UEC and LC of: (a) electricity, (b) water, (c) cooling, (d) process heat.

The advantages of using the levelized cost method are that the cost of steam is considered as an internal cost and it is not necessary to develop an additional assessment, which saves time and reduces the complexity of calculations. Therefore, the evaluator does not require to develop a deep thermodynamic analysis. However, through this approach, the cost of electricity seems more expensive relative to the cost of other products, leading to a distortion in the evaluation, because the allocation of costs does not obey physical parameters as the exergy, which gives the allocation some arbitrariness. Therefore, this method is recommended when it is necessary to perform a first approximation of the costs of each product, but comparing between a polygeneration plant and the stand-alone systems could lead to significant inaccuracies, as the case discussed above.

On the other hand, the advantages of using the thermoeconomic method are that it applies a rational allocation of resources that is not arbitrary since it is based on the exergy, requiring, however, a thorough knowledge of thermodynamics to determine the different exergy flows, which makes the process complex and laborious. Therefore, this method is recommended when a more precise analysis of the costs of each product is needed, and specifically for comparing between polygeneration and the stand-alone schemes.

3.3.2. Production and cost as functions of sizing SM and TES.

Figure 3-9 shows the variation of the capacity factor, in the polygeneration plant, as a function of the solar multiple, the hours of storage, and the hybridization through the BS. An important point that contributes to increasing the capacity factor is the direct normal irradiation. This variable depends on the location (latitude) between other factors, although in this work is not considered a variation on the location. The SM is larger than one to guarantee that the power block is effectively used during the year. The TES allows storing excess energy collected by the SF when it is not used in the power block, and discharges that energy later when the direct normal irradiance is lower. The solar polygeneration plant presents higher dispatchability when hybridized, coupling a backup system. This also allows a more flexible generation strategy to maximize the value of the products generated. Consequently, the annual production of each product is increased too, following the same trends of Figure 3-9.

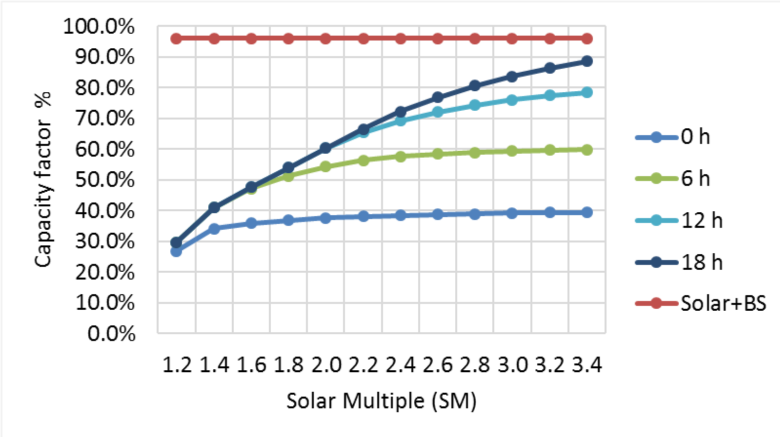

Figure 3- 9: Capacity factor in the polygeneration plant.

On the other hand, the trade-off between the incremental costs of the increased SF, TES, and BS must be balanced against the increase in the production by the rise of the capacity factor. In this context, Figures 3-10 presents the unit exergy cost and levelized cost of each product (electricity, fresh water, cooling, and process heat) as a function of SM and hours of TES of the polygeneration plant. The minimum values of the unit exergy cost and the levelized cost are different in value, but occur at the same points regarding SM and TES.

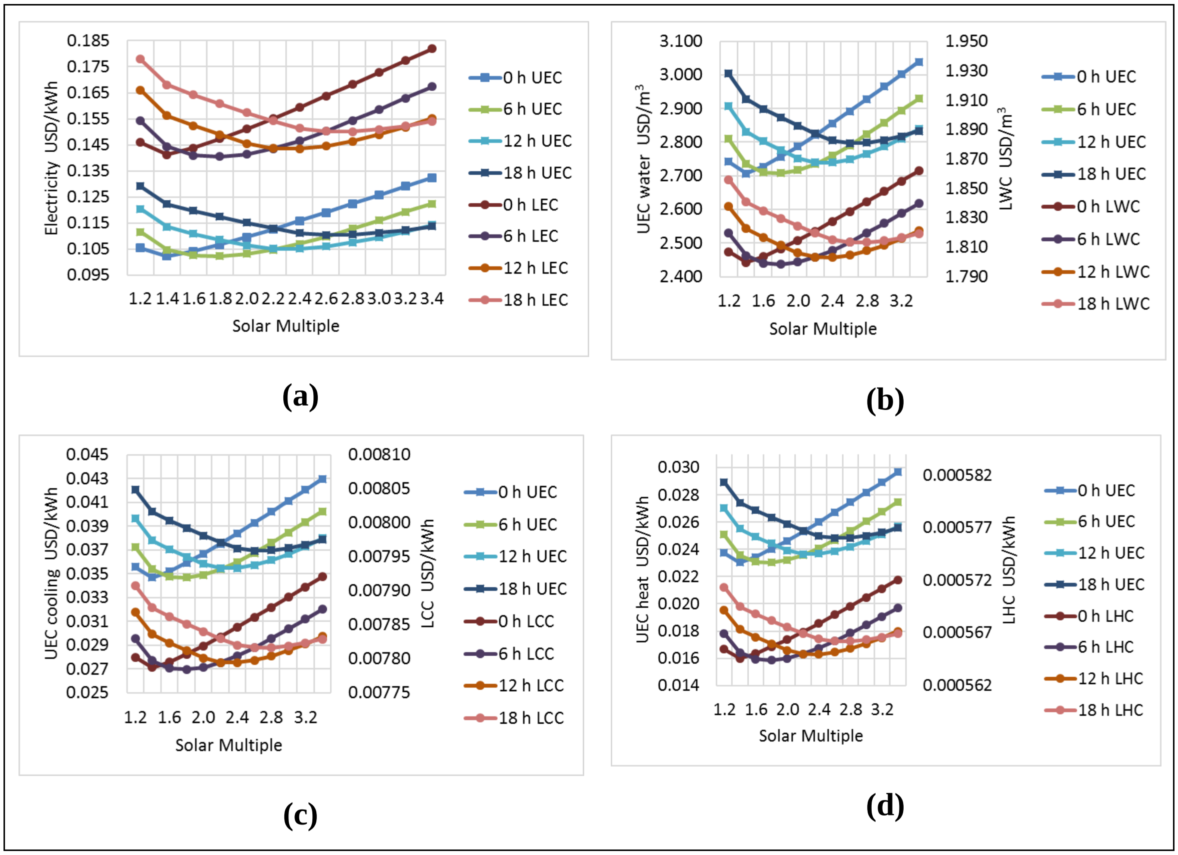

Figure 3- 10: Unit exergy cost (UEC) of electricity (a), water (b), cooling (c), and heat (d), versus Levelized electricity cost (LEC), Levelized water cost (LWC), Levelized cooling cost (LCC), and Levelized heat cost (LHC).

Regarding the values of minimum UEC and LC that are different, the lowest UEC of electricity and LEC are 0.102 and 0.141 USD/kWh, respectively. In the levelized cost method, the electricity cost supports both the *capex* and *opex* of the CSP plant and the fossil fuel cost, whereas in the thermoeconomic method, these costs are shared by the exergy flows, which connect the CSP plant with the MED, REF and PH plants. The lowest UEC of water and LWC are 2.705 and 1.798 USD/m^3, respectively. The LWC is lower than the UEC of water, because the water cost bears the *capex* and *opex* of the MED plant and its own consumption of electricity, but does not consider the thermal cost from CSP plant. In the case of the REF plant, the lowest UEC of cooling and LCC are 0.035 and 0.0078 USD/kWh, respectively. The LCC is lower than the UEC of cooling, for the same reason that in the case of the water cost. Similarly, the minimums UEC of process heat and LHC are 0.023 and 0.00056 USD/kWh, respectively.

The lowest UEC and LC occur at the same point in terms of SM and TES, 1.4 and 3 h, respectively. Therefore, the same plant size (SF and TES) is reached by applying both methods. However, the difference in the unit exergy cost between an SM and TES of 1.4 and 3 h, and the base case (2.56 and 12 h) is 3.8 %, 1.6 %, 3.1 %, and 3.7 % for electricity, water, cooling, and heat, respectively. In the case of levelized cost, the difference is about 3.8 %, 0.5 %, 0.2 %, and 0.2 % for electricity, water, cooling, and heat, correspondingly. The minima UEC and LC coincide at the same plant size because the polygeneration plant is dominated mainly by the solar field size and the thermal energy storage capacity. The variations on the investment cost of SF and TES produce similar variations in both methods, keeping only differences in the magnitude. An optimal solar field area should maximize the time in a year that the field generates enough thermal energy to drive the power cycle at its rated capacity, minimize $capex$ and $opex$, and use TES and backup system efficiently and cost effectively.

Regarding to the stand-alone CSP plant, the minimum UEC of electricity and LEC have the same value and it also occur at the same SM and TES (1.8 and 6 h). Nevertheless, when the stand-alone CSP plant is integrated in the CSP-polygeneration plant, the SM and TES are reduced from 1.8 and 6 h to 1.4 and 3 h respectively, due to the modification of the turbine extraction pressures and the back pressure in the CSP plant to couple the MED, REF, and PH plants.

An optimal sizing of SF and TES should minimize installation and operating costs, and maximize the amount of energy delivered throughout the year. This point is reached with the minimum levelized cost and unit exergy cost. The unit cost in the solar polygeneration plant is dominated by the investment cost of CSP plant. Therefore, the unit cost varies significantly depending on the capacity factor, which in turn depends on the direct normal irradiation, hybridization (BS) levels, and sizing of SF and TES. According to the thermoeconomic method, in an optimization process, the variable to be minimized is the total exergy cost of products, which includes the exergy costs and non-exergy costs of the polygeneration plant. This method allows measuring in the same unit resources and products of very different nature, such as electricity, water, cooling, process heat, resources, and waste. For this reason, the thermoeconomic method is recommended for assessing polygeneration plants.

3.4. Conclusions

The levelized cost method and the thermoeconomic method were applied to a solar polygeneration plant to analyse and compare the cost allocation process, the unit specific costs of products, the energy and exergy efficiencies, as well as the main advantages of each method employed. The solar polygeneration plant consists of a concentrated solar power plant, a multi-effect distillation, an absorption refrigeration, and a process heat plants.

When it is generated only one product by each stand-alone system, it is not necessary to allocate any cost between products, and both methods give the same results. Yet, when more than one product is generated there are common costs associated with the products concerned, and it is necessary to determine the share of costs attributable to one or another product. So, the cost allocation procedure needs an additional rational analysis to prevent allocation from being arbitrary. In this context, the levelized cost method and the thermoeconomic method are used extensively in the evaluation of this kind of plants, in which levelized cost method is a simple and fast method, and a deep knowledge of thermodynamics is not required. In the absence of a detailed knowledge of the plant, the level cost method is a good alternative and presents reasonable results. Therefore, this method is recommended when it is necessary to perform a first approximation of the costs of each product, but comparing between polygeneration plant and the stand-alone systems could lead to different conclusions. On the other hand, the thermoeconomic method is an equitable distribution of the appropriate share of non-exergy-related cost rate ($capex$ and $opex$) and exergy cost rate in each product. It is based on the Second-Law of Thermodynamics and the Economics, in which all costs from resources consumed are charged to their useful products. This method is recommended when it is required to perform a more precise analysis of the costs of each product, and for assessing the benefits of polygeneration schemes, compared to the stand-alone systems. The disadvantages of the thermoeconomic method are its complexity and additional knowledge about the internal parameters of the plant, which could not be available.

Results show that the electricity cost calculated through the levelized cost method is higher than the estimated by the thermoeconomic method. In contrast, the water, cooling, and process heat costs are lower since in the levelized cost method, the cost allocation does not charge all internal cost to MED, REF and PH plants. The allocation of costs based on thermoeconomic method equitably charges each product with the appropriate share of $capex$ and $opex$, that are involved in operating such component according to its exergy rate. Hence, the thermoeconomic method constitutes a rational method to assess a CSP-polygeneration plant, since it is based on the quality of energy assessed.

The analysis shows that the lowest unit exergy and levelized costs happened at the same sizing of SM and TES, however, the unit costs have different values. Hence, independently of the method employed, in an optimization process for sizing of SM and TES, the same results are delivered. Nevertheless, the thermoeconomic method allows measuring resources and products of very different nature, such as energy and water, using the same unit.

In the case of a polygeneration scheme, it is common to use as indicator the utilization factor, which is based on the First-Law of Thermodynamic relating the energy outputs (work, electricity, heat, cooling, heat supplied to the desalting plant, or other) to the energy inputs (sun, fossil fuel, heat, or others). This indicator does not discriminate between the high-quality energy as work or electricity, and low-quality energy as heat. Additionally, when resources and products of different energy nature (as water) are presented, the indicator is limited. A partial solution is to use an appropriate definition, in terms of energy, of those resources and/or products. For that reason, the utilization factor provides a false high-performance impression of the polygeneration plant. Therefore, a better indicator for polygeneration plant is the exergy efficiency.

In future studies, a thermoeconomic assessment with a low aggregation level in the CSP plant should be applied to individual components, such as turbines, preheaters, solar field, among others, to identify the thermodynamic improvements for the polygeneration schemes.

4. EXERGY COST ASSESSMENT OF CSP DRIVEN MULTI-GENERATION SCHEMES: INTEGRATING SEAWATER DESALINATION, REFRIGERATION, AND PROCESS HEAT PLANTS.

Abstract

A thermoeconomic analysis in solar multi-generation plants, that include cogeneration, trigeneration, and polygeneration schemes, for the joint production of electricity, fresh-water, cooling, and process heat, is presented here. The aim is to analyze in depth the exergy cost formation process of the integrated schemes and compare them with stand-alone systems. That comparison allows determining the best configuration in a cogeneration, trigeneration and polygeneration scheme, in terms of unit exergy cost of the product, total exergy cost of product, and exergy efficiency. The solar multi-generation plant considers a concentrated solar power as prime mover, which is integrated to a multi-effect distillation, an absorption refrigeration, and a process heat plants in cogeneration, trigeneration, and polygeneration schemes. The results show that the best configurations found are when the desalination plant replaces the condenser of the power cycle, and the refrigeration plant, as well as the process heat module are coupled to turbine extractions. The main components contributing to the costs formation of electricity are, in this order, solar collectors, evaporator, reheater, economizer, turbine, and super-heater. In the case of the other products generated, the main components are dissipative systems, solar collectors, productive subsystems (multi-effect distillation, absorption refrigeration, and process heat plants), evaporator, reheater, economizer, and superheater. Finally, the present analysis evidences that solar multi-generation plants are more cost effective than stand-alone systems. For instance, the best configuration within the polygeneration schemes analyzed allowed reducing the unit exergy cost about 6.8 %, 59.2 %, 45.6 %, and 32.2 % for electricity, water, cooling, and process heat, respectively.

4.1. Introduction

Polygeneration is the integration of multiple utility outputs, from one or more inputs, for improving the overall performance of energy systems. The performance of a polygeneration system may be assessed from different aspects, such as, thermodynamic, economic, environmental, and social issues. Thus, the main advantages delivered by those systems are measured in terms of the improvement of energy efficiency and cost- effectiveness, use of alternative fuels or energy carriers, and reduction of greenhouse gases emissions. Those advantages constitute polygeneration systems as a competitive technology compared to stand-alone systems delivering equivalent utilities (Serra et al., 2009). In a polygeneration system topping cycle (Al Moussawi et al., 2016), fuel is used in the prime mover, typically in a power cycle such as Rankine, Brayton or Diesel, that generates electricity. Prime mover's hot exhaust is used to supply thermal energy to a secondary unit driven by heat, like thermal distillation, process heat, and/or absorption cooling. Using a Concentrated Solar Power (CSP) plant as a prime mover is an interesting alternative to analyze when it is implemented in a polygeneration scheme; since it produces electricity fueled by solar energy and could be coupled to a thermal energy storage or be hybridized with a fossil fuel or other renewable sources. That integration allows continuous operation, as well as developing capacity factors similar to conventional power plants, enabling plant's dispatchability management, and additionally, taking advantage of the heat rejected from the power block to drive thermal cycles.

The integration of a CSP plant into a polygeneration scheme is a complex process that requires the use of robust methods in its assessment and optimization. In this context, there are several methods for evaluating the integration strategies in polygeneration schemes (Bejan et al., 1996; Nuorkivi, 2010; Serra et al., 2009). Among those methods the Thermoeconomic (or Exergoeconomic) method (Abusoglu & Kanoglu, 2009) is recommended because it provides a compact matrix formulation for the detailed analysis of complex systems based on the physical roots established by the Second Law of Thermodynamics (Valero et al., 2013). Second Law establishes that in some energy carriers, part of the energy cannot be converted into useful energy. It assesses both quantity and quality of energy through exergy, indicating the maximum work that a flow or a system might produce while interacting with the environment. This method is very useful to analyze complex systems because it allows measuring, in the same physical unit, resources and waste flows of different nature, for instance electricity, energy, water, cooling or heat. Commonly, the rationale use of resources in complex systems is evaluated in terms of the exergy cost of mass and/or energy flows, which represents the units of consumed exergy to produce it, i.e. the exergy cost of a flow is the amount of resources expressed in exergy consumed for producing that flow (Valero et al., 2002). The exergy cost allows analyzing and identifying integration possibilities because it enables determining the potential for resources savings. Exergy cost is a conservative magnitude that increases in every process according to the irreversibilities involved. In an integrated process, it is interesting to study in depth how exergy costs are formed, since the process of cost formation provides meaningful information that allows implementing significant improvements to the design and an accurate performance analysis.

As described by Modi et al. (2017) and Jana et al. (2017), CSP technologies could be integrated into polygeneration schemes, with improvements in economics, environmental, and conversion efficiency terms. They presented comprehensive reviews of solar energy-based heat and power plants, and polygeneration schemes as a future sustainable energy solution, in which different studies have focused mainly on determining the final cost of each product by thermoeconomic methods. They concluded that polygeneration schemes constitute an efficient, environment friendly and a rational approach for exploiting the available natural resources. Regarding the thermoeconomic method, Al-Sulaiman et al. (2013a, 2013b) carried out a thermoeconomic optimization of a CSP-trigeneration system, considering an organic Rankine cycle as prime mover, an absorption chiller, and a process heat module. The specific exergy costing method was applied to conduct an evaluation of costs associated to each exergy stream entering and exiting system's components, aiming to determine the final cost (unit exergy cost and exergy cost rate) of each product. The results show that the higher exergy destruction rate is attributed to the solar collectors. In the same line, Calise et al. (2016) carried out an exergetic and exergoeconomic analysis of a hybrid solar geothermal polygeneration system, equipped with an organic Rankine cycle driven by parabolic trough solar collectors and a geothermal well, where a multi-effect distillation unit and an absorption chiller are coupled to the power block. The exergoeconomic accounting method was applied to calculate all the energy and material output costs, comparing on a daily, weekly and annual basis, which allows evaluating the performance of the system and the variability observed during the year. Alternatively, Ortega et al. (2016) presented a thermoeconomic analysis with the integration of seawater desalination processes coupled to a CSP plant, as well as its comparison with stand-alone systems such as multi-effect distillation (MED) and reverse osmosis. The evaluation considered the unit exergy cost of electricity and water. The results showed that the best coupling scenario for CSP-MED configurations was replacing the condenser of the CSP plant by a MED system. Furthermore, the increase on the fresh-water production caused a reduction on the water cost. In this context, Leiva-Illanes et al. (2017) firstly carried out a thermoeconomic assessment of a solar polygeneration plant for producing four products (electricity, fresh-water, cooling and heat) in high direct normal irradiation conditions. Integration of a CSP plant, a MED unit, a single effect absorption chiller (REF), and a process heat (PH) module was analyzed in three configurations, two CSP-polygeneration schemes and one considering stand-alone systems. The plants were evaluated by applying the Bejan et al. method (1996), comparing the unit exergy cost and exergy cost rate of the final products on an annual basis. That study revealed that the solar polygeneration plant evaluated was more efficient and cost-effective than stand-alone systems for a zone with high irradiation conditions and proximity to consumption centers. In a second paper Leiva-Illanes et al. (2018), the levelized cost method (Palenzuela et al., 2015; Short et al., 1995) and the thermoeconomic method (Bejan et al., 1996) were applied to the same solar polygeneration plant to analyze and compare the cost allocation process, the unit specific costs of products, the energy and exergy efficiencies, as well as the main advantages of each method. Through the levelized cost method, the cost associated to the electricity generation was higher than that one found with the thermoeconomic method, whereas the costs of water, cooling and process heat were significantly lower. Those results showed that the thermoeconomic method was an equitable and rational cost allocation method in that solar polygeneration plant based on CSP. The present work constitutes the continuation of that research line, in which a thermoeconomic evaluation is carried out with the exergy cost assessment of the consecutive configurations (stand-alone, cogeneration, trigeneration, and polygeneration schemes) including the CSP, MED, REF, and PH units. Here, the Valero et al. method (2013) is applied (Symbolic Thermoeconomics) since it provides a more detailed information about the cost formation process, the cost decomposition, and the residue cost allocation. Thus, a low aggregation level in the CSP plant (at level of individual components, such as turbines, preheaters, solar field, among others) was carried out to determine the contribution of each component of the CSP plant and the other process units in the production costs. The process of exergy cost formation is crucial for the integration of complex thermal systems since it enables determining where the savings on resources could be found, and therefore, identifying which specific components should be improved. Moreover, this technique could assess the impact of a partial failure in any device of the polygeneration plant over the products costs and the primary energy consumption, what is known as the thermoeconomic diagnosis of the plant operation. To sum up, in this paper Symbolic Thermoeconomics has been used to deepen in the cost formation process of a CSP polygeneration plant, by means of the detailed cost analysis of the sequential integration of selected configurations from stand-alone systems to cogeneration, trigeneration, and finally polygeneration. The main objective is then to find out the potential savings in terms of energy resources, within this complex integrated system.

4.2. Methodology

The present work considers a thermodynamic simulation procedure for modelling and evaluating the performance of multi-generation plants. First, stand-alone systems are modelled and validated against data reported in the technical literature. Then the models of those stand-alone systems are evaluated by integrating them in different solar multi-generation schemes, in which a concentrated solar power plant is considered as the prime mover. Multi-generation plants are configured considering different coupling points to operate in cogeneration, trigeneration, and polygeneration schemes. Validation of the cogeneration, trigeneration, and polygeneration schemes is arranged by the combination of the validated stand-alone systems. Then, the symbolic exergoeconomic methodology (Torres et al., 2008; Usón et al., 2012; Valero et al., 2013) is applied, which is based on the exergy cost theory (Torres et al., 2002). An aggregation level is selected for each physical structure to define the boundaries of the analysis. Then, the productive structure is determined, in which fuel and product streams are established. The model assesses the overall efficiency of the systems and uses variables such as fuel, product, exergy cost and exergy efficiency of each system component. After that, the thermoeconomic model is solved. The main parameters to analyze are the unit exergy cost of each product, their cost formation process, the total exergy cost of product, and the exergy efficiency. Additionally, it is possible to analyze the influence of the individual consumption of each component on the total amount of external resources required to obtain a product. Appendix F provides a flowchart of the overall simulation.

4.2.1. Stand-alone systems

The CSP plant analyzed herein is depicted in Figure 4-1, which is similar to the configuration of Andasol-1 power plant, located in Granada, Spain (NREL, 2013; Wagner & Gilman, 2011). The CSP plant consists of a solar field (SF) with parabolic trough collectors, a thermal energy storage system (TES), a power block, and a backup energy system (BS) (Blanco-Marigorta et al., 2011; NREL, 2013). The SF is composed of EuroTrough collectors, Schott PRT- 70 absorber tubes, and Dowtherm A as heat thermal fluid. The design temperature of the SF is of 393 ºC and 293 ºC as the outlet and inlet temperature. The direct normal irradiance and solar collector efficiency at design point (21st December solar noon for Crucero, Chile) are 1 010 W/m^2 and 0.72, respectively. The solar multiple is defined as 2.56, equivalent to the design point of Andasol-1, leading to a solar field aperture area of 510 120 m^2. The TES consists of a two-tank indirect system using molten salts as storage media, and with a design temperature of 386 ºC and 292 ºC for the hot and cold tanks, respectively. TES was designed to cover 12 hours of continuous operation. The power block consists of a regenerative Rankine cycle with reheat and six extractions, as described by Blanco-Marigorta et al. (2011). The gross power is 55.0 MW_e, the high-pressure turbine inlet pressure is 100.0 bar and the low-pressure turbine backpressure is 0.06 bar. The high and low-pressure turbines have isentropic efficiencies of 85.2 % and 85.0 %, respectively. The generator efficiency is considered as 98.0 %, and pumps' isentropic efficiency is 70.0 %.

The size of the plants has been established to satisfy a large-scale supply from the mining industry, such as observed in northern Chile, Australia, and North-Africa, which operates continuously and consequently presents a constant demand.

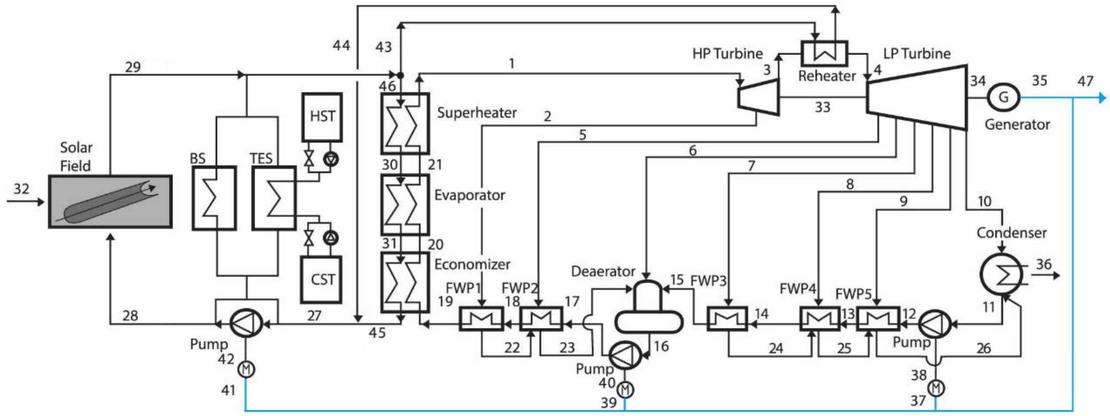

Figure 4- 1: Configuration of the CSP plant (physical structure of the system). CST: cold storage tank, FWP: feed water preheater, G: generator, HP: high pressure, HST: hot storage tank, LP: low pressure.

Figures 4-2 to 4-4 show the configuration of the thermal driven cycles analyzed herein. Each figure represents a simplified physical structure of each stand-alone scheme. Each system is fueled by natural gas (stream 1) to generate heat in the boiler (streams 2 and 3), where this thermal energy drives the multi-effect distillation, single-effect absorption refrigeration, and process heat module, respectively. The electricity supplied from the grid is represented by the Grid module that considers a combined cycle power plant. Additionally, it is considered a dissipative device in the case of the MED and REF; its purpose is to conveniently assess the costs of the residues generated.

Figure 4-2 shows the MED plant that consumes steam from the boiler (streams 2 and 3), seawater (stream 5), and electricity (stream 4) from the Grid. The MED plant generates fresh-water (stream 6) and presents two residues: the cooling seawater (Stream 7) and the brine (stream 8). The desalination plant is modeled considering 12 effects, parallel-cross feed and 11 feed preheaters, as suggested by Zak et al. (2012). The feed seawater intake temperature is considered at 25 °C and its salinity as 0.042 kg/kg; the feed seawater temperature after down condenser is established at 35 °C and the maximum salinity at each effect is 0.072 kg/kg. The top brine temperature is 65 °C, and the concentrate factor is estimated as 1.7. Then, the Gained Output Ratio determined according to the operation condition is 9.1, which is defined as the mass ratio between the distillate produced and the steam supplied to the system, while the specific heat consumption is 245.2 kJ/kg, the specific electricity consumption is 1.5 kWh/m^3, and the fresh-water production is 430.2 kg/s (37 168 m^3/day).

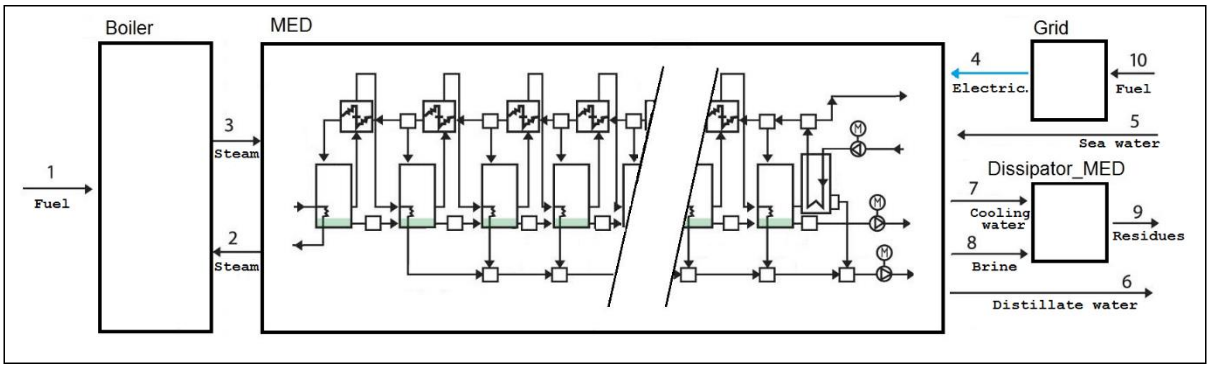

Figure 4- 2: Configuration stand-alone MED plant (simplified physical structure of the system).

Figure 4-3 depicts a stand-alone REF plant, driven by the thermal energy from the boiler (streams 2 and 3) and consuming electricity from the grid (stream 4). The REF plant generates chiller water (stream 5) and the cooling water (streams 6 and 7) is considered as residue. The refrigeration plant is configured by a single-effect LiBr-H_2O absorption chiller, which is modelled as described by Herold et al. (1996). It has a cooling capacity of 5 MW_{th} (1 421.73 tons) and a nominal coefficient of performance of 0.7 (Herold et al., 1996). The chilled water inlet and outlet temperatures are 10 and 6 °C, respectively, while the inlet and outlet cooling water temperatures are 25 and 35 °C, respectively. Finally, the heat medium operating temperature is 108.5 °C.

Regarding the stand-alone PH plant, Figure 4-4 shows its configuration where the module receives thermal energy from the boiler (streams 2 and 3) and electricity from the Grid (stream 4). A countercurrent shell-and-tube heat exchanger is configured to deliver a thermal load of 7 MW_{th} of heating (stream 5). The heat exchanger inlet and outlet temperatures are 63 and 90 °C, respectively.

The thermodynamics modelling of these stand-alone systems were validated by comparing simulations results with the reference cases. The power cycle was validated at the design point using the data of Andasol-1 reported by Blanco-Marigorta et al. (2011). Furthermore, the CSP plant was also validated by comparing the results between the IPSEpro/Matlab model and the case study (Andasol-1) by means of the SAM software (NREL, 2013). The results indicate differences of 3.6 % in terms of annual net electricity, and 1.5 % in thermal efficiency. Regarding the MED plant, it was validated considering the data reported by Zak et al. (2012) and from El-Dessouky et al. (2002). The results show no differences in the total distillate water production, 5.46 % error in terms of specific heat transfer area, and 7.81 % regarding the Gained Output Ratio. Finally, the thermodynamic model of the REF plant was validated using the data reported by Herold et al. (1996). The results show differences lower than 2.6 % in terms of the cooling capacity and COP.

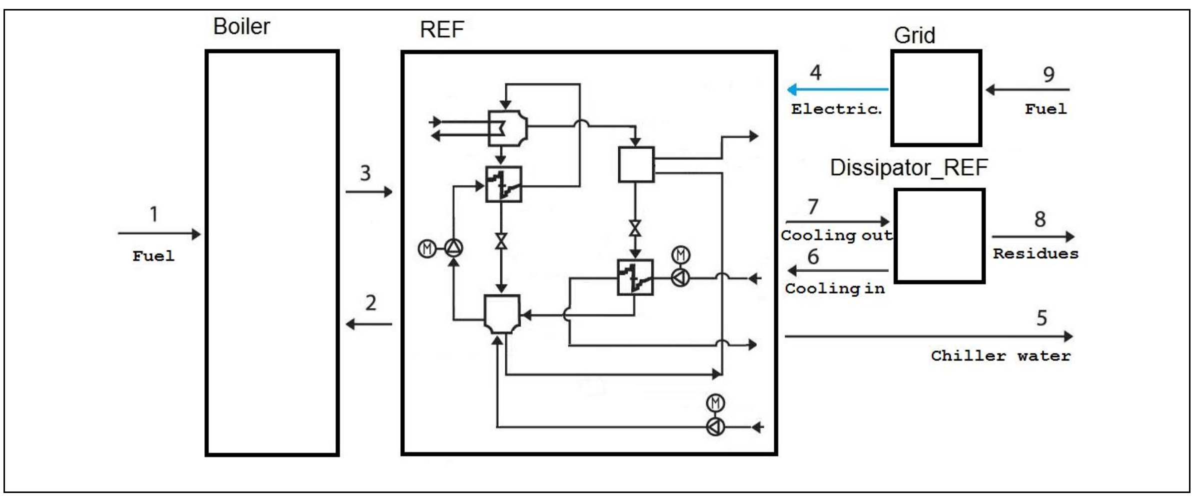

Figure 4- 3: Configuration stand-alone REF plant (physical structure of the system).

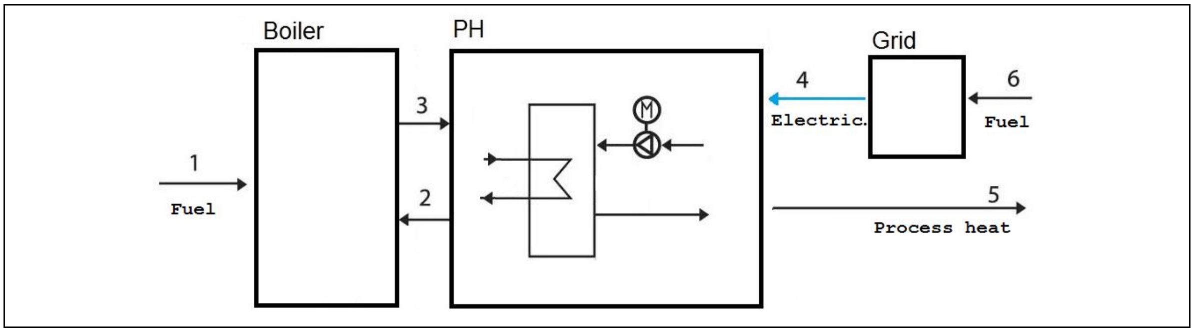

Figure 4- 4: Configuration stand-alone PH plant (physical structure of the system).

4.2.2. Cogeneration schemes

Different cogeneration schemes are configured as listed in Table 4-1, where the coupling points mentioned are related to the stand-alone CSP configuration. As the first effect of the MED plant must operate within a temperature range of 64 to 74 °C (Al-Karaghouli & Kazmerski, 2013), then two configurations of CSP-MED are considered. The first one considers the MED plant substituting the condenser of the power cycle (CSP-MED 1), leading to a modification on the turbine back pressure from 0.06 to 0.37 bar. Hence, to keep the gross power, the solar field aperture area is increased. On the other hand, if the MED plant is coupled to the sixth turbine extraction (CSP-MED 2), it is not necessary to modify the turbine back pressure, yet the solar field aperture area should also be increased, to keep the same gross power output. Regarding the fresh-water production a value of 466.4 kg/s is obtained in CSP-MED 1 configuration, where it is not possible to regulate the production independently because it depends on the electricity production. In the second configuration the production can be regulated, assuming a design point of 300 kg/s. In general, when any plant replaces the condenser of the power cycle, it is not possible to modify the production because the condenser operates according the conditions of the power cycle.

Note that the size of each plant for all solar multi-generation configurations (cogeneration, trigeneration, and polygeneration) is: 55 MW_e, 300 kg/s, 5 MW_{th}, and 7 MW_{th}, for the CSP, MED, REF, and PH plants, respectively. Only in the case that the MED plant replaces the condenser, water production capacity would be different since its production depends on the amount of energy that is rejected in the thermodynamic power cycle.

Table 4- 1: Cogeneration plants.

Cogeneration	Coupling point in CSP plant	Turbine back P bar	Aperture area m^2	Fresh-water kg/s
CSP-MED 1	MED replaces the condenser	0.37	598 452	466.4
CSP-MED 2	MED in 6th extraction	0.06	575 202	300.0
CSP-REF 1	REF in 5th extraction	0.06	520 861	-
CSP-REF 2	REF in 6th extraction	0.37	604 748	-
CSP-PH 1	PH between FWP3-FWP4	0.06	523 991	-
CSP-PH 2	PH in 5th extraction	0.06	520 691	-
CSP-PH 3	PH before collectors in SF	0.06	535 161	-
CSP-PH 4	PH after collectors in SF	0.06	535 169	-

In the case of the CSP-REF schemes, two options are considered, in which, the desorber of the single-effect absorption refrigeration plant should operate between 80 and 110 °C (Sarbu & Sebarchievici, 2015). When the REF plant is coupled to the 5th turbine extraction (CSP-REF 1), it is not necessary to modify the turbine back pressure, but the solar field aperture area must be increased, to keep equivalent power output. Conversely, if the REF plant is coupled to the 6th turbine extraction (CSP-REF 2), the turbine back pressure is modified from 0.06 to 0.37 bar, and the solar field aperture area must be increased too. Note that it is not recommended that the REF plant replaces the condenser of the power cycle because the higher turbine back pressure would mean an important penalty in power block's efficiency. Regarding the cooling production, it can be modified according to the demand in both configurations.

Regarding the CSP-PH, four configurations are analyzed, in which the PH is coupled between feed water preheaters, to the 5th turbine extraction, at the SF inlet, or at the SF outlet. In all of these cases, the turbine back pressure is not modified, however, the solar field should be increased, to deliver equivalent power output. The process heat production could vary depending on the demand in all configurations, but those variations would not affect the point of design of the cogeneration plant.

Note that the output of any product is dependent on the operating parameters of the CSP plant. When the production of any product is reduced, the power cycle needs less energy input to generate the nominal power output, and the control system could either reduce the energy input to the power cycle by partial defocusing solar collectors or reduce the thermal energy output from TES and/or backup system.

4.2.3. Trigeneration schemes

Table 4-2 shows different options of trigeneration schemes analyzed, in which two configurations of CSP-MED-REF, two of CSP-REF-PH, and four schemes of CSP-MED-PH are considered. The turbine back pressure is modified only when the MED plant replaces the condenser, and in all the schemes analyzed the size of the solar field is increased to maintain the same power output. Similarly to the cogeneration schemes, the production of fresh-water is fixed to the production of electricity when the condenser is replaced by the MED plant.

Table 4- 2: Trigeneration plants.

Trigeneration	Coupling point in CSP plant	Turbine back P bar	Aperture area m^2	Fresh-water kg/s
Trigen 1 (CSP-MED-REF 1)	MED replaces the condenser, REF in the 6^{th} extraction	0.37	603 721	443.6
Trigen 2 (CSP-MED-REF 2)	MED in the 6^{th} extraction, REF in the 5^{th} extraction	0.06	585 316	300.0
Trigen 3 (CSP-REF-PH 1)	REF in the 5^{th} extraction, PH in the 4^{th} extraction	0.06	533 768	-
Trigen 4 (CSP-REF-PH 2)	REF in the 5^{th} extraction, PH between FWP3-FWP4	0.06	533 716	-
Trigen 5 (CSP-MED-PH 1)	MED replaces the condenser, PH between FWP3-FWP4	0.37	611 378	453.0
Trigen 6 (CSP-MED-PH 2)	MED in the 6^{th} extraction, PH between FWP3-FWP4	0.06	588 390	300.0
Trigen 7 (CSP-MED-PH 3)	MED replaces the condenser, PH in the 5^{th} extraction	0.37	607 282	448.2
Trigen 8 (CSP-MED-PH 4)	MED in the 6^{th} extraction, PH in the 5^{th} extraction	0.06	585 151	300.0

4.2.4. Polygeneration schemes

Finally, four configurations of polygeneration schemes are analyzed, as listed in Table 4-3. The first configuration named Poly 1 is depicted in Figure 4-5a, where the MED plant replaces the condenser on stream 10, the REF plant is coupled to the 6^{th} turbine extraction on stream 9, and the PH plant is coupled between FWP3 and FWP4 on stream 14. The second scheme called Poly 2 and depicted in Figure 4-5b considers the MED plant coupled to the 6th turbine extraction on stream 9, the REF plant coupled to the 5th turbine extraction on stream 8, and the PH plant coupled between FWP3 and FWP4 on stream 14. The third one, Poly 3 is shown in Figure 4-5c; it is similar to Poly 1 except that the PH plant is coupled to the 5th turbine extraction on stream 8. Finally, in Figure 4-5d, Poly 4 is analogous to Poly 2, but the PH plant is coupled to the 4th turbine extraction on stream 7. Poly 1 and Poly 2 were analyzed in a previous study Leiva-Illanes et al. (2017) focusing on determining the actual cost of each product and establishing the effect of investment, fuel cost, demand, and sizing of the SF and TES in polygeneration plants located in an area with high solar irradiation conditions. Poly 1 was also used in the previous paper Leiva-Illanes et al. (2018) to compare the levelized cost method (Palenzuela et al., 2015; Short et al., 1995) and the thermoeconomic method (Bejan et al., 1996).

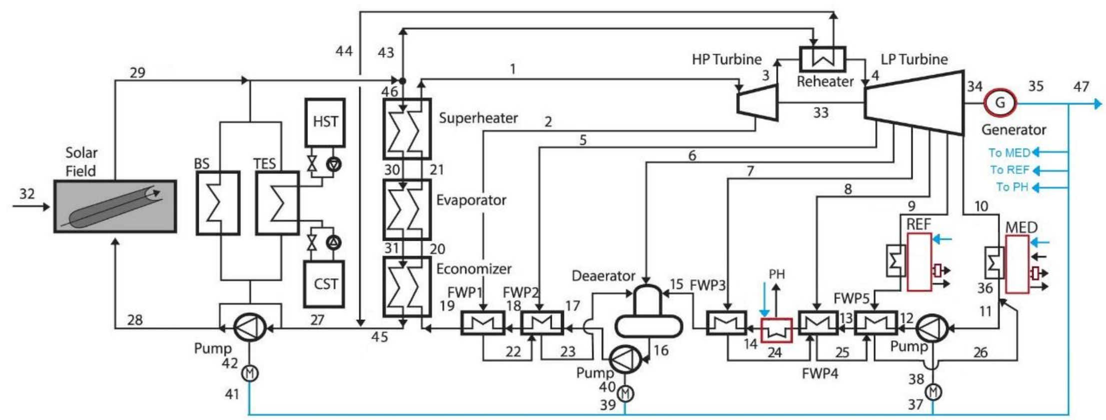
44
43
29
1
HP Turbine
Reheater
LP Turbine
3
4
34
35
47
G
Generator
33
46
Superheater
2
5
Solar
Field
32
BS
TES
HST
CST
30
21
Evaporator
6
7
8
9
10
To MED
To REF
To PH
REF
MED
31
20
Economizer
Deaerator
FWP1
FWP2
15
FWP3
PH
FWP5
36
11
19
18
17
28
27
45
12
13
14
24
25
22
23
16
Pump
42
40
39
41
FWP4
38
37
26

(a)

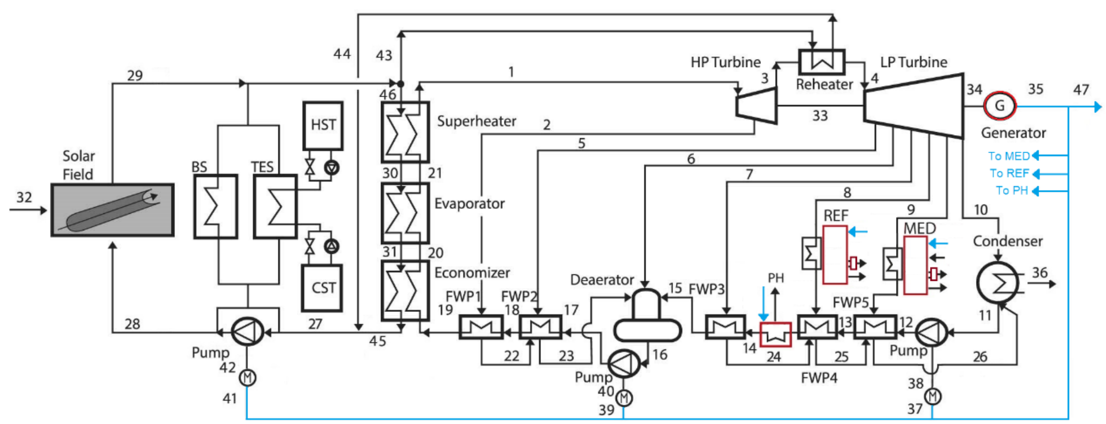
44
43
29
1
HP Turbine
Reheater
LP Turbine
3
4
34
35
47
G
Generator
33
46
Superheater
2
5
Solar
Field
32
BS
TES
HST
CST
30
21
Evaporator
6
7
8
9
10
To MED
To REF
To PH
REF
MED
Condenser
36
31
20
Economizer
Deaerator
FWP1
FWP2
15
FWP3
PH
FWP5
11
19
18
17
28
27
45
12
13
14
24
25
22
23
16
Pump
42
40
39
41
FWP4
38
37
26

(b)

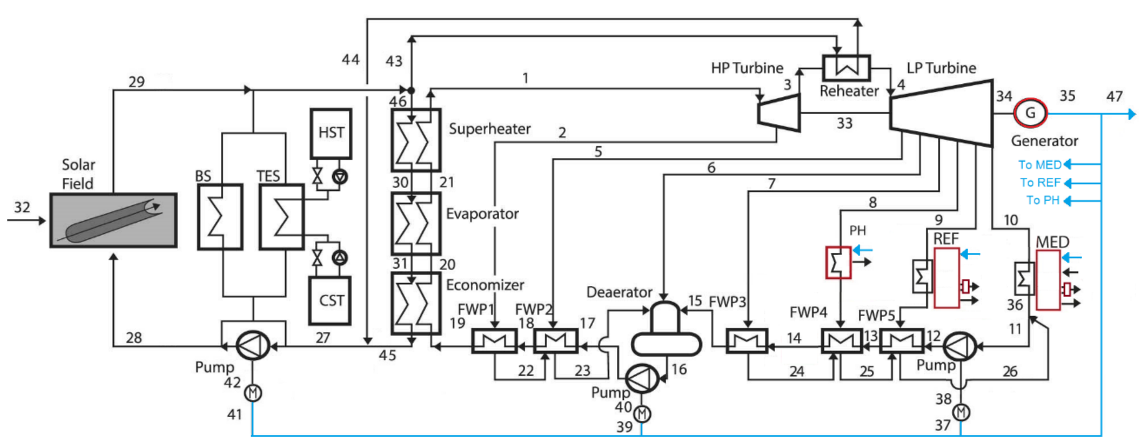
44
43
29
1
HP Turbine
Reheater
LP Turbine
3
4
34
35
47
G
Generator
33
46
Superheater
2
5
Solar
Field
32
BS
TES
HST
CST
30
21
Evaporator
6
7
8
9
10
To MED
To REF
To PH
PH
REF
MED
36
31
20
Economizer
Deaerator
FWP1
FWP2
15
FWP3
FWP4
FWP5
11
19
18
17
28
27
45
12
13
14
24
25
22
23
16
Pump
42
40
39
41
38
37
26

(c)

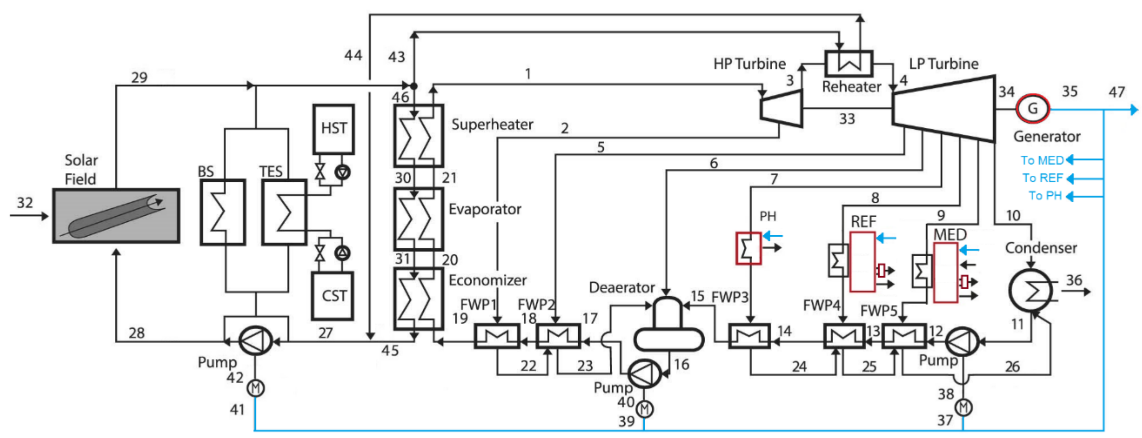

(d)

Figure 4- 5: Configuration CSP-polygeneration schemes. (a) Poly 1, (b) Poly 2, (c) Poly 3, (d) Poly 4.

Table 4- 3: Polygeneration plants.

Polygeneration	Coupling point in CSP plant	Turbine back P bar	Aperture area m^2	Fresh-water kg/s
Poly 1	MED replaces the condenser, REF in the 6th extraction, PH between FWP3-FWP4	0.37	616 650	430.2
Poly 2	MED in the 6th extraction, REF in the 5th extraction, PH between FWP3-FWP4	0.06	598 510	300.0
Poly 3	MED replaces the condenser, REF in the 6th extraction, PH in the 5th extraction	0.37	612 558	425.4
Poly 4	MED in the 6th extraction, REF in the 5th extraction, PH in the 4th extraction	0.06	598 573	300.0

The performance of the solar polygeneration schemes was evaluated, considering the features established by the design point, and considering the data of a meteorological year (Escobar et al., 2014) in a high solar irradiation area. Software IPSEpro (SimTech GmbH, 2011) was employed for modelling and simulating the different systems, were the IPSEpro-MDK and IPSEpro-PSE modules were used. IPSEpro-MDK is a programming environment that offers all the capabilities required to define and build new component models in an existing library or the creation of a new library, and to translate them into a language interpretable by IPSEpro-PSE. IPSEpro-PSE is a process simulation environment that allows establishing mass and energy balances, simulating different kinds of processes, through iterative Newton-Raphson method. The main advantage is the rapid convergence of the system, with an average calculation time of only few seconds. The simulation tool allows determining simulation of steady state operating conditions. Time-dependent phases in plant operation can be simulated using IPSEpro-PSXLink, that allows integrating IPSEpro-PSE projects with Microsoft Excel. The exergoeconomic evaluation was conducted using MATLAB and the ExIO module (Torres & Valero, 2012) as a complement of the Microsoft Excel.

4.2.5. Exergoeconomic method

The symbolic exergoeconomic methodology (Torres et al., 2008; Usón et al., 2012; Valero et al., 2013) is applied, that is based on the exergy cost theory (ECT) (Torres et al., 2002). The method provides a general criterion that enables to assess the efficiency of energy systems and rationally explains the process of cost formation of products. Thus, it is a cost accounting methodology that proposes methods to determine the number of resources required for delivering a specific product. The cost formation process can be easily obtained by using matrix algebra. The exergy cost theory requires a mathematical modelling of the physical and productive structure of the system. This last structure is built according to the purpose of each component and shows the origin of the resources of each component and its products. Each plant has only one physical structure to describe the physical relations between the process units, but various productive structures can be defined depending on the fuel and product definitions as well as the disaggregation level selected. The disaggregation level is interpreted as the degree of accuracy of the analysis. Each subsystem can be part of an equipment, an equipment itself, or a group of equipment. The productive diagram is a graphic representation of the thermoeconomic model of the plant, in which the inputs of a component are its resources, and the outputs of a component are its products. This structure is composed of n components connected by flows characterized by their exergy. Each component consumes resources from other components or from the environment (those resources are named Fuel), to produce useful effects for other components or for the environment (those useful effects are named Product). Fuel (F) is partially transformed into product (P) and partially destroyed as irreversibility (I). A flow from component i to component j is represented by the exergy flow, then, the Fuel and Product is defined as:

$$F_i = P_i + I_i = \sum_{j=0}^{n} E_{ji} \tag{4.1}$$

$$P_i = F_i - I_i = \sum_{j=0}^{n} E_{ij} \tag{4.2}$$

where E_{ij} is the exergy flow, the subscripts i and j are generic components.

The fuel-product presentation is the adjacency matrix of the productive graph, which allows getting all flows within the productive structure, and is based on distribution coefficients y_{ij} that indicate the proportion of the production of the j-th component used as resource for the i-th component. It shows how the product of a component is distributed among the other components and the environment.

$$y_{ij} = \frac{E_{ij}}{P_j} \tag{4.3}$$

Expressing the Equation 1 as function of y_{ij}, it yields:

$$F_i = E_{0i} + \sum_{j=1}^{n} E_{ji} = E_{0i} + \sum_{j=1}^{n} y_{ij} \cdot P_j \tag{4.4}$$

The previous equation in matrix notation is:

$$\boldsymbol{F} = \boldsymbol{F}_e + \langle \boldsymbol{FP} \rangle \cdot \boldsymbol{P} \tag{4.5}$$

where $\boldsymbol{F}$ and $\boldsymbol{P}$ are vectors of all fuels and products, $\boldsymbol{F}_e$ is the vector of external resources, and $\langle \boldsymbol{FP} \rangle$ is a matrix composed of elements y_{ij}.

Similarly, with the same procedure, it is obtained:

$$\boldsymbol{P} = (\boldsymbol{K}_D - \langle \boldsymbol{FP} \rangle)^{-1} \cdot \boldsymbol{F}_e \tag{4.6}$$

where $\boldsymbol{K}_D$ is a diagonal matrix containing the unit exergy consumptions of all components (k_i), defined as:

$$k_i = \frac{F_i}{P_i} = \frac{1}{\psi_i} \tag{4.7}$$

where ψ_i is the exergy efficiency.

The unit exergy cost of a flow c_{ij} is the relation between its exergy cost of a flow C_{ij} and its exergy, where C_{ij} is the amount of exergy resources consumed by that system used to produce this flow.

$$c_{ij} = k_{ij}^* = \frac{C_{ij}}{E_{ij}} \tag{4.8}$$

At the same time, $\boldsymbol{I}$ is a vector of all irreversibilities, and it is expressed as:

$$\boldsymbol{I} = (\boldsymbol{K}_D - \boldsymbol{U}_D) \cdot (\boldsymbol{K}_D - \langle \boldsymbol{FP} \rangle)^{-1} \cdot \boldsymbol{F}_e = (\boldsymbol{K}_D - \boldsymbol{U}_D) \cdot \boldsymbol{P} \tag{4.9}$$

where $\boldsymbol{U}_D$ is the identity matrix.

Equation 4-6 allows calculating the products of all components starting from the external resources consumed by the plant ($\boldsymbol{F}_e$), using the parameters that define the components (unit exergy consumptions and distribution coefficients).

In the thermoeconomic analysis, energy systems, such as polygeneration plants, could present productive and dissipative components. The productive components provide functional products, fuel (resources) to other processes, as well as residue and waste disposals. Likewise, the dissipative components are required to reduce or eliminate the environment impact of residues and waste, to maintain the operating conditions of the system and improve its efficiency.

According to the cost model, the exergy cost of the product is defined as:

$$C_{P,i} = C_{F,i} + C_{R,i} \tag{4.10}$$

where C is the exergy cost, and the subscripts P, F, and R mean product, fuel, and residues, respectively.

The costs of the external resources are known values as:

$$C_{e,i} = E_{0i} \tag{4.11}$$

and the cost of each flow making up the product is proportional to its exergy

$$C_{ij} = c_{P,i} \cdot E_{ij} \tag{4.12}$$

where $c_{P,i}$ is the unit exergy cost of the product of i-th component.

The cost of the fuel used in each component is calculated by

$$C_{F,i} = C_{e,i} + \sum_{r \epsilon V_P} C_{ji} = C_{e,i} + \sum_{r \epsilon V_P} y_{ij} \cdot C_{P,j} \tag{4.13}$$

where C_{ji} is the exergy cost of the j-th component used as fuel in the i-th component, and V_P represents the set of the productive components. In matrix notation it is expressed as

$$\boldsymbol{C}_F = \boldsymbol{C}_e + \langle \boldsymbol{FP} \rangle \cdot \boldsymbol{C}_P \tag{4.14}$$

The exergy cost of residues allocated to each productive unit is:

$$C_{R,i} = \sum_{r \epsilon V_D} C_{ri} = \sum_{r \epsilon V_D} \beta_{ir} \cdot C_{P,r} \tag{4.15}$$

where C_{ri} is the exergy cost of the residues dissipated in the r-th component that has been generated by the i-th productive component, β_{ir} is the residue cost distribution ratio of the dissipative unit, V_D is the set of the dissipative system components. The residue cost distribution ratios represent the portion of the cost of the residue dissipated in the r-th component which has been generated in the i-th productive component. In matrix notation holds:

$$\boldsymbol{C}_R = \langle \boldsymbol{RP} \rangle \cdot \boldsymbol{C}_P \tag{4.16}$$

where $\langle \boldsymbol{RP} \rangle$ is a matrix composed of elements β_{ij}.

Regarding to the production cost decomposition, the exergy cost of the product is decomposed into two parts:

$$\boldsymbol{C}_P = \boldsymbol{C}_e \cdot (\boldsymbol{U}_D - \langle \boldsymbol{FP} \rangle)^{-1} + \boldsymbol{C}_R \cdot (\boldsymbol{U}_D - \langle \boldsymbol{FP} \rangle)^{-1} = \boldsymbol{C}_P^e + \boldsymbol{C}_P^r \tag{4.17}$$

where $\boldsymbol{C}_P^e$ is the exergy cost due to irreversibilities of the components and $\boldsymbol{C}_P^r$ is the exergy cost due to the residues allocation.

The Equation 4-17 could be written including the exergy cost irreversibilities relationship in explicit form. In this equation the residue costs are considered and accounted as external irreversibilities. In matrix notation it is given as:

$$\boldsymbol{C}_P = \{\boldsymbol{P} + (\boldsymbol{U}_D - \langle \boldsymbol{FP} \rangle)^{-1} \cdot \boldsymbol{I}\} + \{(\boldsymbol{U}_D - \langle \boldsymbol{FP} \rangle)^{-1} \cdot \boldsymbol{C}_R\} = \boldsymbol{C}_P^e + \boldsymbol{C}_P^r \qquad (4.18)$$

Clearly, the first term represents the production cost due to the sum of the irreversibilities accumulated along the process, and the second the production cost due to the residues cost. In the same way, the unit exergy cost of the product is decomposed into two parts:

$$c_p = c_P^e + c_P^r \qquad (4.19)$$

where c_P^e is the unit production cost due to irreversibilities of the components and c_P^r is the unit production cost due to the residues. They are calculated by:

$$c_P^e = (\boldsymbol{U}_D - \langle \boldsymbol{FP} \rangle)^{-1} \cdot \boldsymbol{c}_e \qquad (4.20)$$

$$c_P^r = (\boldsymbol{U}_D - \langle \boldsymbol{FP} \rangle)^{-1} \cdot \boldsymbol{c}_R \qquad (4.21)$$

where $\boldsymbol{c}_e$ is the unit exergy cost of the external resources and $\boldsymbol{c}_R$ is the unit exergy cost of the residues.

Summarizing, the process to assess the cost of the flow streams and processes in a polygeneration plant helps to understand the process of cost formation, from the input resources to the final products.

In this analysis, different levels of disaggregation were taken: for the CSP plant, it is considered at the level of components as shown in the physical structure in Figure 4-1, and the systems providing by-products are considered at the level of a unique subsystem as depicted in Figures 4-2 to 4-5. These considerations are due to the fact that the solar polygeneration plant was configured as a topping cycle, in which the priority is the production of electricity while the by-products are generated according to the availability of thermal energy in the power cycle. Therefore, any failure or operation problem in the CSP plant affects the other plants (MED, REF, or PH) and not vice versa, unless one of the other plants replaces the condenser of the power cycle.

Tables 4-4 to 4-7 show the Fuel-Product definition for the stand-alone systems. All the plants have productive and dissipative components, except the stand-alone PH plant that only has productive components. The dissipative components are the condenser in the CSP plant, the Dissipator_MED, and the Dissipator_REF. The purpose of the dissipative devices is to consider the residue generated (that is, that output which is not considered as a product) in the productive unit. In this model, it is assumed that the residues leave a dissipative component, where all the abatement costs of these residues are charged (proportional to the cost of products dissipated). Note that the first row contains the interactions between the system and the environment because the latter is also considered as a process.

Table 4- 4: Fuel-Product definition of the stand-alone CSP plant.

	Component	Fuel	Product
0	Environment	$E_{47}+E_{36}$	E_{32}
1	Collectors	E_{32}	$E_{29}-E_{28}$
2	Pump1	E_{42}	$E_{28}-E_{27}$
3	Motor1	E_{41}	E_{42}
4	Economizer	$E_{31}-E_{45}$	$E_{20}-E_{19}$
5	Evaporator	$E_{30}-E_{31}$	$E_{21}-E_{20}$
6	Superheater	$E_{46}-E_{30}$	$E_{1}-E_{21}$
7	Reheater	$E_{43}-E_{44}$	$E_{4}-E_{3}$
8	HP_Turbine	$E_{1}-E_{2}-E_{3}$	E_{33}
9	LP_Turbine	$E_{4}-E_{5}-E_{6}-E_{7}-E_{8}-E_{9}-E_{10}+E_{33}$	E_{34}
10	Generator	E_{34}	E_{35}
11	Pump3	E_{38}	$E_{12}-E_{11}$
12	Motor3	E_{37}	E_{38}
13	FWP5	$E_{9}+E_{25}-E_{26}$	$E_{13}-E_{12}$
14	FWP4	$E_{8}+E_{24}-E_{25}$	$E_{14}-E_{13}$
15	FWP3	$E_{7}-E_{24}$	$E_{15}-E_{14}$

16	Deaerator	$E_6+E_{15}+E_{23}$	E_{16}
17	Pump2	E_{40}	$E_{17}-E_{16}$
18	Motor2	E_{39}	E_{40}
19	FWP2	$E_5+E_{22}-E_{23}$	$E_{18}-E_{17}$
20	FWP1	E_2-E_{22}	$E_{19}-E_{18}$
21	Node1	$E_{44}+E_{45}$	E_{27}
22	Node2	E_{29}	$E_{43}+E_{46}$
23	Node3	E_{35}	$E_{47}+E_{37}+E_{39}+E_{41}$
24	Condenser	$E_{10}-E_{11}+E_{26}$	E_{36}

Table 4- 5: Fuel-Product definition of the stand-alone MED plant.

	Component	Fuel	Product
0	Environment	E_6+E_9	$E_1+E_{10}+E_5$
1	Boiler	E_1	E_3-E_2
2	MED	$(E_3-E_2)+E_4+E_5$	$E_6+E_7+E_8$
3	Grid	E_{10}	E_4
4	Dissipator_MED	E_7+E_8	E_9

Table 4- 6: Fuel-Product definition of the stand-alone REF plant.

	Component	Fuel	Product
0	Environment	E_5+E_8	E1+E_9
1	Boiler	E_1	E_3-E_2
2	REF	$E_3-E_2+E_4$	$E_5+(E_7-E_6)$
3	Grid	E_9	E_4
4	Dissipator_REF	E_7-E_6	E_8

Table 4- 7: Fuel-Product definition of the stand-alone PH plant.

	Component	Fuel	Product
0	Environment	E_5	E_1+E_6
1	Boiler	E_1	E_3-E_2
2	PH	$(E_3-E_2)+E_4$	E_5
3	Grid	E_6	E_4

Similarly, the same procedure of defining Fuel-Product streams is carried out for the cogeneration, trigeneration, and polygeneration schemes.

Once Fuel-Product streams are defined, the exergy rate of each flow must be calculated. The exergy rate of a matter flow can be expressed in terms of physical, chemical, kinetic, and potential component. While, the exergy rate of heat (E_Q) and work (E_W) are defined as

$$\mathrm{E}_Q = \left(1 - \frac{T_0}{T_j}\right) \cdot \dot{Q}_j \tag{4.22}$$

$$E_W = \dot{W}_j \tag{4.23}$$

where T_0 is the temperature of reference, in K, $\dot{Q}$ is the heat transfer rate, and $\dot{W}$ is the work power. The subscripts Q, j, and W are the heat transfer, control volume, and work, respectively. The reference environment assumed is T_0=25 °C and P_0=1.013 bar. Similarly, the reference mass fraction of LiBr and water salinity is considered of 0.5542 kg/kg (Palacios-Bereche & Gonzales, 2012) and 0.042 kg/kg (Sharqawy et al., 2011), respectively. The exergy rate of fossil fuel is calculated with following relation (Ahmadi et al., 2011):

$$E_{ff} = \dot{m}_{ff} \cdot \xi \cdot LHV \tag{4.24}$$

where ξ is an experimental correlation (Ahmadi et al., 2011), LHV is the lower heating value of the fossil-fuel. The subscript ff denotes fossil-fuel.

$$\xi = 1.033 + 0.0169 \cdot \frac{y}{x} - \frac{0.0698}{x} \tag{4.25}$$

where x and y are the composition $C_xH_y$in a general gaseous fuel. In the present work, the natural gas is considered as methane (CH_4).

The exergy rates of solar radiation are determined by Patela's equation (2010), which is one of the most cited models in the literature. It is defined as:

$$E_{sun} = A \cdot G_b \cdot (1 + \frac{1}{3}\left(\frac{T_0}{T_{sun}}\right)^4 - \frac{4}{3}\left(\frac{T_0}{T_{sun}}\right)) \tag{4.26}$$

where $\boldsymbol{A}$ is the solar field aperture area, $\boldsymbol{G_b}$ is the direct normal irradiance, and $\boldsymbol{T_{sun}}$ is the apparent temperature of the sun, taken as 6 000 K (Petela, 2010).

Other assumptions were adopted throughout the simulation process, as listed below:

- For stand-alone MED, REF, and PH plants, the unit exergy cost of the electricity from the grid is assumed to be 2.44 kW/kW (C. Torres et al., 2008).
- Nominal conditions of all the configurations have been used to perform the exergy costs.

4.3. Results and discussion

4.3.1. Stand-alone plants

The unit exergy cost of product (electricity, water, cooling and heat), the exergy cost of product, and the exergy efficiency in stand-alone systems are shown in Table 4-8. Note that the unit exergy cost represents the amount of exergy required to get a unit of exergy of the product, i.e. the resources required to carry out the production. For instance, a unit of exergy cost of electricity of 3.51 kW/kW means that 3.51 kW of exergy of resources are needed for producing 1 kW of electricity. The exergy cost of product represents the resources required (in exergy units) to carry out the production, for instance, an exergy cost of electricity of 193 476 kW means that 193 476 kW of exergy of resources are needed for producing 55.0 MW_e of electricity. On the other hand, the unit exergy cost and the exergy cost allow measuring in the same unit resources and products of different nature, such as electricity, water, cooling, process heat, resources, and waste. Finally, the exergy efficiency is the ratio between the exergy rate of product and the exergy rate of fuel. Note that $\boldsymbol{c_p}$ and $\boldsymbol{C_p}$ can be transformed into economic costs expressed in USD/kWh and USD/h respectively the validity of the method (Valero & Torres, 2016) is maintained if investment and operation costs are considered. Then, production costs can be broken down into three contributions: the cost of the resources needed to obtain it (due to the irreversibilities of the components), non-thermodynamic costs (due to the investment and operation costs), and waste (residues).

This analysis was already conducted in a previous study (Leiva-Illanes et al., 2017) to Poly 1 and Poly 2 schemes, as well as to stand-alone systems. The stand-alone CSP plant was analyzed considering a turbine back pressure of 0.06 bar. This parameter is modified when is coupled to other technologies as described for the cases of multi-generation. Therefore, if the turbine back pressure is 0.37 bar in a stand-alone CSP plant, the unit exergy cost of electricity would be increased to 4.14 kW/kW. The total exergy cost of the stand-alone systems is distributed as 58.2 %, 37.0 %, 2.4 %, and 2.3 % in electricity, water, cooling, and process heat, respectively. Therefore, in terms of exergy cost, the main impact is reflected in the electricity production, followed by the water production.

Table 4- 8: Unit exergy cost, exergy cost, and exergy efficiency in stand-alone plants.

Stand-alone plant, product	c_p kW/kW	C_p kW	ψ_i %
Stand-alone CSP, electricity	3.51	193 476	29.0
Stand-alone MED, water	55.55	123 102	1.9
Stand-alone REF, cooling	25.22	7 951	4.0
Stand-alone PH, heat process	7.56	7 781	13.2
Stand-alone systems, all products	-	332 310	18.0

The cost decomposition for the stand-alone CSP plant are depicted in Figure 4-6, showing how the unit cost of product is formed as the sum of the irreversibility contributions of the components and the residues (according to Equations 4-18 and 4-19). The contribution on the unit exergy cost of electricity from the productive devices is 3.33 kW/kW and the contribution from the condenser (dissipative device) is 0.18 kW/kW. Note that the contribution from the environment is 1 kW/kW, according to the proposition that says that the cost of external resources is equal to its exergy (Equation 4-11). The main components that contribute to the cost formation of electricity cost (see Generator in the graph and in the eighth column of the table in Figure 4-6), in descending order of importance, are: solar collectors (44.3 %), evaporator (8.1 %), condenser (5.1 %), reheater (3.6 %), low-pressure turbine (2.8 %), economizer (2.4 %), superheater (1.9 %), and Generator (1.2 %). The most significant exergy destruction is observed in the solar field, attributable to the irreversibilities associated to the large temperature difference between the sun and the heat transfer fluid. Furthermore, it is observed that the exergy cost is allocated to the rest of components according to a topping cycle scheme. On the other hand, the condenser as a dissipative component, is allocated to all productive units. It interacts with other components and allows to close the thermodynamic power cycle. As its operating temperature is quite low, from the point of view of the Second Law of Thermodynamics, its contribution to exergy costs is not significant, being the steam generator (or solar collectors in this case) the main inefficient component. It is also possible to analyze the cost decomposition of any other component, such as FWPs, collectors or others; however, in these cases, it is important to study the cost decomposition in which the final product is generated (Generator in Figure 4-6).

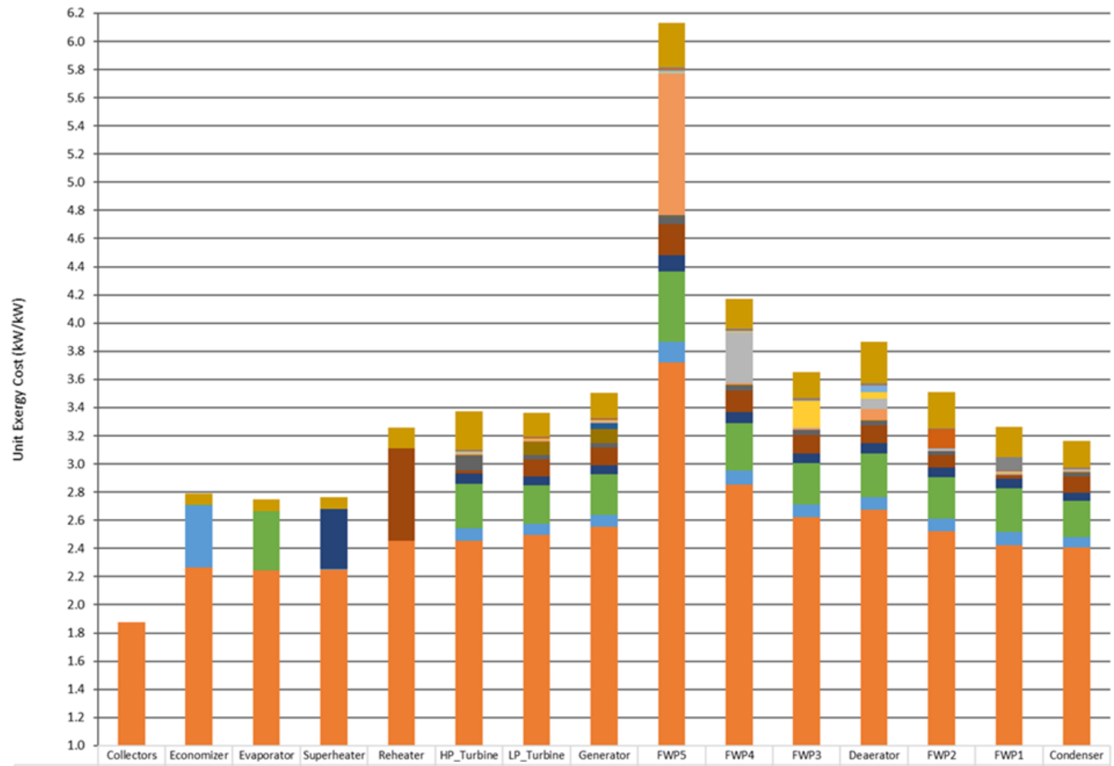

	Collectors	Economizer	Evaporator	Superheater	Reheater	HP_Turbine	LP_Turbine	Generator	FWP5	FWP4	FWP3	Deaerator	FWP2	FWP1	Condenser
Condenser	0.0000	0.0815	0.0802	0.0806	0.1446	0.2722	0.1716	0.1786	0.3125	0.2127	0.1862	0.2956	0.2578	0.2171	0.1884
FWP1	0.0000	0.0000	0.0000	0.0000	0.0000	0.0073	0.0064	0.0066	0.0116	0.0079	0.0069	0.0072	0.0069	0.0897	0.0060
FWP2	0.0000	0.0000	0.0000	0.0000	0.0000	0.0065	0.0056	0.0059	0.0103	0.0070	0.0061	0.0064	0.1342	0.0064	0.0053
Deaerator	0.0000	0.0000	0.0000	0.0000	0.0000	0.0049	0.0042	0.0044	0.0077	0.0052	0.0046	0.0459	0.0046	0.0048	0.0040
FWP3	0.0000	0.0000	0.0000	0.0000	0.0000	0.0053	0.0046	0.0048	0.0084	0.0057	0.1906	0.0502	0.0050	0.0052	0.0044
FWP4	0.0000	0.0000	0.0000	0.0000	0.0000	0.0076	0.0066	0.0069	0.0120	0.3623	0.0072	0.0715	0.0071	0.0074	0.0062
FWP5	0.0000	0.0000	0.0000	0.0000	0.0000	0.0083	0.0072	0.0075	1.0025	0.0090	0.0079	0.0784	0.0078	0.0082	0.0068
Generator	0.0000	0.0002	0.0002	0.0002	0.0003	0.0012	0.0011	0.0423	0.0019	0.0013	0.0012	0.0017	0.0011	0.0012	0.0010
LP_Turbine	0.0000	0.0006	0.0006	0.0006	0.0007	0.0027	0.0947	0.0986	0.0045	0.0031	0.0027	0.0039	0.0027	0.0027	0.0023
HP_Turbine	0.0000	0.0002	0.0002	0.0002	0.0002	0.1077	0.0304	0.0317	0.0555	0.0378	0.0331	0.0322	0.0220	0.0048	0.0286
Reheater	0.0000	0.0007	0.0007	0.0007	0.6545	0.0193	0.1210	0.1259	0.2203	0.1500	0.1313	0.1280	0.0873	0.0190	0.1137
Superheater	0.0000	0.0004	0.0004	0.4254	0.0004	0.0723	0.0630	0.0656	0.1147	0.0781	0.0684	0.0714	0.0683	0.0710	0.0592
Evaporator	0.0000	0.0016	0.4187	0.0016	0.0019	0.3140	0.2734	0.2847	0.4980	0.3390	0.2968	0.3098	0.2963	0.3082	0.2571
Economizer	0.0000	0.4416	0.0005	0.0005	0.0006	0.0937	0.0816	0.0850	0.1486	0.1012	0.0886	0.0925	0.0884	0.0920	0.0767
Collectors	0.8740	1.2656	1.2445	1.2515	1.4523	1.4515	1.4936	1.5552	2.7204	1.8518	1.6213	1.6723	1.5219	1.4247	1.4045
Environment	1.0000	1.0000	1.0000	1.0000	1.0000	1.0000	1.0000	1.0000	1.0000	1.0000	1.0000	1.0000	1.0000	1.0000	1.0000

Figure 4- 6: Cost decomposition in stand-alone CSP plant.

Figure 4-7 shows the cost decomposition in the other stand-alone systems. The unit exergy cost of each product is the sum of the irreversibility contributions of the productive and dissipative devices that preceded the product generated, then the production cost of a component equals the cost of the resources required to obtain such product, as well as the cost of the residues generated. Consequently, the cost of the residues allocated to each productive component may be considered as external resources used to compensate the cost formation of the residues (See MED, REF, and PH in the graph and table in Figure 4-7). The main contribution in the cost of each product comes from the boiler with 49.2 %, 49.5 %, and 80.2 % in MED, REF, and PH respectively, being the higher heat source and then having the higher exergy destruction. Note that since both the MED plant and the REF plant include a dissipative component to operate, they participate in the costs formation with 40.9 % and 38.6 %, respectively. In the case of the PH major exergy costs comes from the boiler and a residual additional cost comes from the heat exchanger (6.5 %) to accommodate the heat supply.

The method described above is based on the classification of the system flows in fuels, products, and residues, in which all costs yielded by the production process must be included in the cost of the final products. The residues are unintended remaining flows of matter or energy in any productive process. That flows could be partially used in further processes or become unusable or unwanted waste disposals (Torres et al., 2008). Additionally, there are dissipative components, whose purpose is to eliminate the undesirable flows.

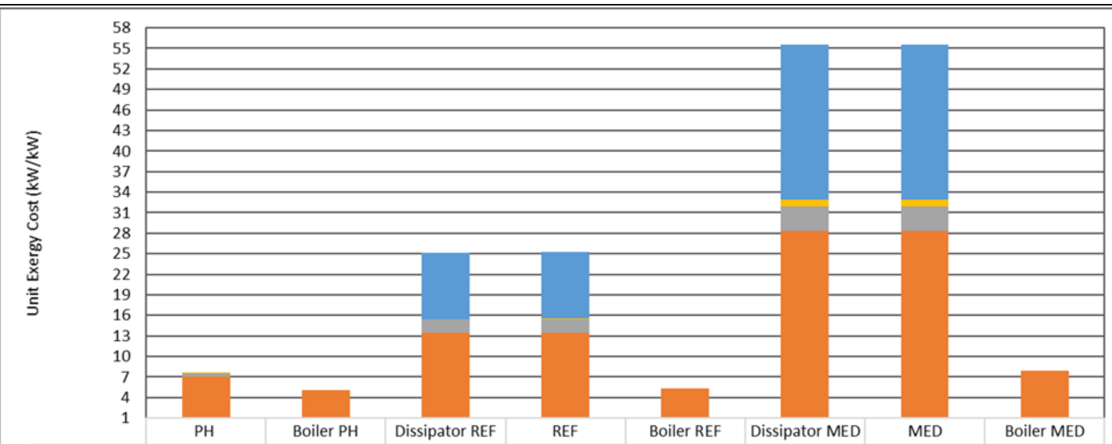

	PH	Boiler PH	Dissipator REF	REF	Boiler REF	Dissipator MED	MED	Boiler MED
Dissipator	0.000	0.000	9.722	9.738	0.000	22.693	22.693	0.000
Grid	0.002	0.000	0.046	0.046	0.000	0.926	0.926	0.000
Equipment	0.493	0.000	1.952	1.955	0.000	3.617	3.617	0.000
Boiler	6.064	4.065	12.467	12.486	4.271	27.310	27.310	6.873
Environment	1.000	1.000	1.000	1.000	1.000	1.000	1.000	1.000

Figure 4- 7: Cost decomposition in stand-alone MED, REF, and PH plants.

4.3.2. Cogeneration plants

The results of cogeneration plants are shown in Table 4-9, in which CSP-MED 1, CSP-REF 1, and CSP-PH 2 are pointed out as the best options for producing electricity-water, electricity-cooling, and electricity-process heat, respectively. These configurations presented the lower unit exergy cost and were reached when MED plant replaced the condenser of the power cycle, the REF plant and the PH plant were coupled in the 5th turbine extraction, in the CSP-MED, CSP-REF, and CSP-PH, respectively. However, CSP-PH 2 is close to CSP-PH 1 in terms of electricity production, but it presents about 12 % of difference in terms of process heat. The unit exergy cost allows to compare schemes presenting the same or different production capacities, however it does not allow to include the unit exergy cost of each product to calculate a total unit exergy cost of the products. On the other hand, the exergy cost of each product can be considered for the assessment of the total exergy cost; however, for comparing plants, they must have the same production capacities. For example, in the case CSP-MED 1, the unit exergy costs (of both products) are lower than in the CSP-MED 2, but the total energy cost is higher. This difference of both indicators is explained by the different capacities of the MED plant; therefore, the total exergy cost is not adequate to compare plants with different production capacities. Similarly, when comparing CSP-PH 3 and CSP-PH 4 schemes, the unit exergy cost of electricity is higher for the CSP-PH 3, but the unit exergy cost of heat is lower. Therefore, it is not possible to discriminate which configuration is better, but considering that both plants have the same production capacities, then the total exergy cost can be used to compare them in detail. Therefore, CSP-PH 4 performs better than CSP-PH 3 because in the CSP-PH 4 scheme the total exergy cost is lower. Regarding the exergy efficiency, when comparing plants, the higher exergy efficiency does not necessarily imply that the plant is more convenient. For instance, in the CSP-MED 1 plant the exergy efficiency is lower than in the CSP-MED 2 plant, nevertheless, CSP-MED 1 is more convenient, as mentioned above.

Table 4- 9: Unit exergy cost, total exergy cost of product, and exergy efficiency in cogeneration plants.

Cogeneration	c_p electricity kW/kW	c_p water kW/kW	c_p cooling kW/kW	c_p heat kW/kW	C_p total kW	ψ_i %
CSP-MED 1	3.26	23.04	-	-	234 849	25.6
CSP-MED 2	3.39	23.86	-	-	223 294	26.3
CSP-REF 1	3.50	-	15.07	-	197 379	28.6
CSP-REF 2	4.08	-	17.64	-	230 226	24.7
CSP-PH 1	3.51	-	-	5.11	198 533	28.8
CSP-PH 2	3.50	-	-	4.49	197 266	29.0
CSP-PH 3	3.52	-	-	8.34	202 679	28.2
CSP-PH 4	3.50	-	-	9.36	202 641	28.2

The comparison between cogeneration and stand-alone systems shows that the analyzed solar cogeneration plants are more cost-effective, except in the cases CSP-PH 3 and CSP-PH 4. These cases are not favorable because the process heat module is coupled close to the SF and operates at a temperature higher than the temperature required by PH.

The cost decomposition in the cogeneration plants are depicted in Appendix G. Each scheme produces two products, electricity-water, electricity-cooling, and electricity-process heat (see Generator, MED, REF, and PH in Tables G.1, G.2, and G.3). Results show that the main contribution to the cost formation of the electricity cost are originated at the solar collectors, evaporator, reheater, and economizer. While regarding the water, cooling, and process heat costs, the main contributions are: dissipative devices (MED and REF), solar collectors, productive subsystems (MED, REF, and PH), evaporator, reheater, economizer, and condenser (if the MED plant does not replace the condenser).

4.3.3. Trigeneration plants

The results of trigeneration plants are shown in Table 4-10, in which Trigen 1 (CSP-MED-REF 1), Trigen 3 (CSP-REF-PH 1), and Trigen 7 (CSP-MED-PH) are the better options of each group of configurations. Similarly to the case of cogeneration plants, the best cases are when the MED plant replaced the condenser of the power cycle, and the REF plant and the PH plant were coupled to a turbine extraction. However, the values are very close also.

Table 4- 10: Unit exergy cost, total exergy cost of product, and exergy efficiency in trigeneration plants.

Trigeneration	c_p electricity kW/kW	c_p water kW/kW	c_p cooling kW/kW	c_p heat kW/kW	C_p total kW	ψ_i %
Trigen 1 (CSP-MED-REF 1)	3.28	22.66	13.74	-	236 567	25.4
Trigen 2 (CSP-MED-REF 2)	3.39	23.37	14.59	-	227 182	26.0
Trigen 3 (CSP-REF-PH 1)	3.48	-	15.02	5.73	202 249	28.4
Trigen 4 (CSP-REF-PH 2)	3.50	-	15.07	5.01	202 254	28.4
Trigen 5 (CSP-MED-PH 1)	3.29	22.79	-	5.02	239 666	25.4
Trigen 6 (CSP-MED-PH 2)	3.39	23.41	-	5.47	228 423	26.2
Trigen 7 (CSP-MED-PH 3)	3.27	22. 67	-	5.12	237 949	25.6
Trigen 8 (CSP-MED-PH 4)	3.39	23.40	-	4.35	227 189	26.3

When comparing trigeneration plants and stand-alone systems, it can be concluded that the solar trigeneration plants analyzed are more cost-effective in all the cases, because the unit exergy cost of each product is lower than stand-alone systems.

Appendix H presents the cost decomposition of the devices that generate each product in the trigeneration schemes analyzed. The main components that contribute to the cost formation of electricity, water, and cooling, in the CSP-MED-REF schemes, are the solar collectors, evaporator, reheater, economizer, LP turbine, and superheater. Additionally, in the case of water and cooling, is included the MED's and REF's dissipative, MED, and REF. Regarding the CSP-REF-PH schemes, the main components that contribute to the cost formation of electricity, cooling, and process heat, are the solar collectors, evaporator, reheater, LP turbine, economizer, condenser, and superheater. In the case of water and cooling, additionally, it is included the REF's dissipative, REF, and PH. Finally, in the CSP-MED-PH schemes, they are the solar collectors, evaporator, reheater, economizer, LP turbine, and superheater. Including the MED's dissipative, MED, and PH in the case of water and process heat.

4.3.4. Polygeneration plants

The results of polygeneration plants are summarized in Table 4.11. According to the unit exergy cost, the best options are Poly 3 and Poly 1. However, the choice between both schemes is complex because the values of unit exergy cost are very close. The total exergy cost is considered to discriminate which configuration is better when the capacity of production is the same, for example in the case of Poly 2 and Poly 4. Then Poly 2 results more attractive than Poly 4, although the differences are quite close. Regarding the exergy costs distribution, the total exergy cost in Poly 3 is distributed as 75.3 %, 20.7 %, 1.8 %, and 2.2 % in electricity, water, cooling, and process heat, respectively. While in Poly 2 it is distributed as 80.2 %, 15.5 %, 2.0 %, and 2.3 %, correspondingly. Therefore, the main impact on the total exergy cost in the polygeneration plants is the electricity production, followed by the water production, similarly to stand-alone systems, but in a different share. In a scheme where the MED plant operates as a base load water station, all configurations allow satisfying the demand, but only Poly 2 and Poly 4 allow adjusting the water production to variable demand without affecting the electricity production. Note that a base load on a system is the minimum level of demand over a span of time.

Finally, a failure event or maintenance stop in the CSP plant would affect all the plants, however, a failure or stop of any of the other plants would not affect the others, except in the case of Poly 1 and Poly 3, in which the MED plant replaces the condenser.

Table 4- 11: Unit exergy cost, total exergy cost of product, and exergy efficiency in polygeneration plants (CSP-MED-REF-PH).

Polygeneration	c_p electricity kW/kW	c_p water kW/kW	c_p cooling kW/kW	c_p heat kW/kW	C_p total kW	ψ_i %
Poly 1	3.29	22.77	13.78	5.07	241 306	25.3
Poly 2	3.38	23.34	14.54	5.28	232 165	25.9
Poly 3	3.27	22.66	13.71	5.13	239 593	25.5
Poly 4	3.38	23.32	14.53	5.47	232 175	25.9

Regarding the comparison between polygeneration plants and standalone systems, the results are presented in Figure 4-10. According to these results, the solar polygeneration plants are more cost-effective than stand-alone systems, since a lower unit exergy costs of electricity, water, cooling and process heat was found with respect to the stand-alone schemes. Poly 3, that is the best configuration analyzed, allows reducing the unit exergy cost by 6.8 %, 59.2 %, 45.6 %, and 32.2 % for electricity, water, cooling, and process heat, respectively.

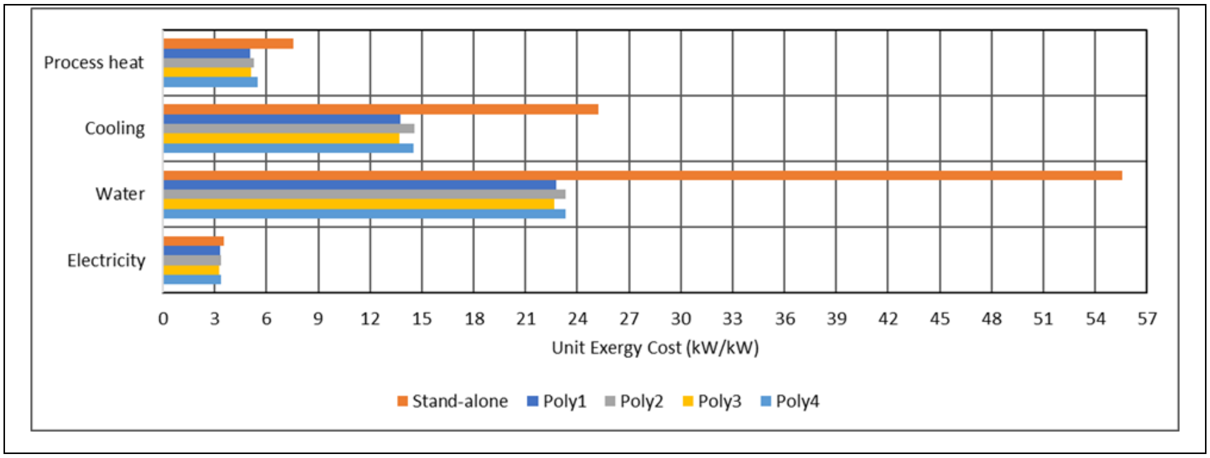

Figure 4- 8: Unit exergy cost of each product in stand-alone plants and polygeneration schemes.

The cost decomposition of the Generator, MED, REF, and PH, in the polygeneration schemes analyzed, are summarized in Figure 4-9 and shown in detail in Appendix I. The products such as electricity, fresh-water, cooling, and heat are generated in Generator, MED, REF and PH, respectively. The main components that contribute to the costs formation of electricity are: solar collectors, evaporator, and reheater. In the case of water, the components are: MED's dissipative, solar collector, MED, evaporator, and reheater. In the case of cooling, the devices that provoke its cost are: REF's dissipative, solar collector, REF, evaporator, and reheater. Finally, in the case of process heat, its end cost comes mainly from: solar collectors, PH, evaporator, and reheater. To reduce the costs of products, it is necessary to first consider these components in an in-depth process of analysis and optimization.

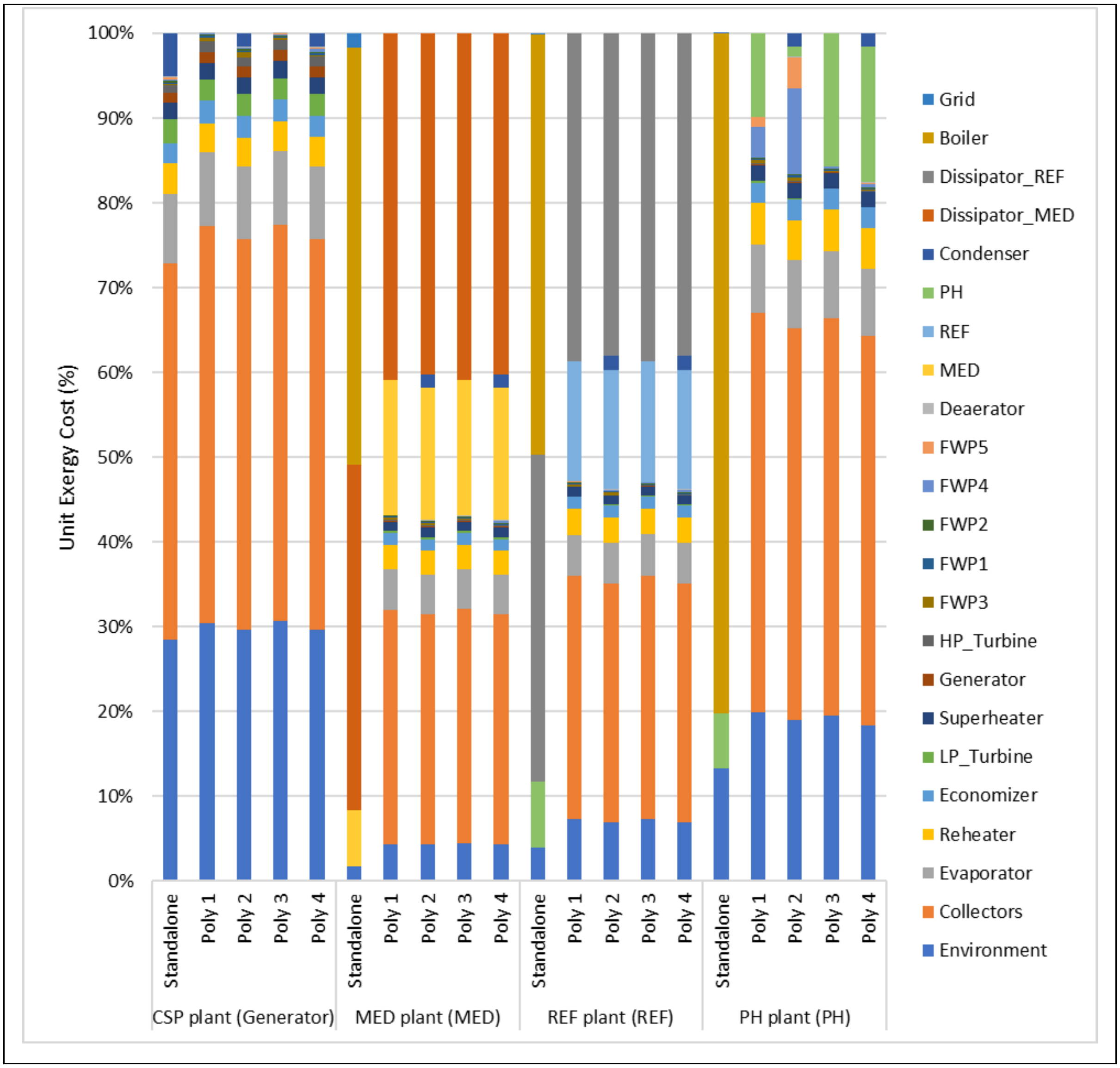

Figure 4- 9: Cost decomposition in polygeneration schemes.

In summary, the solar collectors (solar field) represent the main contribution on cost formation of electricity and process heat, and it is the second for the water and cooling, while the MED's dissipative and REF's dissipative are the main components in cost formation of water and cooling, respectively. Lastly, exergy cost theory allows finding some interactions between different plant components that are not necessarily very close one from the other, such as the solar collectors, the MED's dissipative and REF's dissipative.

4.4. Conclusions

The exergy cost theory (ECT) was applied to different solar multi-generation plants, including cogeneration, trigeneration, polygeneration, and stand-alone systems to analyze the process of exergy cost formation and establish the best configuration among these complex integrated schemes. The solar multi-generation plants considered a concentrated solar power as prime mover, and were simulated in a location with high direct normal irradiation conditions.

Symbolic Thermoeconomics is a branch of the ECT that provides a set of numerical procedures and general formulation, which is valid for any state of the system that depends only on the productive structure and its interaction with the environment. Also, it allows decomposing the production costs into the contributions of the components irreversibilities and residues cost, thus it describes the cost formation process in that solar multi-generation scheme. This method delivers information that is crucial for the design and optimization process of those complex schemes, since it allows identifying the components that present the higher contribution to the unit exergy cost of product.

The results show that the recommended configurations for the integrated solar multi-generation plants (cogeneration, trigeneration, and polygeneration) are those in which the MED plant replaces the condenser of the power cycle, and the REF plant, as well as the PH module are coupled to turbine extractions. Those plants deliver lower unit exergy costs of electricity, water, cooling, and heat.

According to the results, the main components that contribute to the costs formation of electricity in a solar polygeneration plant, in descending order of importance (considering the best configuration of polygeneration scheme as reference), are: solar collectors (46.6 %), evaporator (8.7 %), and reheater (3.4 %). On the other hand, in the case of the other products generated, the main components are dissipative device systems (40.9 % in MED and 38.6 % in REF), solar collectors (46.6 % to 27.6 %), productive subsystems (16.0 % in MED, 14.3 % in REF, and 15.6 % in PH plants), evaporator (8.0 % to 4.8 %), and reheater (4.9 % to 2.8 %). Therefore, these components constitute the key equipment where the design should be improved. Regarding the cost of dissipative devices, there are residues that cannot be reused internally yet, despite the integration. Hence, it is recommended to searching for new integrations inside of the multi-generation schemes to reduce the effect of these residues.

The unit exergy cost, the total exergy cost, and the exergy efficiency are used to compare different configurations of polygeneration schemes. The unit exergy cost allows comparing any configuration, but in the case of the total exergy cost, it is used to compare only when the plants have the same production capacities. On the other hand, a higher exergy efficiency does not imply that the plant is more convenient in thermoeconomic terms because, in general, the minimum total exergy cost and the maximum exergy efficiency are not reached for the same design point.

The analysis shows that the integrated solar multi-generation plants (cogeneration, trigeneration, and polygeneration) are more cost-effective than stand-alone systems since these produce the lower unit exergy cost of electricity, water, cooling and heat under the conditions analyzed. In which, the best configuration of polygeneration scheme allowed reducing the unit exergy cost on 6.8 %, 59.2 %, 45.6 %, and 32.2 %, for electricity, water, cooling, and process heat, respectively. Therefore, the solar multi-generation plants constitute a promising application of a polygeneration system topping cycle, in which the CSP technology is the prime mover.

In future challenges, symbolic exergoeconomic methodology could be extended applied to perform a thermoeconomic diagnosis of the operation of a CSP-polygeneration plant, in the sense of analyzing the impact due to the degradation of a component that forces other components to adapt their behavior to keep their production conditions, and thus increase their irreversibilities (malfunction) and production demand (dysfunction).

5. CONCLUSIONS

Solar multi-generation plants, whose prime mover is a concentrated solar power plant, and stand-alone systems to produce power, desalted water, cooling, and process heat, are modeled, analyzed and evaluated applying two thermoeconomic methods and the levelized cost method, to determine the specific cost of each product and to conduct a sensitivity analysis of the main parameters, to optimize the solar polygeneration in term of the sizing of the solar field and the thermal energy storage, to compare and analysis the cost allocation applying the thermoeconomic and the levelized cost methods, to analyze in depth the process of exergy cost formation, and finally to establish the best configuration in a cogeneration, trigeneration and polygeneration schemes in term of unit exergy cost of the product, total exergy cost of the product, and exergy efficiency. The technologies evaluated consist of a concentrated solar power plant as prime mover, a multi-effect distillation, an absorption refrigeration, and a process heat plant. The evaluation considers that the multi-generation plants are located in an area with high solar irradiation conditions and large demands of energy and water.

The major conclusions of this research associated with each journal paper answers to the first, second and third specific objective of this dissertation, are the follows:

- Solar multi-generation plants, that include cogeneration, trigeneration, and polygeneration schemes, are a promising alternative for the supply of electricity, fresh-water, cooling, and process heat for a zone with high irradiation conditions, scarcity of water, availability of flat terrain, and a short distance to consumption centers. Besides, they are more cost-effective than stand-alone systems since these produce the lower unit exergy cost of each product. Therefore, the multi-generation schemes analyzed are a competitive option compared to stand-alone systems.
- Solar polygeneration plants might increase the economic profit with the sale of carbon credits (certified emission reductions) and credits of the renewable energy quota established by Kyoto Protocol (clean development mechanism) and Chilean legislation, respectively.
- The recommended configurations for the integrated solar multi-generation plants (cogeneration, trigeneration, and polygeneration) are those in which the MED plant

replaces the condenser of the power cycle, and the refrigeration plant, as well as the process heat module are coupled to turbine extractions. Those plants were the most cost-effective configuration.

- The key equipment, on which the design should be improved in solar multi-generation plants, are: solar collector, productive subsystems (MED, REF, and PH plants), evaporator, and reheater because they are the main components that contribute to the costs formation of electricity, water, cooling, and process heat.
- It is recommended searching for new integrations inside of the multi-generation schemes to reduce the effect of the residues, such as recovering the heat in the dissipative devices to be used in other processes.
- The key areas, where cost reductions produce the higher impacts on the unit exergy cost, are the investment cost of the SF and the TES in a solar polygeneration plant.
- The levelized cost method is a simple and fast method, and a deep knowledge of thermodynamics is not required. In the absence of a detailed knowledge of the plant, the level cost method is a good alternative and presents reasonable results. Therefore, this method is recommended when is necessary to perform a first approximation of the costs of each product. However, comparing polygeneration plant and the stand-alone systems could lead to different conclusions.
- The thermoeconomic method constitutes a rational method to assess a CSP-polygeneration plant since it is based on the quality of energy assessed. It is an equitable distribution of the appropriate share of non-exergy-related cost rate ($capex$ and $opex$) and exergy cost rate in each product according to its exergy rate. All costs from resources consumed are charged to their useful products. Additionally, the thermoeconomic method allows measuring resources and products of very different nature, such as energy and water, using the same unit.
- The thermoeconomic method is recommended when is required to perform a more precise analysis of the costs of each product, and to assess the benefits of polygeneration schemes compared to the stand-alone systems. The disadvantages of the thermoeconomic method are its complexity and additional knowledge about the internal parameters of the plant, which could not be available.

- For selecting the optimal size of a CSP-polygeneration plant, the lowest unit costs happened at the same sizing of SM and TES when it is used the levelized cost and the thermoeconomic methods, although, the unit costs have different values. However, the thermoeconomic method uses exergy as a criterion to allocate costs and allows performing an assessment considering the conversion efficiencies and economic benefits offered by the system.
- The unit exergy cost, the total exergy cost, and the exergy efficiency are used to compare different configurations of polygeneration schemes. The unit exergy cost allows comparing any configuration, but in the case of the total exergy cost, it is used to compare only when the plants have the same production capacities. On the other hand, a higher exergy efficiency does not imply that the plant is more convenient in thermoeconomic terms because, in general, the minimum total exergy cost and the maximum exergy efficiency are not reached in the same design point.
- The utilization factor as thermodynamic indicator, which relating the energy outputs to the energy inputs, provides a false high-performance impression of the polygeneration plant because it does not discriminate between the high-quality energy as work or electricity, and low-quality energy as heat. Additionally, when resources and products of different energy nature (as water) are presented, the indicator is limited. Therefore, a better thermodynamic indicator for polygeneration plant is the exergy efficiency.

REFERENCES

Abusoglu, A., & Kanoglu, M. (2009). Exergoeconomic analysis and optimization of combined heat and power production: A review. *Renewable and Sustainable Energy Reviews*, *13*(9), 2295–2308. http://doi.org/10.1016/j.rser.2009.05.004

Ahmadi, P., Dincer, I., & Rosen, M. A. (2011). Exergy, exergoeconomic and environmental analyses and evolutionary algorithm based multi-objective optimization of combined cycle power plants. *Energy*, *36*(10), 5886–5898. http://doi.org/10.1016/j.energy.2011.08.034

Al-Karaghouli, A., & Kazmerski, L. L. (2013). Energy consumption and water production cost of conventional and renewable-energy-powered desalination processes. *Renewable and Sustainable Energy Reviews*, *24*, 343–356. http://doi.org/10.1016/j.rser.2012.12.064

Al-Sulaiman, F. A., Dincer, I., & Hamdullahpur, F. (2013a). Thermoeconomic optimization of three trigeneration systems using organic Rankine cycles: Part I – Formulations. *Energy Conversion and Management*, *69*, 199–208. http://doi.org/10.1016/j.enconman.2012.12.030

Al-Sulaiman, F. A., Dincer, I., & Hamdullahpur, F. (2013b). Thermoeconomic optimization of three trigeneration systems using organic Rankine cycles: Part II – Applications. *Energy Conversion and Management*, *69*, 209–216. http://doi.org/10.1016/j.enconman.2012.12.032

Al Moussawi, H., Fardoun, F., & Louahlia-Gualous, H. (2016). Review of tri-generation technologies: Design evaluation, optimization, decision-making, and selection approach. *Energy Conversion and Management*, *120*, 157–196. http://doi.org/10.1016/j.enconman.2016.04.085

Antofagasta, A. (2016). Aguas Antofagasta, tarifas actuales, 2016. Retrieved September 21, 2016, from http://www3.aguasantofagasta.cl/empresa/informacion-comercial/tarifas/tarifas-actuales.html

Baghernejad, A., & Yaghoubi, M. (2011). Exergoeconomic analysis and optimization of an Integrated Solar Combined Cycle System (ISCCS) using genetic algorithm. *Energy Conversion and Management*, *52*(5), 2193–2203. http://doi.org/10.1016/j.enconman.2010.12.019

Bejan, A., Tsatsaronis, G., & Moran, M. (1996). *Thermal Design and Optimization* (1 edition). John Wiley & Sons. Retrieved from http://books.google.com/books?hl=en&lr=&id=sTi2crXeZYgC&pgis=1

Beretta, G. P., Iora, P., & Ghoniem, A. F. (2014). Allocating resources and products in multi-hybrid multi-cogeneration: What fractions of heat and power are renewable in hybrid fossil-solar CHP? *Energy*, *78*, 587–603. http://doi.org/10.1016/j.energy.2014.10.046

Blanco-Marigorta, A. M., Victoria Sanchez-Henríquez, M., & Peña-Quintana, J. A. (2011). Exergetic comparison of two different cooling technologies for the power cycle of a thermal power plant. *Energy*, *36*(4), 1966–1972. http://doi.org/10.1016/j.energy.2010.09.033

Calise, F., d'Accadia, M. D., Macaluso, A., Piacentino, A., & Vanoli, L. (2016). Exergetic and exergoeconomic analysis of a novel hybrid solar–geothermal polygeneration system producing energy and water. *Energy Conversion and Management*, *115*, 200–220. http://doi.org/10.1016/j.enconman.2016.02.029

CNE. (2015). Informe de Proyección de precios de combustibles 2015-2030. Retrieved November 21, 2017, from https://www.cne.cl/wp-content/uploads/2015/11/ResEx541_2015_Comb-informe-final-Informe-Proyecciones-Precios-Combustibles.pdf

COCHILCO. (2015a). Proyecciones del consumo de agua en la minería del cobre al 2026. http://doi.org/DEPP 16/2015

COCHILCO. (2015b). Proyecciones del consumo de electricidad en la minería del cobre 2015-2016. http://doi.org/DE 21/2015

COCHILCO. (2016). Informe de actualización del consumo energético de la minería del cobre al año 2015. http://doi.org/DE 11/2016

Dincer, I., & Rosen, M. (2012). *Exergy. Energy, environment and sustainable development*. (Elsevier, Ed.) (second edi). Elsevier Science.

ELECDA. (2016). Tarifas actuales de suministro electrico. Retrieved November 21, 2017, from http://www.elecda.cl/wp-content/uploads/2016/10/Tarifas-de-Suministro_ELECDA_-Noviembre-2016.pdf

Escobar, R. A., Cortés, C., Pino, A., Pereira, E. B., Martins, F. R., & Cardemil, J. M. (2014). Solar energy resource assessment in Chile: Satellite estimation and ground station measurements. *Renewable Energy*, *71*, 324–332. http://doi.org/10.1016/j.renene.2014.05.013

Escobar, R. A., Cortés, C., Pino, A., Salgado, M., Pereira, E. B., Martins, F. R., … Cardemil, J. M. (2015). Estimating the potential for solar energy utilization in Chile by satellite-derived data and ground station measurements. *Solar Energy*, *121*, 139–151. http://doi.org/10.1016/j.solener.2015.08.034

Fernández-García, A., Zarza, E., Valenzuela, L., & Pérez, M. (2010). Parabolic-trough solar collectors and their applications. *Renewable and Sustainable Energy Reviews*, *14*(7), 1695–1721. http://doi.org/10.1016/j.rser.2010.03.012

Fylaktos, N., Mitra, I., Tzamtzis, G., & Papanicolas, C. N. (2014). Economic analysis of an electricity and desalinated water cogeneration plant in Cyprus. *Desalination and Water*

Treatment, *3994*(September 2015), 1–18. http://doi.org/10.1080/19443994.2014.940219

Gochenour, C. (2003). *Regulation of Heat and Electricity Produced in Combined Heat and Power Plants*. *The World Bank Washington, D.C.* Retrieved from http://www.globalregulatorynetwork.org/Resources/CHPRegionalStudy.pdf

H. El-Dessouky, & H. Ettouney. (2002). *Fundamentals of Salt Water Desalination*. Elsevier.

Herold, K., Radermacher, R., & Klein, S. (1996). *Absorption Chillers and Heat Pumps*. (T. & F. Group, Ed.) (1st editio). CRC Press; 1 edition (January 18, 1996).

Houda, J., Trieb, F., Scharfe, J., Kern, J., Nieseor, T., Cottret, N., & Glueckstern, P. (2009). *Combined Solar Power and Desalination Plants : Techno-Economic Potential in Mediterranean Partner Countries and Desalination Configurations (MED-CSD).*

IEA. (2011). *Co-generation and Renewables*.

IEA. (2016). *Key World Energy Statistics 2016*. *Statistics*. Retrieved from http://www.oecd-ilibrary.org/energy/key-world-energy-statistics-2009_9789264039537-en

IEA-NEA. (2015). Projected costs of generating electricity 2015, 16. http://doi.org/10.1787/cost_electricity-2015-en

Inodú. (2014). Utilización de bloques horarios en licitación de suministro a distribuidoras, 2014. Caso licitación SIC 2013/03-2º llamado. Retrieved September 21, 2016, from http://www.acera.cl/wp-content/uploads/2015/02/Minuta-Acera-20122014b.pdf

IRENA. (2012). *Concentrating Solar Power* (Vol. 1).

IRENA. (2015). *Renewable Power Generation Costs in 2014 : An Overview*. Retrieved from http://www.irena.org/DocumentDownloads/Publications/IRENA_RE_Power_Costs_2014_report.pdf

Jana, K., Ray, A., Majoumerd, M. M., Assadi, M., & De, S. (2017). Polygeneration as a future sustainable energy solution – A comprehensive review. *Applied Energy*, *202*, 88–111. http://doi.org/10.1016/j.apenergy.2017.05.129

Leiva-Illanes, R., Escobar, R., Cardemil, J. M., & Alarcón-Padilla, D. (2017). Thermoeconomic assessment of a solar polygeneration plant for electricity, water, cooling and heating in high direct normal irradiation conditions. *Energy Conversion and Management*, *151*(May), 538–552. http://doi.org/10.1016/J.ENCONMAN.2017.09.002

Leiva-Illanes, R., Escobar, R., Cardemil, J. M., & Alarcón-Padilla, D. (2018). Comparison of the levelized cost and thermoeconomic methodologies – Cost allocation in a solar polygeneration plant to produce power, desalted water, cooling and process heat. *Energy Conversion and Management*, *168*, 215–229.

http://doi.org/10.1016/j.enconman.2018.04.107

Mata-Torres, C., Escobar, R. A., Cardemil, J. M., Simsek, Y., & Matute, J. A. (2017). Solar polygeneration for electricity production and desalination: Case studies in Venezuela and northern Chile. *Renewable Energy*, *101*, 387–398. http://doi.org/10.1016/j.renene.2016.08.068

Ministerio-de-energia-Chile. (2017). Balance nacional de energía 2015. Retrieved September 21, 2016, from http://dataset.cne.cl/Energia_Abierta/Reportes/Minenergia/Reporte BNE 2015.pdf

Ministerio de economía. (2008). Ley 20257. Introduce modificaciones a la ley general de servicios eléctricos respecto de la generación de energía eléctrica con fuentes de energías renovables no convencionales. Retrieved September 21, 2016, from http://www.leychile.cl/Navegar/?idNorma=270212&idVersion=2008-04-01&idParte

Modi, A., Bühler, F., Andreasen, J. G., & Haglind, F. (2017). A review of solar energy based heat and power generation systems. *Renewable and Sustainable Energy Reviews*, *67*, 1047–1064. http://doi.org/10.1016/j.rser.2016.09.075

Montes, M. J., Abánades, A., Martínez-Val, J. M., & Valdés, M. (2009). Solar multiple optimization for a solar-only thermal power plant, using oil as heat transfer fluid in the parabolic trough collectors. *Solar Energy*, *83*(12), 2165–2176. http://doi.org/10.1016/j.solener.2009.08.010

Moser, M., Trieb, F., Fichter, T., & Kern, J. (2013). Renewable desalination: a methodology for cost comparison. *Desalination and Water Treatment*, *51*(4–6), 1171–1189. http://doi.org/10.1080/19443994.2012.715446

Moser, M., Trieb, F., Fichter, T., Kern, J., & Hess, D. (2014). A flexible techno-economic model for the assessment of desalination plants driven by renewable energies. *Desalination and Water Treatment*, *3994*(October 2014), 1–15. http://doi.org/10.1080/19443994.2014.946718

Noro, M., & Lazzarin, R. M. (2014). Solar cooling between thermal and photovoltaic: An energy and economic comparative study in the Mediterranean conditions. *Energy*, *73*, 453–464. http://doi.org/10.1016/j.energy.2014.06.035

NREL. (2013). System Advisor Model (SAM) Case Study: Andasol-1, 1–10. Retrieved from https://sam.nrel.gov/sites/sam.nrel.gov/files/content/case_studies/sam_case_csp_physical_trough_andasol-1_2013-1-15.pdf

NREL. (2017). Aalborg CSP-Brønderslev CSP with ORC project. Retrieved July 6, 2017, from https://www.nrel.gov/csp/solarpaces/project_detail.cfm/projectID=8316

Nuorkivi, A. (2010). Allocation of Fuel Energy and Emissions to Heat and Power in CHP.

Retrieved August 24, 2017, from http://era17.fi/wp-content/uploads/2012/02/Report-Nordic-CHP-Allocation_Energy-AN-Consulting_2010-9-7.pdf

Olwig, R., Hirsch, T., Sattler, C., Glade, H., Schmeken, L., Will, S., … Messalem, R. (2012). Techno-economic analysis of combined concentrating solar power and desalination plant configurations in Israel and Jordan. *Desalination and Water Treatment*, *41*(1–3), 9–25. http://doi.org/10.1080/19443994.2012.664674

Ortega-Delgado, B., García-Rodríguez, L., & Alarcón-Padilla, D. (2016). Thermoeconomic comparison of integrating seawater desalination processes in a concentrating solar power plant of 5 MWe. *Desalination*, *392*, 102–117. http://doi.org/10.1016/j.desal.2016.03.016

Palacios-Bereche Reynaldo, Gonzales R, N. S. (2012). Exergy calculation of lithium bromide–water solution and its application in the exergetic evaluation of absorption refrigeration systems LiBr–H2O. *International Journal of Energy Research*, *36*, 166–181. http://doi.org/10.1002/er.1790

Palenzuela, P., Alarcón-Padilla, D., & Zaragoza, G. (2015). Large-scale solar desalination by combination with CSP: Techno-economic analysis of different options for the Mediterranean Sea and the Arabian Gulf. *Desalination*, *366*, 130–138. http://doi.org/10.1016/j.desal.2014.12.037

Palenzuela, P., Hassan, A. S., Zaragoza, G., & Alarcón-Padilla, D.-C. (2014). Steady state model for multi-effect distillation case study: Plataforma Solar de Almería MED pilot plant. *Desalination*, *337*, 31–42. http://doi.org/10.1016/j.desal.2013.12.029

Perdichizzi, A., Barigozzi, G., Franchini, G., & Ravelli, S. (2015). Performance Prediction of a CSP Plant Integrated with Cooling Production. *Energy Procedia*, *75*, 436–443. http://doi.org/10.1016/j.egypro.2015.07.413

Petela, R. (2010). *Engineering Thermodynamics of Thermal Radiation for solar Power Utilization*. (McGraw-Hill, Ed.) (1 edition). McGraw-Hill Education; 1 edition.

Piacentino, A. (2015). Application of advanced thermodynamics, thermoeconomics and exergy costing to a Multiple Effect Distillation plant: In-depth analysis of cost formation process. *Desalination*, *371*, 88–103. http://doi.org/10.1016/j.desal.2015.06.008

Sarbu, I., & Sebarchievici, C. (2015). General review of solar-powered closed sorption refrigeration systems. *Energy Conversion and Management*, *105*, 403–422. http://doi.org/10.1016/j.enconman.2015.07.084

SENDECO2. (2016). Precios del CO2. Retrieved November 21, 2016, from http://www.sendeco2.com/es/precios-co2

Serra, L. M., Lozano, M.-A., Ramos, J., Ensinas, A. V., & Nebra, S. A. (2009). Polygeneration and efficient use of natural resources. *Energy*, *34*(5), 575–586.

http://doi.org/10.1016/j.energy.2008.08.013

Sharqawy, M. H., Lienhard V, J. H., & Zubair, S. M. (2011). On exergy calculations of seawater with applications in desalination systems. *International Journal of Thermal Sciences*, *50*(2), 187–196. http://doi.org/10.1016/j.ijthermalsci.2010.09.013

Short, W., Packey, D., & Holt, T. (1995). A manual for the economic evaluation of energy efficiency and renewable energy technologies. *University Press of the Pacific*, *2*(March), 120. http://doi.org/NREL/TP-462-5173

SimTech GmbH. (2011). *IPSEpro Process Simulation Environment* (Rev 5.0). SimTech Simulation Technology. Retrieved from http://www.simtechnology.com/CMS/index.php/ipsepro/system-description

Tereshchenko, T., & Nord, N. (2015). Uncertainty of the allocation factors of heat and electricity production of combined cycle power plant. *Applied Thermal Engineering*, *76*, 410–422. http://doi.org/10.1016/j.applthermaleng.2014.11.019

Torres, C., & Valero, A. (2012). ExIO, Thermoeconomic analysis of thermal systems.

Torres, C., Valero, A., Rangel, V., & Zaleta, A. (2008). On the cost formation process of the residues. *Energy*, *33*(2), 144–152. http://doi.org/10.1016/j.energy.2007.06.007

Torres, C., Valero, A., Serra, L., & Royo, J. (2002). Structural theory and thermoeconomic diagnosis. *Energy Conversion and Management*, *43*(9–12), 1503–1518. http://doi.org/10.1016/S0196-8904(02)00032-8

Turton, R., Bailie, R., Whiting, W., Shaeiwitz, J., & Bhattacharyya, D. (2012). *Analysis, Synthesis, and Design of Chemical Processes*. (Prentice Hall, Ed.) (4th editio). Prentice Hall; 4 edition (July 2, 2012).

Usón, S., Valero, A., & Agudelo, A. (2012). Thermoeconomics and Industrial Symbiosis. Effect of by-product integration in cost assessment. *Energy*, *45*(1), 43–51. http://doi.org/10.1016/j.energy.2012.04.016

Valero, A., Correas, L., Zaleta, A., Lazzaretto, A., Verda, V., Reini, M., & Rangel, V. (2004). On the thermoeconomic approach to the diagnosis of energy system malfunctionsPart 2. Malfunction definitions and assessment. *Energy*, *29*(12–15), 1889–1907. http://doi.org/10.1016/j.energy.2004.03.008

Valero, A., Lerch, F., Serra, L., & Royo, J. (2002). Structural theory and thermoeconomic diagnosis. *Energy Conversion and Management*, *43*(9–12), 1519–1535. http://doi.org/10.1016/S0196-8904(02)00033-X

Valero, A., & Torres, C. (2016). *Thermoeconomic Analysis*. *Exergy, Energy System Analysis and Optimization - Encyclopedia of Life Support Systems (EOLSS)*.

Valero, A., Usón, S., Torres, C., Valero, A., Agudelo, A., & Costa, J. (2013).

Thermoeconomic tools for the analysis of eco-industrial parks. *Energy*, *62*, 62–72. http://doi.org/10.1016/j.energy.2013.07.014

Wagner, M. J., & Gilman, P. (2011). Technical manual for the SAM physical trough model. *Contract*, *303*(June), 275–3000. Retrieved from http://www.nrel.gov/docs/fy11osti/51825.pdf

Wang, J., & Mao, T. (2015). Cost allocation and sensitivity analysis of multi-products from biomass gasification combined cooling heating and power system based on the exergoeconomic methodology. *Energy Conversion and Management*, *105*, 230–239. http://doi.org/10.1016/j.enconman.2015.07.081

Wang, Y., & Lior, N. (2007). Fuel allocation in a combined steam-injected gas turbine and thermal seawater desalination system. *Desalination*, *214*(1), 306–326. http://doi.org/10.1016/j.desal.2007.01.001

Ye, X., & Li, C. (2013). A novel evaluation of heat-electricity cost allocation in cogenerations based on entropy change method. *Energy Policy*, *60*, 290–295. http://doi.org/10.1016/j.enpol.2013.05.015

Zak, G., Mitsos, A., & Hardt, D. (2012). *Master Thesis. Thermal Desalination : Structural Optimization and Integration in Clean Power and Water*. Massachusetts Institute of Technology.

APPENDICES

APPENDIX A: Model development kit (MDK) of software IPSEpro.

The software IPSEpro (SimTech GmbH, 2011) was used for the simulations of stand-alone systems and the solar multi-generation plants. Three modules of IPSEpro were employed: IPSEpro-MDK, IPSEpro-PSE, and IPSEpro-PSXLink. The model development kit (IPSEpro-MDK module) offers all the capabilities required to define and build new component models and to translate them into a form that can be used by IPSEpro-PSE module. MDK consists of two functional units: MDK Model Editor and MDK Model Compiler. The Model Editor uses the model description language (MDL), which allows to design icons that represent the models and to describe their behavior mathematically. In this context, in order to be able to study the different configurations a new library was developed. This new library, named polygeneration library, integrates the Concentrated Solar Power, Refrigeration Process, and Desalination Process libraries, as shown in Figure A-1. Additionally, it was modified the libraries' codes in order to calculate the co-enthalpy and the exergy flow in each component, and the exergy rate from solar radiation in the solar collectors.

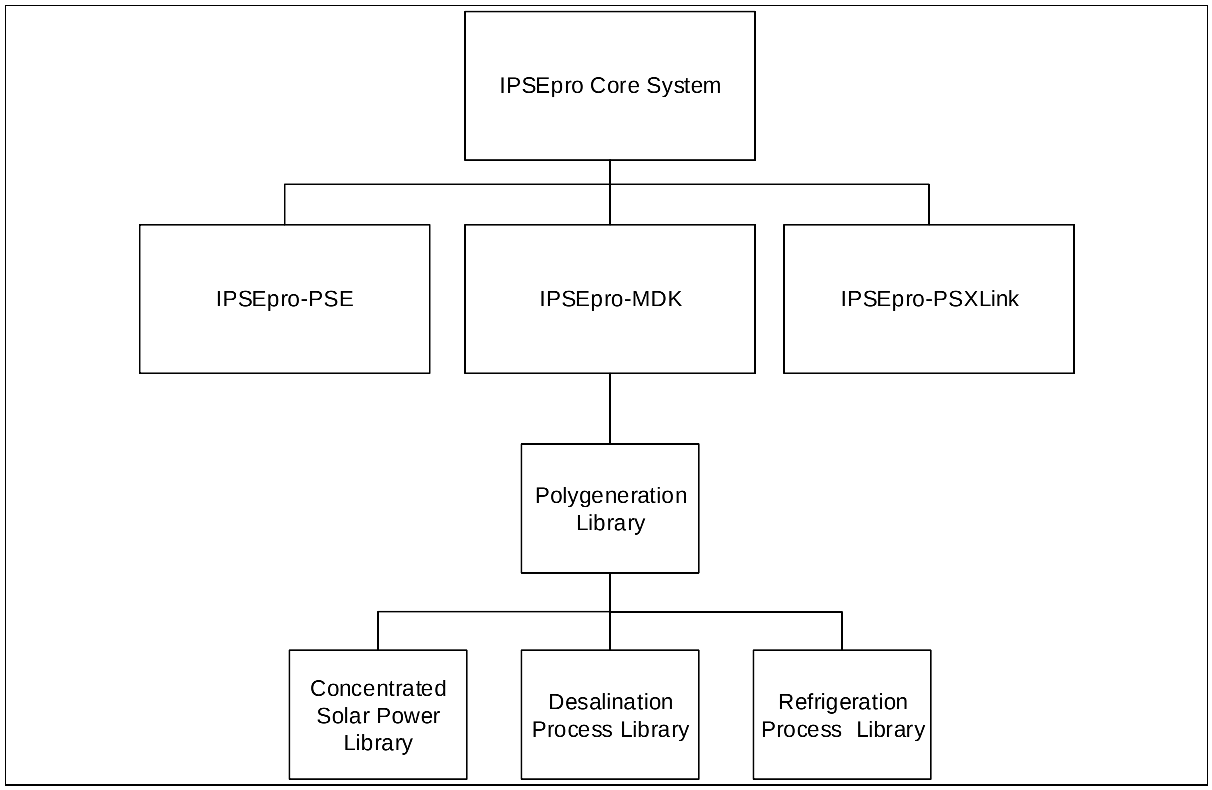

Figure A- 1: Polygeneration library.

APPENDIX B: Validation of the stand-alone CSP plant.

The CSP plant was validated by comparing the results between the IPSEpro/Matlab model and the case study (Andasol-1) by means of the SAM software (NREL, 2013). Table B-1 shows the results of the validation of the stand-alone CSP plant.

Table B- 1: Comparison between IPSEpro/Matlab model and SAM model.

Net electricity	IPSEpro/Matlab model	SAM model	Difference
	GWh	GWh	
January	29.5	28.0	5.1%
February	20.7	19.8	4.5%
March	31.6	30.5	3.4%
April	23.3	23.3	0.0%
May	24.3	23.2	4.6%
June	20.4	19.0	6.9%
July	20.5	19.5	4.6%
August	27.1	27.4	-1.2%
September	29.2	29.2	0.2%
October	33.8	31.6	6.7%
November	32.4	31.4	3.4%
December	33.5	31.9	4.7%
Average	27.2	26.2	3.6%

APPENDIX C: Exergy rate and unit exergy cost in polygeneration plants.

Table C- 1: Exergy rate and unit exergy cost in Poly 1.

Stream	$\dot{E}$ kW	c USD/kWh
1	162 677.9	0.0000
2	2 202.8	0.1058
3	1 896.6	0.1058
4	3 432.2	0.1058
5	455.4	0.1058
6	1 956.1	0.1058
7	720.2	0.1058
8	15 609.9	0.1058
9	55 070.2	0.1058
10	1 866.0	0.1058
11	2 410.7	0.1058
12	0.0	0.0000
13	2 216.2	1.9494
14	340.0	0.0000
15	1 190.8	0.0000
16	16.4	0.1058
17	198.2	0.0000
18	494.8	0.6251
19	810.0	0.6251
20	-0.3	0.0000
21	1.3	0.1058
22	582.4	0.1616
23	1 611.8	0.1616
24	47 517.9	0.0324

Table C- 2: Exergy rate and unit exergy cost in Poly 2.

Stream	$\dot{E}$ kW	c USD/kWh
1	15 7421.2	0.0000
2	2 202.8	0.1114
3	648.2	0.1114
4	1 741.3	0.1114
5	2 397.6	0.1114
6	3 945.9	0.1114
7	502.2	0.1114
8	10 885.3	0.1114
9	55 070.2	0.1114
10	1 791.3	0.1114
11	1 679.8	0.1114
12	0.0	0.0000
13	1 544.7	2.1360
14	237.2	0.0000
15	830.4	0.0000
16	16.4	0.1114
17	198.5	0.0000
18	495.1	0.6690
19	810.3	0.6690
20	-0.1	0.0000
21	1.3	0.1114
22	582.4	0.1221
23	1 611.8	0.1221
24	46 523.2	0.0324

APPENDIX D: Exergy rate and unit exergy cost in stand-alone systems.

Table D- 1: Exergy rate and unit exergy cost in Stand-alone CSP plant.

Stream	$\dot{E}$ kW	c USD/kWh
1	136 506.98	0.000
2	37 809.13	0.032
3	89 179.54	0.000
4	55 069.53	0.122
5	3 727.01	0.122

Table D- 2: Exergy rate and unit exergy cost in Stand-alone MED plant.

Stream	$\dot{E}$ kW	c USD/kWh
1	117 221	0.032
2	720	0.253
3	15 610	0.256
4	2 411	0.098
5	0	0.000
6	2 216	2.865
7	340	0.000
8	1 191	0.000

Table D- 3: Exergy rate and unit exergy cost in Stand-alone REF plant.

Stream	$\dot{E}$ kW	c USD/kWh
1	7 910.8	0.032
2	453.0	0.176
3	1 953.6	0.176
4	16	0.098
5	198	0.000
6	495	0.958
7	810	0.958
8	-0.34	0.000

Table D- 4: Exergy rate and unit exergy cost in Stand-alone PH plant.

Stream	$\dot{E}$ kW	c USD/kWh
1	7 777.8	0.032
2	1 882.2	0.169
3	3 416.8	0.169
4	1.3	0.098
5	582.4	0.256
6	1 611.8	0.256

APPENDIX E: Flowchart of the simulation in chapter 3.

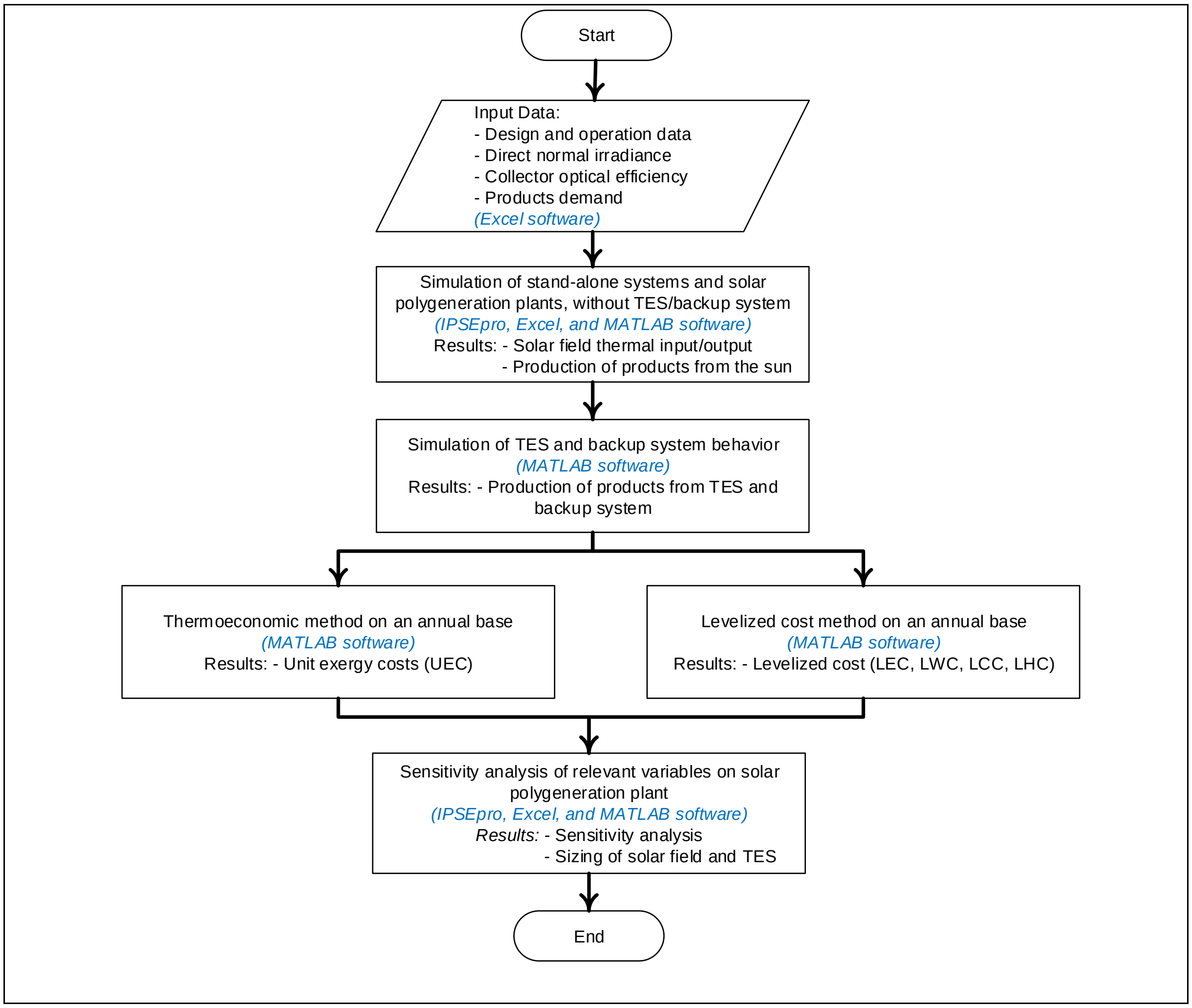

Figure E- 1: Flowchart of the simulation in chapter 3.

APPENDIX F: Flowchart of the simulation in chapter 4.

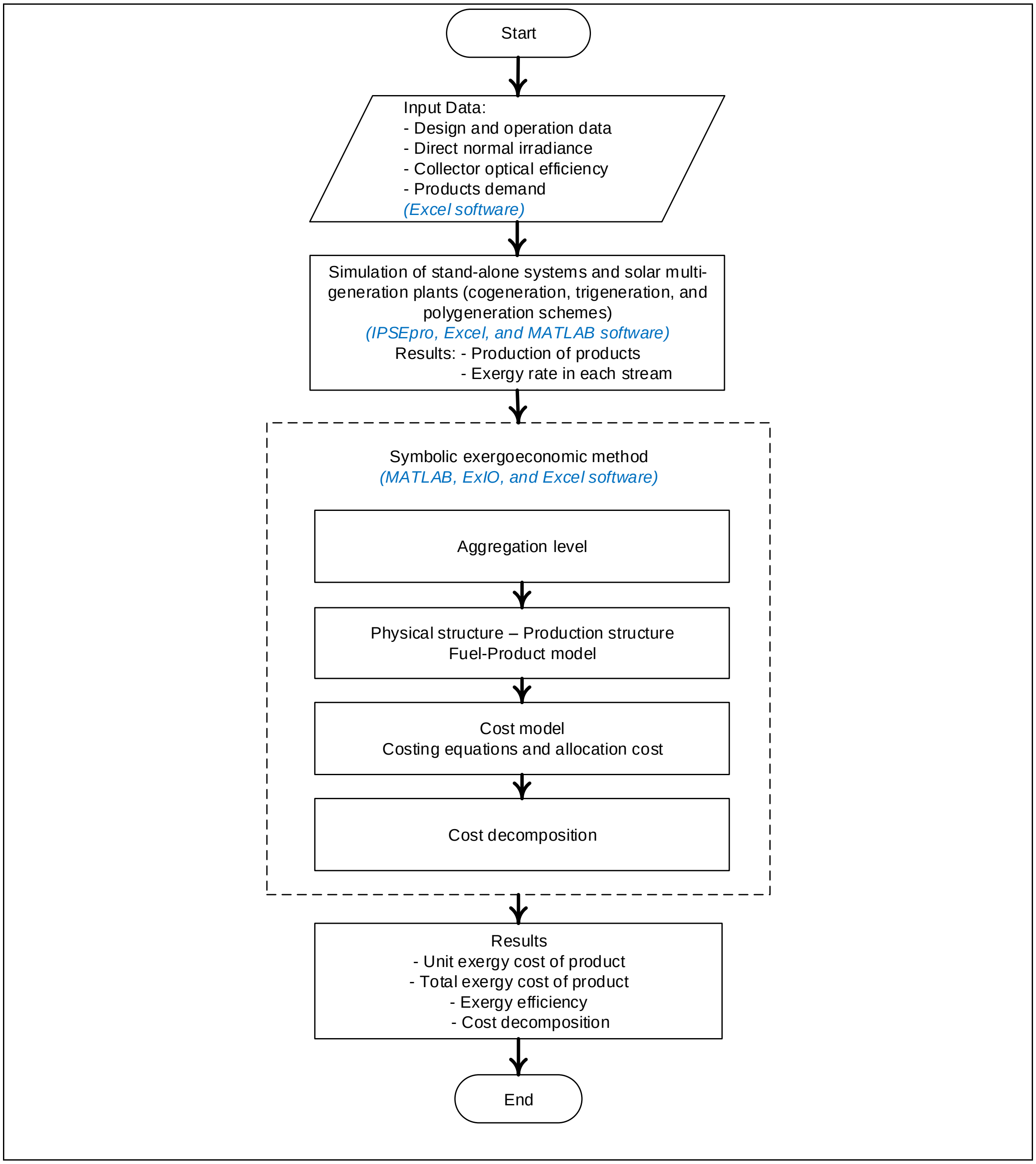

Figure F- 1: Flowchart of the simulation in chapter 4.

APPENDIX G: Cost decomposition in the cogeneration plants.

Table G- 2: Cost decomposition of Generator and MED in CSP-MED plants.

	Generator		MED	
Device	CSP-MED 1	CSP-MED 2	CSP-MED 1	CSP-MED 2
Environment	30.7%	29.5%	4.3%	4.2%
Collectors	46.6%	45.7%	27.6%	27.0%
Evaporator	8.6%	8.4%	5.1%	5.0%
Reheater	3.7%	3.7%	2.2%	2.2%
LP_Turbine	2.6%	2.6%	0.3%	0.3%
Economizer	2.6%	2.5%	1.5%	1.5%
Superheater	2.0%	1.9%	1.2%	1.1%
Generator	1.3%	1.3%	0.1%	0.1%
HP_Turbine	1.0%	0.9%	0.6%	0.6%
FWP1	0.2%	0.2%	0.1%	0.1%
FWP4	0.2%	0.4%	0.1%	0.3%
FWP3	0.1%	0.1%	0.1%	0.1%
FWP2	0.1%	0.2%	0.1%	0.1%
FWP5	0.1%	0.1%	0.0%	0.1%
Deaerator	0.0%	0.1%	0.0%	0.1%
MED	0.0%	0.0%	15.7%	15.2%
Condenser	-	2.0%	-	2.0%
Dissipator_MED	0.0%	0.0%	40.9%	40.1%

Table G- 3: Cost decomposition of Generator and REF in CSP-REF plants.

	Generator		REF	
Device	CSP-REF 1	CSP-REF 2	CSP-REF 1	CSP-REF 2
Environment	28.6%	24.5%	6.6%	5.7%
Collectors	44.4%	37.3%	27.2%	22.9%
Economizer	8.1%	2.0%	5.0%	1.3%
Generator	3.6%	3.0%	2.2%	1.8%
FWP5	2.8%	0.1%	0.1%	0.1%
LP_Turbine	2.4%	6.8%	1.5%	4.2%
Superheater	1.9%	1.6%	1.1%	1.0%
FWP1	1.2%	2.0%	0.0%	0.0%
HP_Turbine	0.9%	0.8%	0.6%	0.5%
FWP3	0.2%	0.0%	0.1%	0.0%
Deaerator	0.2%	0.0%	0.1%	0.0%
Evaporator	0.1%	0.1%	0.1%	0.0%
FWP4	0.0%	1.0%	0.0%	0.0%
Reheater	0.0%	0.0%	0.0%	0.0%
FWP2	0.0%	0.1%	0.0%	0.0%
REF	0.0%	0.0%	13.3%	11.2%
Condenser	4.8%	20.1%	4.8%	20.1%
Dissipator_REF	0.0%	0.0%	36.8%	30.9%

Table G- 4: Cost decomposition of Generator and PH in CSP-PH plants.

	Generator				PH			
Device	CSP-PH 1	CSP-PH 2	CSP-PH 3	CSP-PH 4	CSP-PH 1	CSP-PH 2	CSP-PH 3	CSP-PH 4
Environment	28.5%	28.6%	28.4%	28.5%	19.6%	22.3%	12.0%	10.7%
Collectors	44.4%	44.4%	44.3%	44.3%	44.4%	44.4%	46.6%	46.6%
Evaporator	8.1%	8.1%	8.1%	8.1%	8.1%	8.1%	0.1%	0.1%
Reheater	3.6%	3.6%	3.7%	3.6%	3.6%	3.6%	0.1%	0.0%
LP_Turbine	2.8%	2.8%	2.8%	2.8%	0.2%	0.1%	0.0%	0.0%
Economizer	2.4%	2.4%	2.4%	2.4%	2.4%	2.4%	0.0%	0.0%
Superheater	1.9%	1.9%	1.9%	1.8%	1.9%	1.9%	0.0%	0.0%
Generator	1.2%	1.2%	1.2%	1.2%	0.1%	0.0%	0.0%	0.0%
HP_Turbine	0.9%	0.9%	0.9%	0.9%	0.9%	0.9%	0.0%	0.0%
FWP3	0.5%	0.2%	0.1%	0.1%	0.5%	0.2%	0.0%	0.0%
FWP1	0.2%	0.2%	0.2%	0.2%	0.2%	0.2%	0.0%	0.0%
FWP2	0.2%	0.2%	0.2%	0.2%	0.2%	0.2%	0.0%	0.0%
Deaerator	0.1%	0.1%	0.1%	0.1%	0.1%	0.1%	0.0%	0.0%
FWP5	0.1%	0.2%	0.2%	0.2%	5.8%	0.2%	0.0%	0.0%
FWP4	0.1%	0.2%	0.2%	0.2%	5.3%	0.2%	0.0%	0.0%
PH	0.0%	0.0%	0.0%	0.0%	1.4%	10.2%	40.8%	42.3%
Condenser	4.8%	4.8%	5.1%	5.1%	4.8%	4.8%	0.1%	0.1%

APPENDIX H: Cost decomposition in the trigeneration plants.

Table H- 1: Cost decomposition of Generator, MED, and REF in CSP-MED-REF plants (Trigen 1 and Trigen 2).

	Generator		MED		REF	
Device / Trigen	1	2	1	2	1	2
Environment	30.5%	29.5%	4.4%	4.3%	7.3%	6.9%
Collectors	46.6%	45.8%	27.6%	27.1%	28.6%	28.1%
Evaporator	8.7%	8.5%	4.8%	4.7%	4.9%	4.8%
Reheater	3.4%	3.4%	2.8%	2.7%	3.0%	3.0%
Economizer	2.6%	2.5%	1.4%	1.4%	1.5%	1.4%
LP_Turbine	2.5%	2.6%	0.3%	0.3%	0.1%	0.0%
Superheater	2.0%	2.0%	1.1%	1.1%	1.1%	1.1%
Generator	1.3%	1.3%	0.1%	0.1%	0.0%	0.0%
HP_Turbine	1.2%	1.1%	0.1%	0.1%	0.0%	0.0%
FWP1	0.2%	0.2%	0.1%	0.1%	0.1%	0.1%
FWP4	0.2%	0.4%	0.1%	0.2%	0.1%	0.2%
FWP3	0.2%	0.2%	0.1%	0.1%	0.1%	0.1%
FWP2	0.1%	0.2%	0.1%	0.1%	0.1%	0.1%
FWP5	0.1%	0.1%	0.0%	0.1%	0.0%	0.1%
Deaerator	0.0%	0.1%	0.0%	0.1%	0.0%	0.1%
MED	0.0%	0.0%	16.0%	15.5%	0.0%	0.0%
REF	0.0%	0.0%	0.0%	0.0%	14.3%	14.1%
Condenser	-	1.7%	-	1.7%	-	1.7%
Dissipator_MED	0.0%	0.0%	40.9%	40.2%	0.0%	0.0%
Dissipator_REF	0.0%	0.0%	0.0%	0.0%	38.6%	38.0%

Table H- 2: Cost decomposition of Generator, REF, and PH in CSP-REF-PH plants (Trigen 3 and Trigen 4).

	Generator		REF		PH	
Device / Trigen	3	4	3	4	3	4
Environment	28.7%	28.6%	6.7%	6.6%	17.4%	20.0%
Collectors	44.5%	44.5%	27.3%	27.3%	44.5%	44.5%
Evaporator	8.2%	8.2%	5.0%	5.0%	8.2%	8.2%
Reheater	3.6%	3.6%	2.2%	2.2%	3.6%	3.6%
LP_Turbine	2.7%	2.7%	0.1%	0.1%	0.1%	0.2%
Economizer	2.4%	2.4%	1.5%	1.5%	2.4%	2.4%
Superheater	1.9%	1.9%	1.2%	1.2%	1.9%	1.9%
Generator	1.2%	1.2%	0.0%	0.0%	0.0%	0.1%
HP_Turbine	0.9%	0.9%	0.6%	0.6%	0.9%	0.9%
FWP5	0.2%	0.1%	0.1%	0.0%	0.2%	6.2%
FWP1	0.2%	0.2%	0.1%	0.1%	0.2%	0.2%
FWP4	0.2%	0.1%	0.1%	0.0%	0.2%	5.1%
FWP2	0.2%	0.2%	0.1%	0.1%	0.2%	0.2%
FWP3	0.1%	0.5%	0.1%	0.3%	0.1%	0.5%
Deaerator	0.1%	0.1%	0.1%	0.1%	0.1%	0.1%
REF	0.0%	0.0%	13.3%	13.3%	0.0%	0.0%
PH	0.0%	0.0%	0.0%	0.0%	15.1%	0.9%
Condenser	4.5%	4.5%	4.5%	4.5%	4.5%	4.5%
Dissipator_REF	0.0%	0.0%	36.9%	36.9%	0.0%	0.0%

Table H- 3: Cost decomposition of Generator and MED in CSP-MED-PH plants (Trigen 5 to Trigen 8).

	Generator				MED			
Device / Trigen	5	6	7	8	5	6	7	8
Environment	30.4%	29.5%	30.5%	29.5%	4.4%	4.3%	4.4%	4.3%
Collectors	46.6%	45.8%	46.6%	45.8%	27.6%	27.1%	27.6%	27.1%
Evaporator	8.7%	8.5%	8.7%	8.5%	4.8%	4.7%	4.8%	4.7%
Reheater	3.4%	3.4%	3.4%	3.4%	2.8%	2.7%	2.8%	2.7%
Economizer	2.6%	2.5%	2.6%	2.5%	1.4%	1.4%	1.4%	1.4%
LP_Turbine	2.5%	2.6%	2.5%	2.6%	0.3%	0.3%	0.3%	0.3%
Superheater	2.0%	2.0%	2.0%	2.0%	1.1%	1.1%	1.1%	1.1%
Generator	1.3%	1.2%	1.3%	1.3%	0.1%	0.1%	0.1%	0.1%
HP_Turbine	1.2%	1.1%	1.2%	1.1%	0.1%	0.1%	0.1%	0.1%
FWP3	0.5%	0.5%	0.2%	0.2%	0.3%	0.3%	0.1%	0.1%
FWP1	0.2%	0.2%	0.2%	0.2%	0.1%	0.1%	0.1%	0.1%
FWP2	0.1%	0.2%	0.1%	0.2%	0.1%	0.1%	0.1%	0.1%
FWP4	0.1%	0.2%	0.1%	0.4%	0.0%	0.1%	0.1%	0.2%
FWP5	0.0%	0.1%	0.1%	0.1%	0.0%	0.0%	0.0%	0.1%
Deaerator	0.0%	0.1%	0.0%	0.1%	0.0%	0.1%	0.0%	0.1%
MED	0.0%	0.0%	0.0%	0.0%	15.9%	15.5%	16.0%	15.5%
PH	0.0%	0.0%	0.0%	0.0%	0.0%	0.0%	0.0%	0.0%
Condenser	-	1.8%	-	1.8%	-	1.8%	-	1.8%
Dissipator_MED	0.0%	0.0%	0.0%	0.0%	40.9%	40.1%	40.9%	40.1%

Table H- 4: Cost decomposition of PH in CSP-MED-PH plants (Trigen 5 to Trigen 8).

	PH			
Device / Trigen	5	6	7	8
Environment	19.9%	18.3%	19.5%	23.0%
Collectors	46.6%	45.8%	46.6%	45.8%
Evaporator	8.0%	7.9%	8.0%	7.8%
Reheater	4.9%	4.8%	4.9%	4.8%
Economizer	2.4%	2.3%	2.4%	2.3%
LP_Turbine	0.1%	0.1%	0.1%	0.1%
Superheater	1.8%	1.8%	1.8%	1.8%
Generator	0.1%	0.1%	0.0%	0.0%
HP_Turbine	0.1%	0.1%	0.0%	0.0%
FWP3	0.4%	0.5%	0.1%	0.2%
FWP1	0.2%	0.2%	0.2%	0.2%
FWP2	0.1%	0.2%	0.1%	0.2%
FWP4	3.1%	10.5%	0.1%	0.4%
FWP5	1.5%	3.2%	0.1%	0.1%
Deaerator	0.0%	0.1%	0.0%	0.1%
MED	0.0%	0.0%	0.0%	0.0%
PH	9.8%	1.8%	15.6%	11.1%
Condenser	-	1.8%	-	1.8%
Dissipator_MED	0.0%	0.0%	0.0%	0.0%

APPENDIX I: Cost decomposition in the polygeneration plants.

Table I- 1: Cost decomposition of Generator and MED in CSP-MED-REF-PH plants (Poly 1 to Poly 4).

	Generator				MED			
Device / Poly	1	2	3	4	1	2	3	4
Environment	30.4%	29.6%	30.5%	29.6%	4.4%	4.3%	4.4%	4.3%
Collectors	46.6%	45.9%	46.6%	45.9%	27.6%	27.1%	27.6%	27.1%
Evaporator	8.7%	8.6%	8.7%	8.6%	4.8%	4.7%	4.8%	4.7%
Reheater	3.4%	3.4%	3.4%	3.4%	2.8%	2.7%	2.8%	2.7%
Economizer	2.6%	2.6%	2.6%	2.6%	1.4%	1.4%	1.4%	1.4%
LP_Turbine	2.5%	2.5%	2.5%	2.5%	0.3%	0.3%	0.3%	0.3%
Superheater	2.0%	2.0%	2.0%	2.0%	1.1%	1.1%	1.1%	1.1%
Generator	1.3%	1.3%	1.3%	1.3%	0.1%	0.1%	0.1%	0.1%
HP_Turbine	1.2%	1.2%	1.2%	1.2%	0.1%	0.1%	0.1%	0.1%
FWP3	0.5%	0.5%	0.2%	0.1%	0.2%	0.3%	0.1%	0.1%
FWP1	0.2%	0.2%	0.2%	0.2%	0.1%	0.1%	0.1%	0.1%
FWP2	0.1%	0.2%	0.1%	0.2%	0.1%	0.1%	0.1%	0.1%
FWP4	0.1%	0.1%	0.2%	0.4%	0.1%	0.1%	0.1%	0.2%
FWP5	0.0%	0.1%	0.1%	0.1%	0.0%	0.0%	0.0%	0.1%
Deaerator	0.0%	0.1%	0.0%	0.1%	0.0%	0.1%	0.0%	0.1%
MED	0.0%	0.0%	0.0%	0.0%	15.9%	15.5%	16.0%	15.5%
REF	0.0%	0.0%	0.0%	0.0%	0.0%	0.0%	0.0%	0.0%
PH	0.0%	0.0%	0.0%	0.0%	0.0%	0.0%	0.0%	0.0%
Condenser	-	1.5%	-	1.5%	-	1.6%	-	1.6%
Dissipator_MED	0.0%	0.0%	0.0%	0.0%	40.9%	40.2%	40.9%	40.2%
Dissipator_REF	0.0%	0.0%	0.0%	0.0%	0.0%	0.0%	0.0%	0.0%

Table I- 2: Cost decomposition of REF and PH in CSP-MED-REF-PH plants (Poly 1 to Poly 4).

	REF				PH			
Device / Poly	1	2	3	4	1	2	3	4
Environment	7.3%	6.9%	7.3%	6.9%	19.7%	18.9%	19.5%	18.3%
Collectors	28.6%	28.2%	28.6%	28.2%	46.6%	45.9%	46.6%	45.9%
Evaporator	4.9%	4.8%	4.9%	4.8%	8.0%	7.9%	8.0%	7.9%
Reheater	3.0%	3.0%	3.0%	3.0%	4.8%	4.8%	4.9%	4.8%
Economizer	1.5%	1.4%	1.5%	1.4%	2.4%	2.4%	2.4%	2.3%
LP_Turbine	0.1%	0.0%	0.1%	0.0%	0.2%	0.2%	0.1%	0.1%
Superheater	1.1%	1.1%	1.1%	1.1%	1.8%	1.8%	1.8%	1.8%
Generator	0.0%	0.0%	0.0%	0.0%	0.1%	0.1%	0.0%	0.0%
HP_Turbine	0.0%	0.0%	0.0%	0.0%	0.1%	0.1%	0.0%	0.0%
FWP3	0.3%	0.3%	0.1%	0.1%	0.4%	0.5%	0.1%	0.1%
FWP1	0.1%	0.1%	0.1%	0.1%	0.2%	0.2%	0.2%	0.2%
FWP2	0.1%	0.1%	0.1%	0.1%	0.1%	0.2%	0.1%	0.2%
FWP4	0.1%	0.1%	0.1%	0.2%	3.6%	10.0%	0.1%	0.4%
FWP5	0.0%	0.0%	0.0%	0.1%	1.2%	3.6%	0.1%	0.1%
Deaerator	0.0%	0.1%	0.0%	0.1%	0.0%	0.1%	0.0%	0.1%
MED	0.0%	0.0%	0.0%	0.0%	0.0%	0.0%	0.0%	0.0%
REF	14.2%	14.1%	14.3%	14.1%	0.0%	0.0%	0.0%	0.0%
PH	0.0%	0.0%	0.0%	0.0%	9.7%	1.2%	15.6%	15.9%
Condenser	-	1.6%	-	1.6%	-	1.6%	-	1.6%
Dissipator_MED	0.0%	0.0%	0.0%	0.0%	0.0%	0.0%	0.0%	0.0%
Dissipator_REF	38.6%	38.0%	38.6%	38.0%	0.0%	0.0%	0.0%	0.0%